

## Comprehensive analysis of prognostic significance of cadherin (CDH) gene family in breast cancer

Su-Chi Ku<sup>1,2,3,\*</sup>, Hsin-Liang Liu<sup>4,\*</sup>, Che-Yu Su<sup>4</sup>, I-Jeng Yeh<sup>4,5</sup>, Meng-Chi Yen<sup>4,5</sup>, Gangga Anuraga<sup>2,6</sup>, Hoang Dang Khoa Ta<sup>2</sup>, Chung-Chieh Chiao<sup>2</sup>, Do Thi Minh Xuan<sup>1</sup>, Fidelia Berenice Prayugo<sup>1,7</sup>, Wei-Jan Wang<sup>8,9</sup>, Chih-Yang Wang<sup>1,2,10</sup>

<sup>1</sup>Graduate Institute of Cancer Biology and Drug Discovery, College of Medical Science and Technology, Taipei Medical University, Taipei 11031, Taiwan

<sup>2</sup>Ph.D. Program for Cancer Molecular Biology and Drug Discovery, College of Medical Science and Technology, Taipei Medical University and Academia Sinica, Taipei 11031, Taiwan

<sup>3</sup>Department of General Medicine, Taipei Medical University Hospital, Taipei 11031, Taiwan

<sup>4</sup>Department of Emergency Medicine, Kaohsiung Medical University Hospital, Kaohsiung Medical University, Kaohsiung 80708, Taiwan

<sup>5</sup>Graduate Institute of Clinical Medicine, College of Medicine, Kaohsiung Medical University, Kaohsiung 80708, Taiwan

<sup>6</sup>Department of Statistics, Faculty of Science and Technology, Universitas PGRI Adi Buana, Surabaya 60234, Indonesia

<sup>7</sup>International Master/PhD Program in Medicine, College of Medicine, Taipei Medical University, Taipei 11031, Taiwan

<sup>8</sup>Department of Biological Science and Technology, Research Center for Cancer Biology, China Medical University, Taichung 406040, Taiwan

<sup>9</sup>Research Center for Cancer Biology, China Medical University, Taichung 40676, Taiwan

<sup>10</sup>TMU Research Center of Cancer Translational Medicine, Taipei Medical University, Taipei 11031, Taiwan

\*Equal contribution

**Correspondence to:** Wei-Jan Wang, Chih-Yang Wang; email: [cvcsky@cmu.edu.tw](mailto:cvcsky@cmu.edu.tw), [chihyang@tmu.edu.tw](mailto:chihyang@tmu.edu.tw)

**Keywords:** cadherin, bioinformatics, prognosis, breast cancer, therapeutic targets

**Received:** January 22, 2022

**Accepted:** September 23, 2022

**Published:** October 30, 2022

**Copyright:** © 2022 Ku et al. This is an open access article distributed under the terms of the [Creative Commons Attribution License](https://creativecommons.org/licenses/by/3.0/) (CC BY 3.0), which permits unrestricted use, distribution, and reproduction in any medium, provided the original author and source are credited.

### ABSTRACT

Breast cancer is one of the leading deaths in all kinds of malignancies; therefore, it is important for early detection. At the primary tumor site, tumor cells could take on mesenchymal properties, termed the epithelial-to-mesenchymal transition (EMT). This process is partly regulated by members of the cadherin (CDH) family of genes, and it is an essential step in the formation of metastases. There has been a lot of study of the roles of some of the CDH family genes in cancer; however, a holistic approach examining the roles of distinct CDH family genes in the development of breast cancer remains largely unexplored. In the present study, we used a bioinformatics approach to examine expression profiles of CDH family genes using the OncoPrint, Gene Expression Profiling Interactive Analysis 2 (GEPIA2), cBioPortal, MetaCore, and Tumor IMMune Estimation Resource (TIMER) platforms. We revealed that CDH1/2/4/11/12/13 messenger (m)RNA levels are overexpressed in breast cancer cells compared to normal cells and were correlated with poor prognoses in breast cancer patients' distant metastasis-free survival. An enrichment analysis showed that high expressions of CDH1/2/4/11/12/13 were significantly correlated with cell adhesion, the extracellular matrix remodeling process, the EMT, WNT/beta-catenin, and interleukin-mediated immune responses. Collectively, CDH1/2/4/11/12/13 are thought to be potential biomarkers for breast cancer progression and metastasis.

## INTRODUCTION

Breast cancer is one of the most common malignancies among women and the second leading cause of death after lung cancer [1, 2]. The prognosis of breast cancer is better with early detection and improved treatment. Because of the poor prognosis of advanced breast cancer, research on breast cancer has recently focused on precise detection of invasion and metastasis with accurate tumorigenic biomarkers [3–9]. Despite progress in developing diagnostic screening tools, distant metastases at the time of diagnosis indicates a worse prognosis with only 23% of patients surviving 5 years post-diagnosis [10]. Therefore, novel research on genetic alterations and signal transduction pathways is playing important roles in both early breast cancer detection and treatment in advanced stages [11–13].

The cadherins (CDHs) are a superfamily of calcium-dependent adhesion molecules which have functions in cell recognition, tissue morphogenesis, and tumor suppression [14, 15]. The *CDH* family consists of 23 members, from *CDH1* to *CDH26*, as documented in the GeneCards database [16]. Basic characteristics of the *CDH* gene family, including gene IDs and aliases, are presented in Table 1. Classic cadherins have mostly been thoroughly studied, including epithelial (E)-cadherin (*CDH1*), neural (N)-cadherin (*CDH2*), placental (P)-cadherin (*CDH3*), and retinal (R)-cadherin (*CDH4*) [17].

It is widely accepted that the epithelial-to-mesenchymal transition (EMT) of epithelial cells results in strong cell-cell adhesion and more invasive features [18]. The EMT is essential for this phenomenon and is considered a promoter of metastasis, and metastatic processes associated with mesenchymal features are similar among various cancers such as advanced breast cancer. The EMT has also received a lot of interest in cancer research and is thought to be an important step in metastases [19, 20]. As a result, finding new molecules that can inhibit this mechanism is an important subject of scientific study. A feature of the EMT is in part a result of downregulation of *CDH1* and parallel upregulation of other cadherins like *CDH2*, which plays an essential role during early invasion and metastasis [21]. Loss of *CDH1* alone might be insufficient to induce the EMT [22]. Instead, *CDH1* expression was observed in invasive lobular carcinomas (ILCs) and invasive ductal carcinomas (IDCs) [23]. Other cadherins and molecules such as  $\beta$ -catenin, which forms an important membrane complex, are often detached from the cell membrane and are translocated to the nucleus to induce EMT signaling events [24–26].

Previous studies reported the roles of cadherins in breast cancer. However, interactions and pathways among all

*CDH* family members and related molecules in tumorigenesis are still unclear, and challenges remain in discovering suitable biomarkers for precision treatment and detection.

The present study is the first study to perform a bioinformatics analysis of the entire *CDH* family in patients with breast cancer by analyzing several large online databases. A flowchart depicting the investigative strategies we utilized in this study, including expression levels, clinical survival, and functional enrichment analyses, of *CDH* family members in breast cancer is presented in Figure 1. First, original data were retrieved from the Molecular Taxonomy of Breast Cancer International Consortium (METABRIC) and The Cancer Genome Atlas (TCGA) databases. Second, differential expression levels were analyzed using the OncoPrint and Tumor Immune Estimation Resource (TIMER) databases. Third, Kaplan-Meier (KM) plots were utilized to reveal the significance of *CDH* family in the prognosis of breast cancer patients. Incorporating these results, we selected targeted genes due to higher expression levels and lower survival for further analysis. Then, the Cancer Cell Lines Encyclopedia (CCLE) and Gene Expression Profiling Interactive Analysis 2 (GEPIA2) databases were used to discover differences in expressions between breast cancer and normal tissues [27–31]. Afterwards, we used the MethSurv database to determine single CpG methylation expression patterns. In addition, we studied the gene potential thoroughly through a functional enrichment analysis and micro (mi)RNA-regulated networks, including biological processes (BPs), cellular components (CCs), molecular functions (MFs), signaling pathways, and potentially regulated miRNAs. Ultimately, we utilized the TIMER2.0 database to uncover correlations between *CDH* genes and immune cell markers in breast cancer. The flowchart is presented to offer insights into our comprehensive approach and possibly suggest a theoretical foundation for future research.

## MATERIALS AND METHODS

### OncoPrint analysis

OncoPrint (<https://www.oncoPrint.com/>) is an online database established to show information of gene expressions in major cancers compared to their respective normal samples [32]. In this study, individual expression levels of *CDH* family members in various cancers were obtained from the OncoPrint database with  $p < 0.05$  and fold change (FC) defined as 1.5 [33–37].

### TIMER and GEPIA2 analyses

The TIMER database was utilized to identify complements or regulatory factors that are upregulated

**Table 1. Basic characteristics of the CDH gene family.**

Approved symbol	HGNC ID	Gene ID	Aliases	Location on chromosome
CDH1	1748	999	Cadherin 1; Uvomorulin; CD324; UVO; Cadherin 1, Type 1, E-Cadherin (Epithelial)	16q22.1
CDH2	1759	1000	Cadherin 2; CDHN; CD325; NCAD; Cadherin 2, Type 1, N-Cadherin (Neuronal)	18q12.1
CDH3	1762	1001	Cadherin 3; CDHP; PCAD; Cadherin 3, Type 1, P-Cadherin (Placental)	16q22.1
CDH4	1763	1002	Cadherin 4; R-Cadherin; Cadherin 4, Type 1, R-Cadherin (Retinal)	20q13.33
CDH5	1764	1003	Cadherin 5; VE-Cadherin; CD144; 7B4	16q21
CDH6	1765	1004	Cadherin 6; Cadherin 6, Type 2, K-Cadherin (Fetal Kidney)	5p13.3
CDH7	1766	1005	Cadherin 7; Cadherin 7, Type 2; Cadherin-7; CDH7L1	18q22.1
CDH8	1767	1006	Cadherin 8; Cadherin 8, Type 2; Cadherin-8; Nbla04261	16q21
CDH9	1768	1007	Cadherin 9; Cadherin-9; Cadherin 9, Type 2 (T1-Cadherin)	5p14.1
CDH10	1749	1008	Cadherin 10; Cadherin-10; T2-Cadherin; Cadherin 10, Type 2, (T2-Cadherin)	5p14.2-p14.1
CDH11	1750	1009	Cadherin 11; CAD11; OB; Cadherin 11, Type 2, OB-Cadherin (Osteoblast)	16q21
CDH12	1751	1010	Cadherin 12; Br-Cadherin; CDHB; Neural Type Cadherin 2	5p14.3
CDH13	1753	1012	Cadherin 13; CDHH; T-Cadherin; H-Cadherin (Heart)	16q23.3
CDH15	1754	1013	Cadherin 15; CDH 14; CDH3; Cadherin 15, Type 1, M-Cadherin (Myotubule)	16q24.3
CDH16	1755	1014	Cadherin 16; Cadherin 16, KSP-Cadherin; Kidney-Specific Cadherin	16q22.1
CDH17	1756	1015	Cadherin 17; HPT-1; Intestinal Peptide-Associated Transporter HPT-1	8q22.1
CDH18	1757	1016	Cadherin 18; CDH14; Cadherin 18, Type 2	5p14.3
CDH19	1758	28513	Cadherin 19; CDH7; Cadherin 19, Type 2	18q22.1
CDH20	1760	28316	Cadherin 20; CDH7L3; Cdh7	18q21.33
CDH22	13251	64405	Cadherin 22; DJ998H6.1; C20orf25	20q13.12
CDH23	13733	64072	Cadherin 23; CDHR23; Cadherin-Related Family Member 23	10q22.1
CDH24	14265	64403	Cadherin 24; CDHH11L; Cadherin 24, Type 2	14q11.2
CDH26	15902	60437	Cadherin 26; VR20; Cadherin-Like Protein VR20	20q13.33

or downregulated in tumor samples compared to normal tissues. To analyze differences in gene expressions of each *CDH* family member between breast cancer and normal tissues, differentially expressed genes (DEGs) in breast invasive carcinoma (BRCA) in TCGA dataset were identified via TIMER. The threshold  $|\log_2[FC]|$  was set to 1, and the value of  $q$  was 0.05. GEPIA2 (<http://gepia2.cancer-pku.cn/#index>) is a web platform that contains RNA sequencing (RNA-Seq) expression data from 9736 tumors and 8587 normal samples from TCGA and GTEx projects [38]. An independent t-test was used to calculate  $p$  values, and  $p < 0.05$  was considered statistically significant;  $\Pr(>F) < 0.05$  was based on Student's t-test [39–44].

### KM plotter survival analysis

The KM plotter (<http://kmplot.com/analysis/>) contains 54,000 genes associated with survival in 21 types of cancer [45], including breast cancer samples ( $n=7830$ ), which can be analyzed to examine the effects of *CDH* gene family members on survival times of patients with breast cancer. Results are presented by plotting the survival curve and hazard ratios (HRs) with 95% confidence intervals (CIs) and log-rank  $p$  values [46]. To assess the prognosis of breast cancer patients, distant metastasis-free survival (DMFS) was applied to evaluate the survival of advanced breast cancer patients.

### Genetic alterations and protein expression analysis

The cBioPortal (<http://www.cbioportal.org/>) is an open platform providing large-scale visualization, analysis, and downloading of cancer genomic datasets for various types of cancer [47, 48]. Cancer genome profiles can be obtained by a portal query interface, allowing researchers to explore and compare genetic alterations across samples. This study used the cBioPortal to explore alterations, correlations, and networks of the *CDH* gene family. *CDH* family protein expressions were evaluated by the Human Protein Atlas (HPA) platform. HPA contains images of pathologic tissues labeled with antibodies in conjunction with 11,250 human proteins. Microarrays include sections from forty-six normal tissues and more than twenty types of human cancers [49–51]. This study used the HPA to obtain the intensities of labeled antibodies in pathologic malignant tissues. Bar charts represent the quantification of four classifications, “negative”, “weak”, “moderate”, and “strong”, of IHC staining intensities in breast cancer samples with different antibodies.

### Expression modules in breast cancer gene-expression analysis

“Breast cancer gene-expression miner” (bc-GenExMiner), which contains published annotated breast

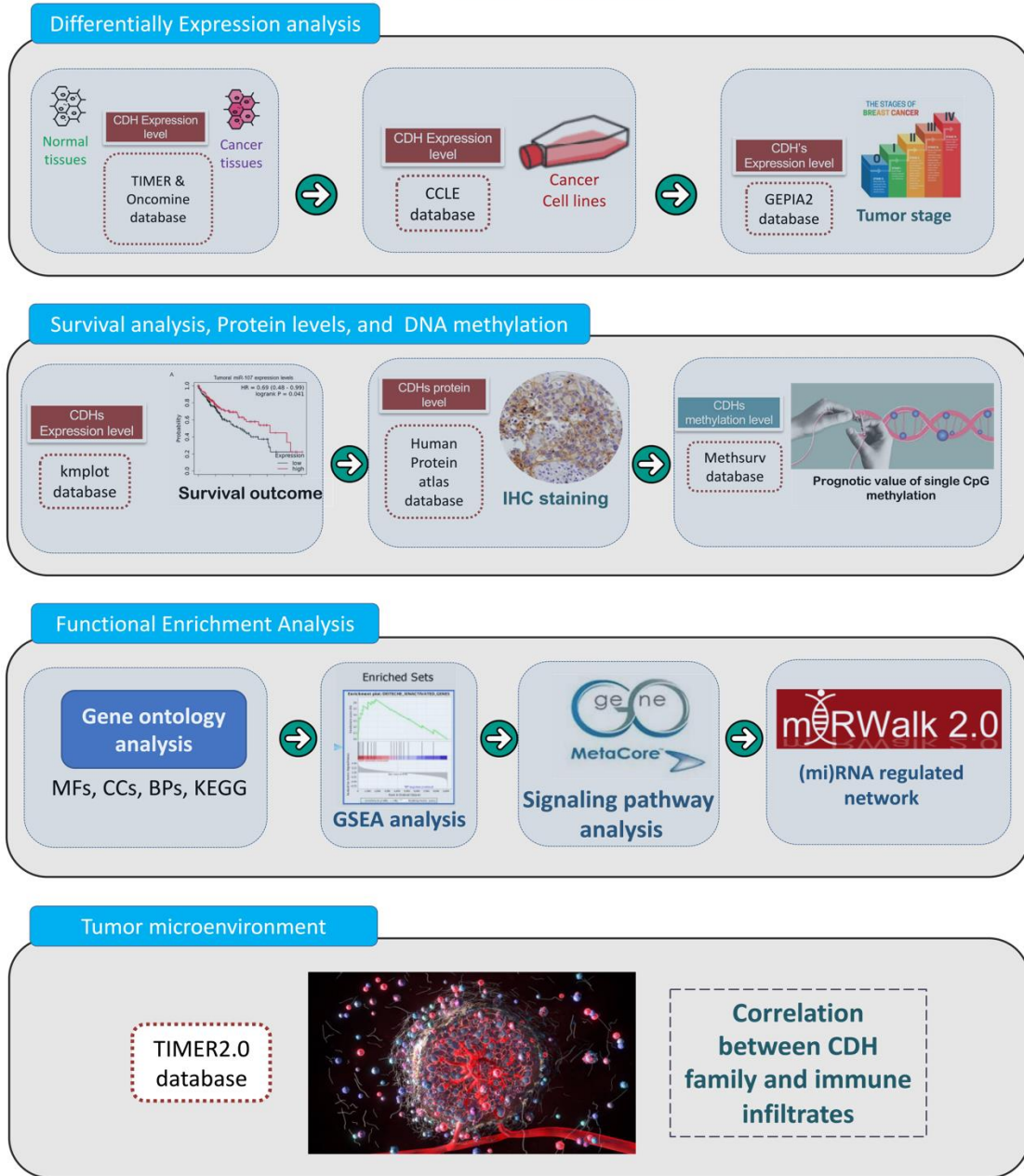
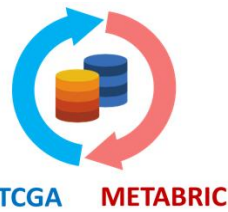


**Figure 1. Flowchart of the study design and analytical steps in the present study.** Gene data were retrieved from TCGA and METABRIC databases. To select targeted genes among the cadherin (CDH) family, we observed results of simultaneous higher expression levels in cancer cells than normal tissues and poorer prognoses in breast cancer patients. Afterwards, through four steps of a “differential expression analysis”, “survival analysis, protein levels, and DNA methylation”, “functional enrichment analysis”, and “tumor microenvironment”, a comprehensive analysis was conducted with the following databases and analytical methods. TCGA, The Cancer Genome Atlas; METABRIC, Molecular Taxonomy of Breast Cancer International Consortium; TIMER, Tumor IMMune Estimation Resource; CCLC, Cancer Cell Line Encyclopedia; GEPIA2, Gene Expression Profiling Interactive Analysis 2; KM, Kaplan-Meier; IHC, immunohistochemistry; BPs, biological processes; MFs, molecular functions; CCs, cellular components; KEGG, Kyoto Encyclopedia of Genes and Genomes; GSEA, Gene Set Enrichment Analysis; miRNA, micro-RNA.

cancer transcriptomic data (DNA microarrays [ $n=11,359$ ] and RNA-Seq [ $n=4421$ ]), is a breast cancer-associated web portal (<http://bcgenex.ico.unicancer.fr>) that conducts several differential gene expression analyses. We obtained data from Affymetrix® median probe data. To evaluate the difference in a gene's expression among different groups, Welch's test was used. Moreover, Dunnett-Tukey-Kramer's test was used for two-by-two comparisons (allowing determination of the significance levels but not giving a precise  $p$  value) when there were more than three different groups and Welch's  $p$  value was significant. Variant corresponding clinical or pathological data is contained in bc-GenExMiner version 4.5, which stresses that the Expression Module can be utilized for both exploratory and validation purposes [52].

### Cancer cell line encyclopedia (CCLE) analysis

Over 1100 cell lines among 37 cancer types are contained in the CCLE database (<https://portals.broadinstitute.org/ccle>). The CCLE dataset provides extensive genomic data, computational analyses, and visualization [53]. For the present study, we used the CCLE dataset to investigate messenger (m)RNA expression levels of *CDH* family members to further verify their participation in cancer cell lines [54–57].

### DNA methylation analysis

The MethSurv (<https://biit.cs.ut.ee/methsurv/>) database was utilized to determine single CpG methylation expression patterns and establish a heatmap of the different DNA methylated regions [58]. DNA methylation values are presented as beta values (ranging from 0 to 1). We used the formula of  $M / (M + U + 100)$  to calculate each single methylation of CpG, where  $M$  and  $U$  respectively represent methylated and unmethylated intensity values.

### Functional enrichment and miRNA-regulated network analyses

The METABRIC and TCGA datasets in the cBioPortal database were accessed for functional enrichment analyses [59, 60]. There were two parts of the MetaCore analysis (<https://portal.genego.com>). The first part was to find overlapping genes coexpressed in the two datasets with Venny version 2.1. The second part was to uncover BPs, disease biomarker networks, breast neoplasm signaling pathways, and drug target networks [61–65]. Moreover, a gene ontology (GO) analysis was implemented to discover the functional significance of genes with BPs, MFs, CCs, and the Kyoto Encyclopedia of Genes and Genomes (KEGG) with  $p$  values of  $<0.05$  indicating statistical significance [66–70]. Next, we used the median expression of targeted genes and then

performed a differential analysis with an algorithm in the “DESeq2” package in R/Bioconductor. After the differential analysis, results were utilized for the gene set enrichment analysis (GSEA) with the Hallmark database [71–73]. Then, we used the “fgsea” packages in R Studio software to evaluate enriched pathways in transcriptional data by the GSEA, and online platform (<http://www.bioinformatics.com.cn/>) and used “SRplot” for visualization (<http://www.bioinformatics.com.cn/srplot>) [74, 75]. The level of statistical significance was presented via  $p$  values, and a normalized enrichment score (NES) reflected the rank of gene classes. In addition, the gene potential of the *CDH* family was conducted using the miRWalk database (<http://mirwalk.umm.uni-heidelberg.de/>) to investigate the regulatory potential of miRNAs and to analyze regulated pathways and networks by an Ingenuity Pathway Analysis (IPA) [76–79].

### Cox regression analysis in TIMER

The TIMER web server was accessed for a Cox regression analysis [80, 81]. We used the “Survival” module to explore the clinical significance of covariates in a multivariable Cox proportional hazard model. Clinical factors such as age, gender, ethnicity, and tumor stage and gene expression were covariates in the analysis. TIMER presents Cox regression results including hazard ratios (HRs) and statistical significance. For outputs of the Cox model,  $\text{Surv}(\text{CancerType}) \sim \text{variables}$  is the formula of the user-defined Cox regression model, which is fitted by the function `coxph()` from the R package ‘survival’. In the results, the coefficient reads as a regression coefficient. The 95% confidence intervals (CIs) are shown.

### Data availability

The present study is based on open-source data. Users could download relevant data in public databases for research.

## RESULTS

### Differential expressions of *CDH* family members in breast cancer

To understand differences in expressions between breast cancer and normal tissues, all 24 *CDH* family members were investigated in the Oncomine database (Figure 2A, 2B). Findings of this database revealed that at the transcriptional level, *CDH1/2/4/6/7/11/12/13/15/22/23/24* were overexpressed in breast cancer samples compared to normal tissues, while transcriptional levels of *CDH1/3/5/8/9/10/16/17/18/19/20/26/28* were downregulated compared to normal tissues. In addition, complement expressions were explored across TCGA

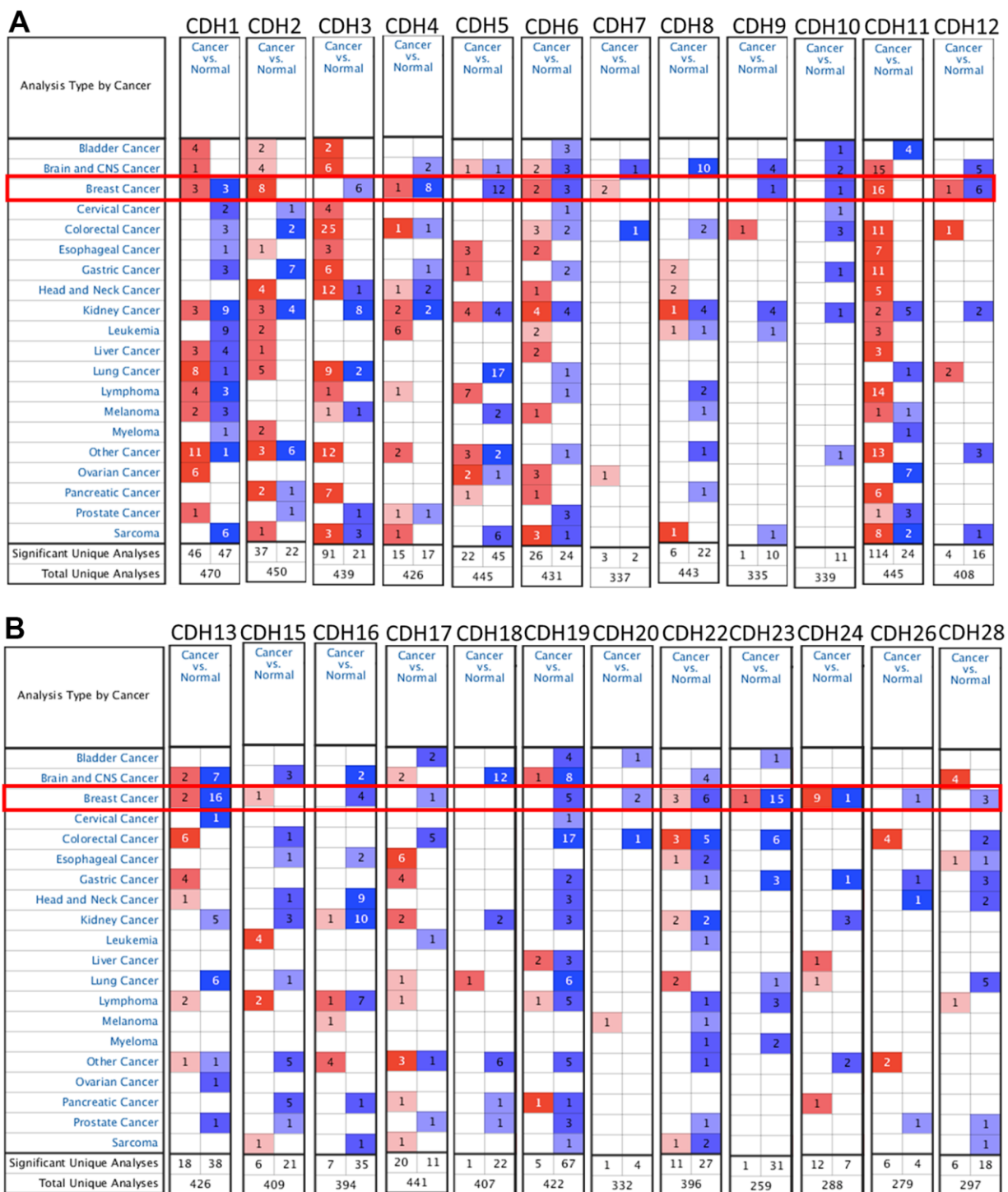


**Figure 2. mRNA transcription levels of cadherin (CDH) gene family members (ONCOMINE).** A red background with numbers indicates studies including expression levels of CDH family members corresponding to our selection standards (with  $p$  values  $<0.05$ , fold changes of  $>1.5$ , and the expressed gene rank in the top 10% as selection thresholds) in cancer tissues; blue (the same selection threshold) in normal tissues. The number for the significant unique analyses means that the queried genes significantly differed in these studies. The number for the total unique analyses means the total number of queried genes in these studies. (A) mRNA transcription levels of CDH1/2/4/6/7/11/12 were overexpressed in breast cancer samples compared to normal tissues, while transcriptional levels of CDH1/3/4/5/6/9/10/12 were downregulated compared to normal tissues. (B) mRNA transcription levels of CDH13/15/22/23/24 were overexpressed in breast cancer samples compared to normal tissues, while transcriptional levels of CDH13/16/17/19/20/22/23/24/26/28 were downregulated compared to normal tissues. Red indicates upregulation, and blue indicates downregulation compared to normal tissues.



database via the TIMER database (Figure 3A). We investigated expression levels of CDH family members in breast cancer cell lines using the CCLE database as well (Figure 3B). Results revealed that expression levels were upregulated or downregulated in BRCA samples compared to non-tumor samples. Compared to normal tissues, expression levels of *CDH2/3/4/5/6/7/8/10/11/12/13/15/17/19/20/22/23/24/26* were significantly higher in BRCA tissues. In contrast, expression levels of *CDH1/18* were significantly lower in BRCA tissues. The molecular subtypes of cell lines are also shown in Supplementary Figure 1. *CDH1* and *CDH7* were highly expressed in luminal A cell lines; *CDH5* was mostly expressed in human epidermal growth factor receptor-2 (HER2) cell lines; *CDH2/3/4/6/11/12/13/15/18/19/22/23* showed high expressions in multiple triple-negative breast cancer cell lines; and other *CDH* genes showed no specific expressions in molecular subtypes of breast cancer cell lines.

### Prognostic analysis of the *CDH* family via Kaplan-Meier analyses

The impact of the entire *CDH* family on breast cancer survival was evaluated through the KM plotter database. Distant metastasis-free survival (DMFS) was analyzed due to its significance in clinical prognosis of advanced breast cancer. Results demonstrated that most *CDH* family genes were associated with the prognosis of BRCA patients including *CDH1/2/3/4/5/7/9/10/11/12/13/15/16/19/26* (Figure 4 and Table 2). High expression levels of *CDH1* (HR=1.32, 95% CI=1.13~1.55,  $p=0.0058$ ), *CDH2* (HR=1.39, 95% CI=1.17~1.64,  $p=0.00012$ ), *CDH3* (HR=1.55, 95% CI=1.32~1.82,  $p=6.4e-8$ ), *CDH4* (HR=1.27, 95% CI=1.08~1.5,  $p=0.0036$ ), *CDH7* (HR=1.34, 95% CI=1.14~1.58,  $p=0.00048$ ), *CDH9* (HR=1.21, 95% CI=1.03~1.43,  $p=0.02$ ), *CDH10* (HR=1.34, 95% CI=1.13~1.58,  $p=0.00059$ ), *CDH11* (HR=1.42, 95% CI=1.04~1.96,  $p=0.028$ ), *CDH12* (HR=1.21, 95% CI=1.03~1.41,  $p=0.019$ ), *CDH13* (HR=1.31, 95% CI=1.12~1.54,  $p=0.00089$ ), *CDH15* (HR=1.22, 95% CI=1.03~1.44,  $p=0.023$ ), *CDH16* (HR=1.28, 95% CI=1.09~1.5,  $p=0.003$ ), and *CDH26* (HR=1.68, 95% CI=1.28~2.19,  $p=0.00012$ ) were correlated with poorer DMFS in BRCA patients. On the other hand, high expressions of *CDH5* (HR=0.84, 95% CI=0.71~0.98,  $p=0.031$ ) and *CDH19* (HR=0.71, 95% CI=0.54~0.92,  $p=0.01$ ) were associated with a good prognosis in BRCA patients. Other family members in the *CDH* family showed negative results.

A univariate Cox regression analysis was conducted to validate our results from clinical breast cancer patients, data of which were obtained from the TIMER database. The univariate Cox regression demonstrated that high levels of *CDH13* were an independent risk factor for

poor overall survival (OS) (Supplementary Table 1A) in breast cancer patients. In addition, subtypes of breast cancer, including luminal, HER2, and basal, were analyzed. The luminal subtype showed no significance among *CDHs* (Supplementary Table 1B). *CDH12* was a significant risk factor for poor OS in the HER2 subtype (Supplementary Table 1C). *CDH11* and *CDH12* were significant risk factors for poor OS in the basal subtype (Supplementary Table 1D).

To further understand correlations of expression levels of *CDH* family members in breast cancer, some clinical and pathological factors were analyzed in specific genes among the *CDH* family. Among all *CDH* family members, *CDH1/2/3/4/7/9/10/11/12/13/15/16/26* were significantly positively associated with a lower DMFS (Figure 4), and *CDH1/2/4/6/7/11/12/13/15/22/23/24* mRNA expression levels were higher in breast cancer than in normal tissues in the Oncomine database (Figure 2A, 2B). Results demonstrated that the eight *CDH1/2/4/7/11/12/13/15* genes simultaneously expressed significance in the gene database and clinical survival analysis. Therefore, in this study, these eight specific genes were further analyzed with an extensive database, clinical factors, and bioinformatics tools and were demonstrated to be potential biomarkers for breast cancer.

### Correlations of *CDH1*, *CDH2*, *CDH4*, *CDH7*, *CDH11*, *CDH12*, *CDH13*, and *CDH15* expressions with prognosis and different clinical and pathological factors

As *CDH1/2/4/7/11/12/13/15* were positive in terms of both gene expressions and with the KM survival analysis, immunohistochemical (IHC) patterns from the HPA were utilized to validate clinical applications by pathology (Figure 5A, 5B). *CDH1*, *CDH2*, and *CDH12* exhibited strong intensities in cell nuclei in breast cancer samples. Otherwise, other members of the *CDH* family showed negative or weak intensities in pathological samples. The relative staining intensities of *CDH1* were negative (two cases), moderate (one case), and strong (eight cases) in breast cancer samples. *CDH2* staining intensities were negative (nine cases), weak (three cases), and strong (one case) in breast cancer samples. *CDH12* staining intensities were negative (one case), weak (three cases), moderate (one case), and strong (seven cases) in breast cancer samples. There was no IHC pattern for *CDH4* obtained from the HPA. Other staining intensities of *CDH* family members are shown in Figure 5A, 5B. *CDH* staining expressions, magnification in 4x, were displayed among *CDH* family except *CDH13* and *CDH15* due to negative intensities.

Correlations of expression levels of *CDH1/2/4/7/11/12/13/15* with pathological stages of breast cancer are



shown in violin plots in Figure 6A. mRNA levels of *CDH1/11/13* were relatively high in breast cancer

patients classified as stage IV with metastasis but without statistical significance.

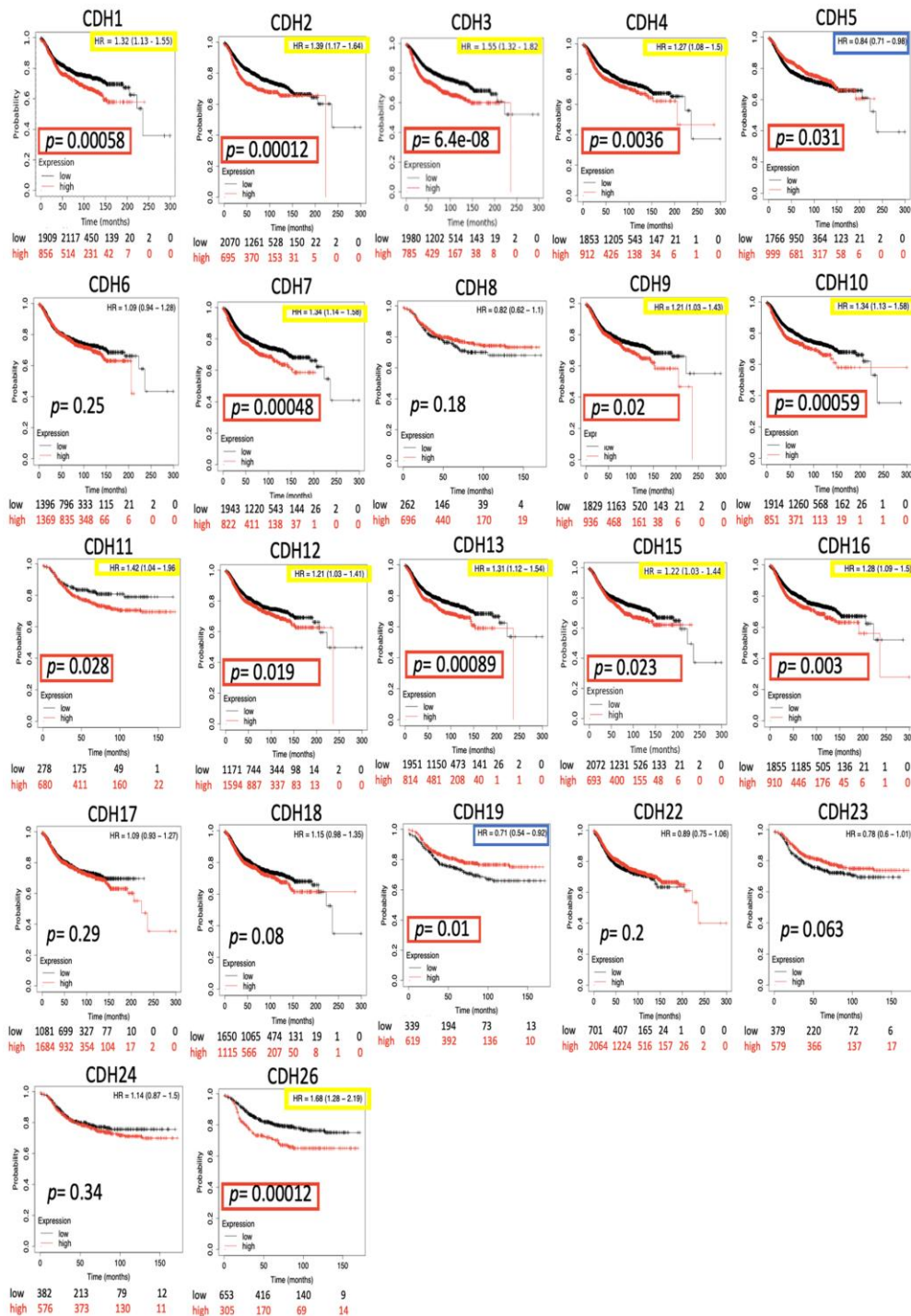


**Figure 4. Kaplan-Meier (KM) analysis of cadherin (CDH) family genes in the distant metastasis-free survival (DMFS) of breast cancer patients.** The hazard ratio (HR) represents a prognostic value of breast cancer patients. Log[rank *p*] was utilized to find out the level of prognostic significance of breast cancer patients. In addition, log[rank *p*] of <0.05 was considered a significant difference in the prognosis of breast cancer patients. High expressions of *CDH1/2/3/4/5/7/9/10/11/12/13/15/16/19/26* were significant compared to low expressions, which are highlighted with *p* values in red boxes. The HRs of *CDH1/2/3/4/7/9/10/11/12/13/15/16/26* were significantly higher, which are marked in yellow boxes, indicating poor prognostic outcomes in breast cancer. In contrast, the HRs of *CDH5/19* were significantly lower, which were marked in blue boxes, indicating better prognostic outcomes in breast cancer.

**Table 2. Kaplan-Meier analysis of CDH family genes in distant metastasis-free survival (DMFS) in breast cancer.**

Gene	HR (95% CI)	p value	Gene	HR (95% CI)	p value
<i>CDH1</i>	1.32 (1.13~1.55)	0.0058	<i>CDH12</i>	1.21 (1.03~1.41)	0.019
<i>CDH2</i>	1.39 (1.17~1.64)	0.00012	<i>CDH13</i>	1.31 (1.12~1.54)	0.00089
<i>CDH3</i>	1.55 (1.32~1.82)	6.4e-08	<i>CDH15</i>	1.22 (1.03~1.44)	0.023
<i>CDH4</i>	1.27 (1.08~1.5)	0.0036	<i>CDH16</i>	1.28 (1.09~1.5)	0.003
<i>CDH5</i>	0.84 (0.71~0.98)	0.031	<i>CDH17</i>	1.09 (0.93~1.27)	0.29
<i>CDH6</i>	1.09 (0.94~1.28)	0.25	<i>CDH18</i>	1.15 (0.98~1.35)	0.08
<i>CDH7</i>	1.34 (1.14~1.58)	0.00048	<i>CDH19</i>	0.71 (0.54~0.92)	0.01
<i>CDH8</i>	0.82 (0.62~1.1)	0.18	<i>CDH22</i>	0.89 (0.75~1.06)	0.2
<i>CDH9</i>	1.21 (1.03~1.43)	0.02	<i>CDH23</i>	0.78 (0.6~1.01)	0.063
<i>CDH10</i>	1.34 (1.13~1.58)	0.00059	<i>CDH24</i>	1.14 (0.87~1.5)	0.34
<i>CDH11</i>	1.42 (1.04~1.96)	0.028	<i>CDH26</i>	1.68 (1.28~2.19)	0.00012

High expressions of *CDH1/2/3/4/5/7/9/10/11/12/13/15/16/19/26* were significant compared to low expressions.

Scarff-Bloom-Richardson (SBR) grading is a clinical prognostic predictor associated with cell proliferation and an indicator of the response to chemotherapy (Figure 6B). A determination of an association between the SBR grade and responsiveness would be clinically useful [82]. SBR1 indicates good differentiation, SBR2 moderate differentiation, and SBR3 poor differentiation. Figure 6B demonstrates that *CDH1*, *CDH2*, and *CDH11* with the poorest prognoses were assigned to grade SBR3.

The Nottingham prognostic index (NPI) is used to predict a prognosis after breast cancer surgery, and is calculated by three pathological factors: the tumor size, the number of involved lymph nodes, and the tumor grade (Figure 6C). Values are used to define three subsets of patients with different survival chances of breast cancer: 1) good prognosis, comprising 29% of patients with an 80% chance of 15-year survival; 2) moderate prognosis, 54% of patients with a 42% chance of 15-year survival; and 3) poor prognosis, 17% of patients with a 13% chance of 15-year survival [83]. The NPI can also be used to evaluate the effect of adjuvant treatment like chemotherapy or radiotherapy. Figure 6C demonstrates that only *CDH1* expression was correlated with higher NPI values, indicating poor prognoses in patients with *CDH1* gene expression. Otherwise, *CDH11* and *CDH13* expressions demonstrated lower NPI values with better prognoses. Other *CDH* family members showed no significance.

Other clinical predictors were also analyzed in terms of *CDH* family gene expressions in breast cancer (Supplementary Figure 2 in Supplementary Materials). Estrogen receptor (ER)/progesterone receptor (PR)-positive samples showed a high probability of positive

effects of hormone therapy such as with tamoxifen. HER2 samples corresponded to positive effects of targeted therapy with trastuzumab. Subtypes of breast cancer including basal-like, HER2-E, luminal A, and luminal B were correlated with different pathological characteristics and clinical prognoses. Mutations of breast cancer gene-1 (*BRCA1*) and *BRCA2* were also analyzed with respect to *CDH* family gene expressions, which represent breast cancer oncogenes (Supplementary Figure 2D). Supplementary Figure 2A demonstrates that ER-/PR- expressions were correlated with higher expressions of *CDH2* and *CDH11*, indicating a poorer response to hormone therapy. Supplementary Figure 2B demonstrates that HER2-negative expression was found to be associated with *CDH7* and *CDH11*, suggesting a poorer response to targeted therapy. Supplementary Figure 2C demonstrates relationships of different subtypes of breast invasive carcinoma with *CDH* family gene expressions. *CDH1* was highly expressed by the HER2-E and luminal B types; *CDH2* was highly expressed by the HER2-E type; *CDH4* was highly expressed by the basal-like type; *CDH7* and *CDH11* were highly expressed by the luminal A type; *CDH12* and *CDH13* were highly expressed by the basal-like and luminal A types; and *CDH15* expression was significantly associated with no types.

#### Gene mutation analysis of *CDH1/2/4/7/11/12/13/15* in breast cancer

Genomic changes in the *CDH* family were analyzed via the cBioPortal database, which demonstrated changes in *CDH1* (14%), *CDH2* (6%), *CDH4* (11%), *CDH7* (5%), *CDH11* (5%), *CDH12* (7%), *CDH13* (4%), and *CDH15* (4%) (Figure 7A). Our results of mutated gene

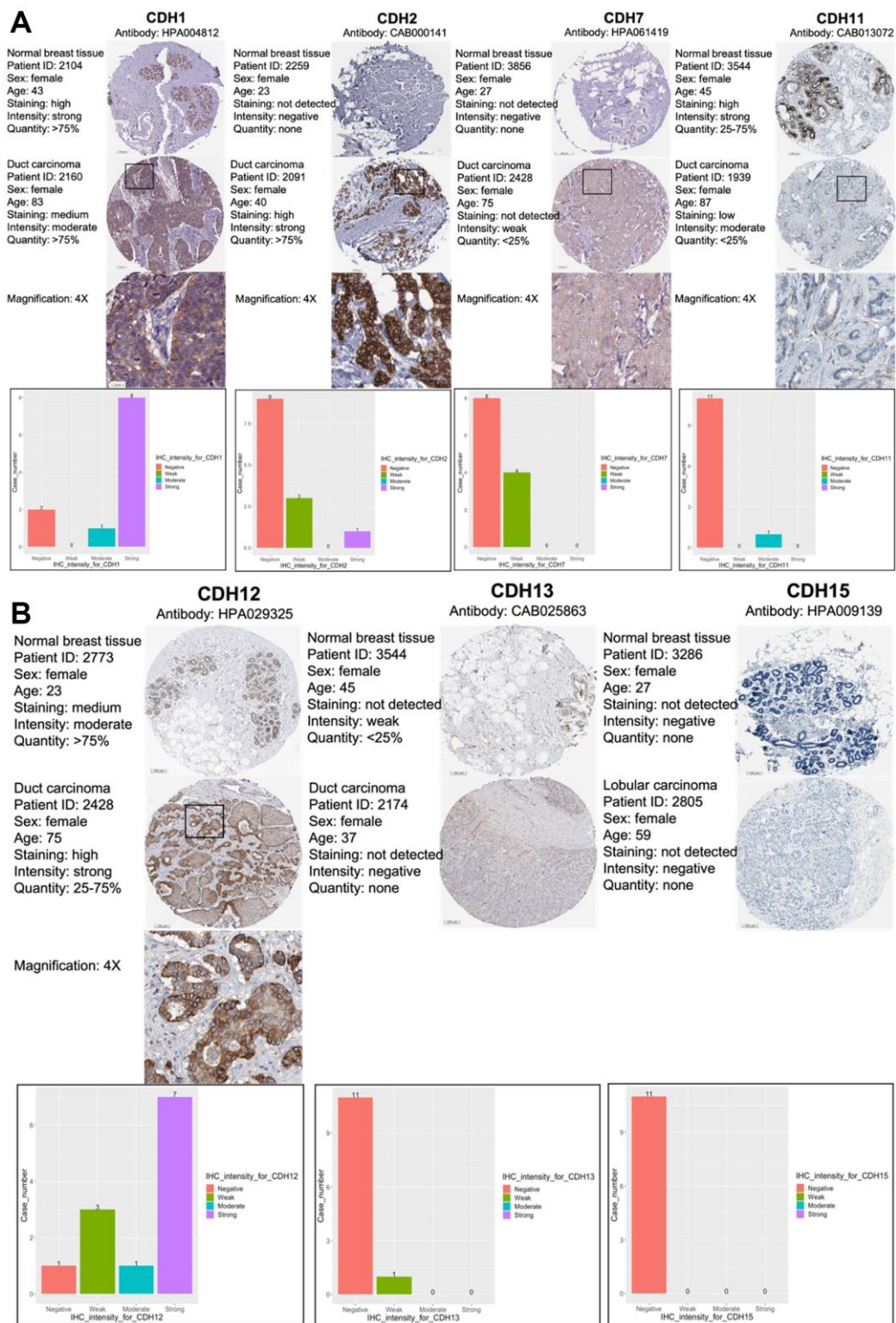


**Figure 5. Protein expression levels of members of cadherin (CDH) family genes in all clinical breast cancer specimens from the Human Protein Atlas (HPA).** (A) Images of immunohistochemistry (IHC) of *CDH1/2/7/11* show their staining intensities. IHC images and patients' information were obtained from the HPA. Normal and tumor samples are listed, and bar charts represent the quantification of IHC staining in breast cancer samples. There were strong intensities of *CDH1* and *CDH2* in breast cancer samples. (B) IHC images of *CDH12/13/15* show their staining intensities. IHC images and patient information were obtained from the HPA. Normal and tumor samples are listed, and bar charts present quantification of IHC staining in breast cancer samples. There were strong intensities of *CDH12* in breast cancer samples.

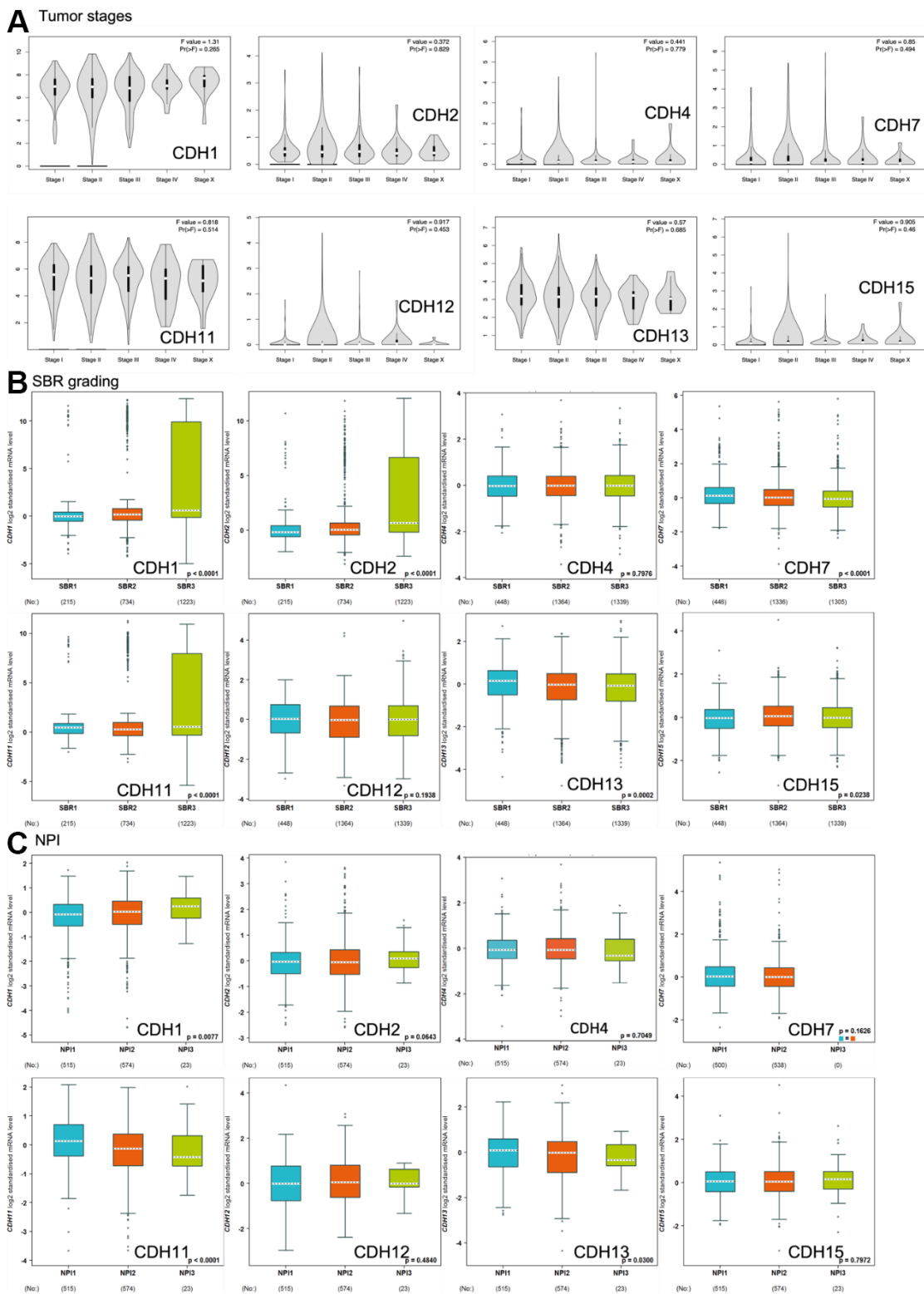


**Figure 6. Expression of cadherin (CDH) family genes in subgroups of breast cancer patients. (A)** Gene expression analysis among the stages of *CDH* genes in a breast cancer (GEPiA2) database. The violin plot displayed comparisons of *CDH* genes expressions from TCGA dataset of breast cancer. An independent *t*-test was utilized for *p* values;  $p < 0.05$  meant statistically significant;  $Pr(>F) < 0.05$  was based on Student's *t*-test. **(B)** Scarff-Bloom-Richardson (SBR) grading of *CDH* family genes. Associations between *CDH1/2/4/7/11/12/13/15* and SBR grading were analyzed via the bc-GenExMiner dataset. **(C)** The Nottingham prognostic index (NPI) of *CDH* family genes. Associations between *CDH1/2/4/7/11/12/13/15* and NPI values were analyzed via the bc-GenExMiner dataset.

frequencies demonstrated that those of *CDH1* and *CDH4* were >10%. Altered genes at higher frequencies affect signaling pathways and cellular processes and can induce tumorigenesis based on previous studies [84–86]. *CDH1* showed more gene alterations of truncating mutations and deep deletions, and low mRNA expression, while in contrast, *CDH4* showed more amplifications and high mRNA expression. In the METABRIC dataset, *CDH1* acted more like a TSG, and *CDH4* acted like an oncogene in breast cancer. A previous study demonstrated that loss of E-cadherin was a key hallmark of ILCs [87]. In Giovanni et al. [86], *CDH1* was one of the most recurrently mutated genes in breast cancer. In mixed ILC-IDC samples, genetic alterations of ILC tumors were found at a frequency of 14%. Mutations targeting *CDH1* were mostly truncated mutations, and this result was similar to our mutation analysis.

We also used Pearson's correlations to calculate correlations between *CDH* family members based on mRNA expressions (Figure 7B). *CDH11* was significantly positively correlated with *CDH13*. Other genes in the *CDH* family otherwise showed no relative correlations with each other (Figure 7B). In addition, a protein-protein interacting (PPI) network analysis of the *CDH* family was conducted via STRING at various transcription levels to investigate potential relationships. The STRING analysis revealed that linkages among *CDH* gene family members were complicated. Using a three-group k-means algorithm, it was found that the group consisting of *CDH1*, *CDH13*, and *CDH15* had a close relationship, and *CDH2*, *CDH4*, and *CDH11* comprised another related group. A third group consisted of *CDH7* and *CDH12* (Figure 7C).

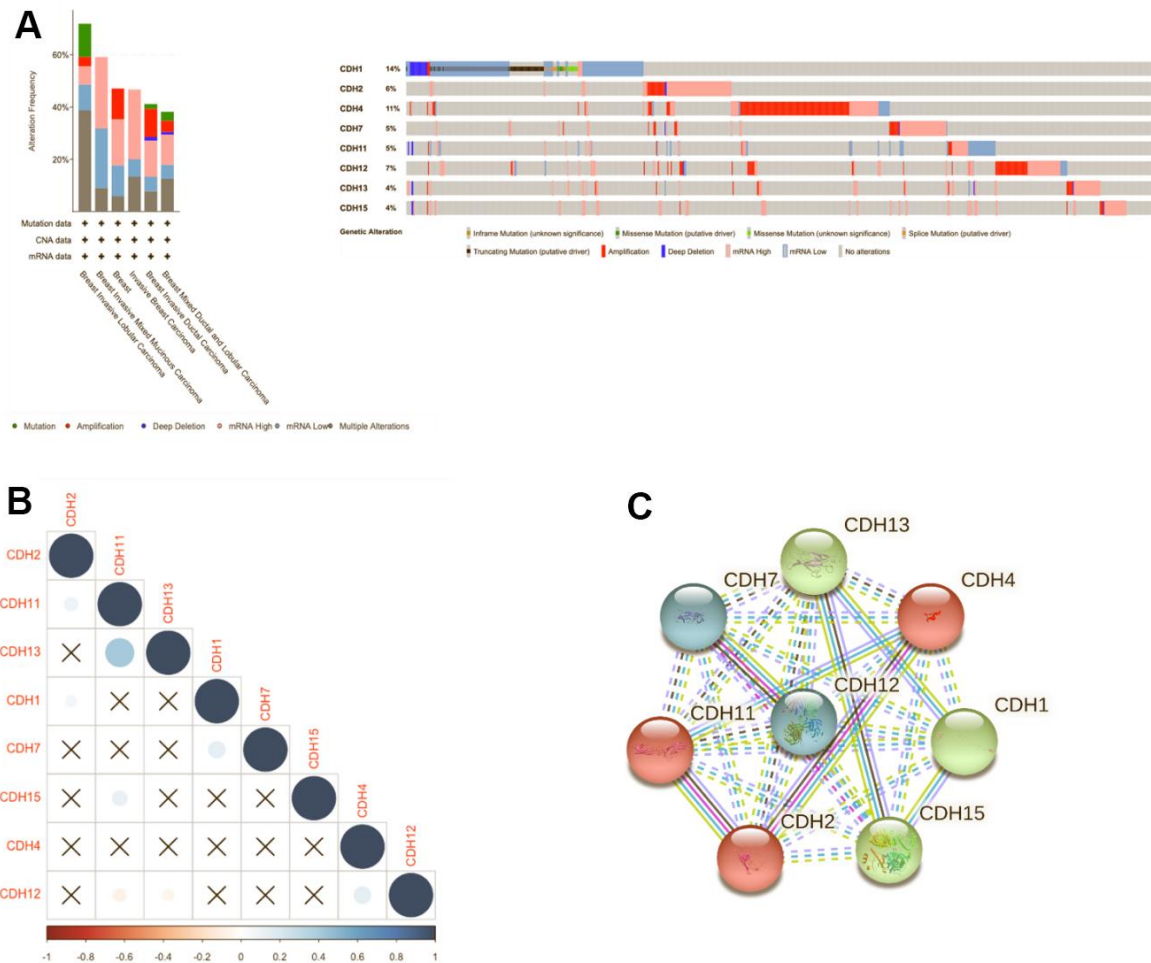


**Figure 7. Genomic alterations of differentially expressed cadherin 1 (*CDH1*)/2/4/7/11/12/13/15 genes in breast cancer. (A)** The cBioPortal database was used to reveal levels of gene amplification, deep deletions, and associated nucleotide substitutions of the *CDH1/2/4/7/11/12/13/15* genes in breast cancer progression in the METABRIC dataset. **(B)** Correlation plot of the *CDH1/2/4/7/11/12/13/15* genes in breast cancer (cBioPortal) database. Insignificant correlation values were displayed by crosses;  $p < 0.01$  was considered statistically significant. **(C)** Protein-protein interactions (PPIs) of *CDH1/2/4/7/11/12/13/15* (STRING database). Highly interacting proteins were represented as hub protein nodes in the PPI network.

## DNA methylation analysis of *CDH1/2/4/11/12/13* in breast cancer

We present a heatmap of DNA methylated locations of *CDH1/2/4/11/12/13* in breast cancer in Supplementary Figure 3 in “Supplementary Materials”. In total, 18 methylated CpG sites were determined for *CDH1*, with six CpG sites presenting high expressions. Among them, cg26508465 and cg09220040 showed the highest levels of DNA methylation. In total, 20 methylated CpG sites of *CDH2* were determined with six CpG sites presenting high expressions. Among them, cg24776465 showed the highest level of DNA methylation. In total, there were 26 methylated CpG sites of *CDH11*, with 19 CpG sites presenting high expressions. Among them, cg02724025 showed the highest level of DNA methylation. Over half of the CpG sites of *CDH11* presented high levels of methylation and relevance to breast cancer. These results provide a potential mechanism by which *CDH11* can serve as an oncogene for breast cancer.

## Regulated networks of *CDH1/2/4/7/11/12/13/15* in breast cancer

To understand how DEG lists are linked to downstream CDH-regulated networks in various biological pathways and diseases, an enrichment analysis was performed using MetaCore software. After uploading genes coexpressed with *CDH1* from Metabric and TCGA databases into MetaCore, we found that numerous pathways and networks were related to cell cycle (Figure 8 and Supplementary Table 2 in Supplementary Materials) including “Immune response\_B cell antigen receptor (BCR) pathway”, “Oxidative stress ROS-induced cellular signaling”, “Development\_negative regulation of WNT/Beta-catenin signaling in the cytoplasm”, and “Immune response\_IFN-alpha/beta signaling via PI3K and NF-κB pathways”.

Similar pathway analyses of *CDH2*, *CDH4*, *CDH7*, *CDH11*, *CDH12*, *CDH13*, and *CDH15* are displayed in “Supplementary Materials” (Supplementary Figures 4–9 and Supplementary Tables 3–9). Genes coexpressed with *CDH2* were correlated with “Cell adhesion\_ECM remodeling” and “Cytoskeleton remodeling\_Regulation of actin cytoskeleton organization by the kinase effectors of Rho GTPases” (Supplementary Figure 4). Genes coexpressed with *CDH4* were correlated with “Protein folding and maturation POMC processing”, “Beta-catenin-dependent transcription regulation in colorectal cancer”, and “Cell adhesion\_ECM remodeling” (Supplementary Figure 5). Genes coexpressed with *CDH7* were correlated with “Cell cycle\_Chromosome condensation in prometaphase” and “Cell cycle\_the metaphase checkpoint” (Supplementary Figure 6).

Genes coexpressed with *CDH11* were correlated with “Cell adhesion\_ECM remodeling”, “IL-1 beta-and endothelin-1-included fibroblast/myofibroblast migration and extracellular matrix production in asthmatic airways”, and “Development regulation of epithelial to mesenchymal transition (EMT)” (Supplementary Figure 7). Genes coexpressed with *CDH12* were correlated with “Cytoskeleton remodeling\_Regulation of actin cytoskeleton organization by the kinase effectors of Rho GTPases” and “Development negative regulation of WNT/Beta catenin signaling in the cytoplasm”. Genes coexpressed with *CDH13* were correlated with “Development\_Regulation of epithelial-to-mesenchymal transition (EMT)”, “Role of stellate cells in progression of pancreatic cancer”, and “Cell adhesion ECM remodeling” (Supplementary Figure 8). Genes coexpressed with *CDH15* were correlated with “Transcription\_HIF-1 targets”, “Oxidative stress\_ROS-induced cellular signaling”, and “Development\_negative regulation of WNT/Beta catenin signaling in the cytoplasm”. In summary, genes coexpressed with *CDH11* and *CDH13* were both correlated with regulation of the EMT, while genes coexpressed with *CDH2*, *CDH4*, *CDH11*, and *CDH13* were all correlated with cell adhesion.

## Comprehensive results of *CDH1/2/4/11/12/13* in the functional enrichment analysis

### Gene ontology (GO) enrichment analysis

For comprehensive analysis, we obtained data from the METABRIC and TCGA datasets to acquire GO enrichment results including BPs, CCs, MFs, and KEGG (Supplementary Figures 9A–14A in Supplementary Materials). The BP analysis demonstrated that *CDH1* was correlated with T-cell activation; the CC analysis showed correlations with cell-cell junctions and vacuolar membranes; MFs revealed significant relationships with phospholipid binding and actin binding, while KEGG ontology indicated the role of the mitogen-activated protein kinase (MAPK) signaling pathway and cytokine-cytokine receptor interactions (Supplementary Figure 9A). For *CDH2*, BPs demonstrated correlations with positive regulation of catabolic processes; the CC analysis showed correlations with mitochondrial matrix and cell-cell junctions; MFs revealed significant relationships with actin binding and protein serine/threonine kinase activity, while KEGG ontology indicated the role of the phosphatidylinositol 3-kinase (PI3K)-Akt signaling pathway (Supplementary Figure 10A). For *CDH4*, BPs demonstrated correlations with proteasomal protein catabolic process; the CC analysis showed correlations with the mitochondrial inner membrane and mitochondrial matrix; MFs revealed significant relationships with actin binding and ion channel activity, while KEGG ontology indicated the

role of pathways of multiple neurodegenerative diseases (Supplementary Figure 11A). For *CDH11*, BPs demonstrated correlations with non-coding (nc)RNA metabolic processes; the CC analysis showed correlations with the mitochondrial inner membrane and mitochondrial matrix; MFs revealed significant relationships with transcription coregulator activity and actin binding, while KEGG ontology indicated the role of pathways of multiple neurodegenerative diseases (Supplementary Figure 12A). For *CDH12*, BPs demonstrated correlations with positive regulation of catabolic processes; the CC analysis showed correlations with cell-cell junctions and the mitochondrial matrix; MFs revealed significant relationships with phospholipid binding and actin binding, while KEGG ontology

indicated the role of pathways of multiple neurodegenerative diseases (Supplementary Figure 13A). For *CDH13*, BPs demonstrated correlations with positive regulation of catabolic processes; the CC analysis showed correlations with cell-cell junctions and the mitochondrial matrix; MFs revealed significant relationships with transcription coregulator activity, while KEGG ontology indicated the role of neuroactive ligand-receptor interactions (Supplementary Figure 14A).

**High expression levels of *CDH2/4/11/12* were related to the epithelial-mesenchymal transition (EMT) in the GSEA analysis**

GSEA results indicated that the Hallmark pathway analysis of *CDH1* was significantly associated with

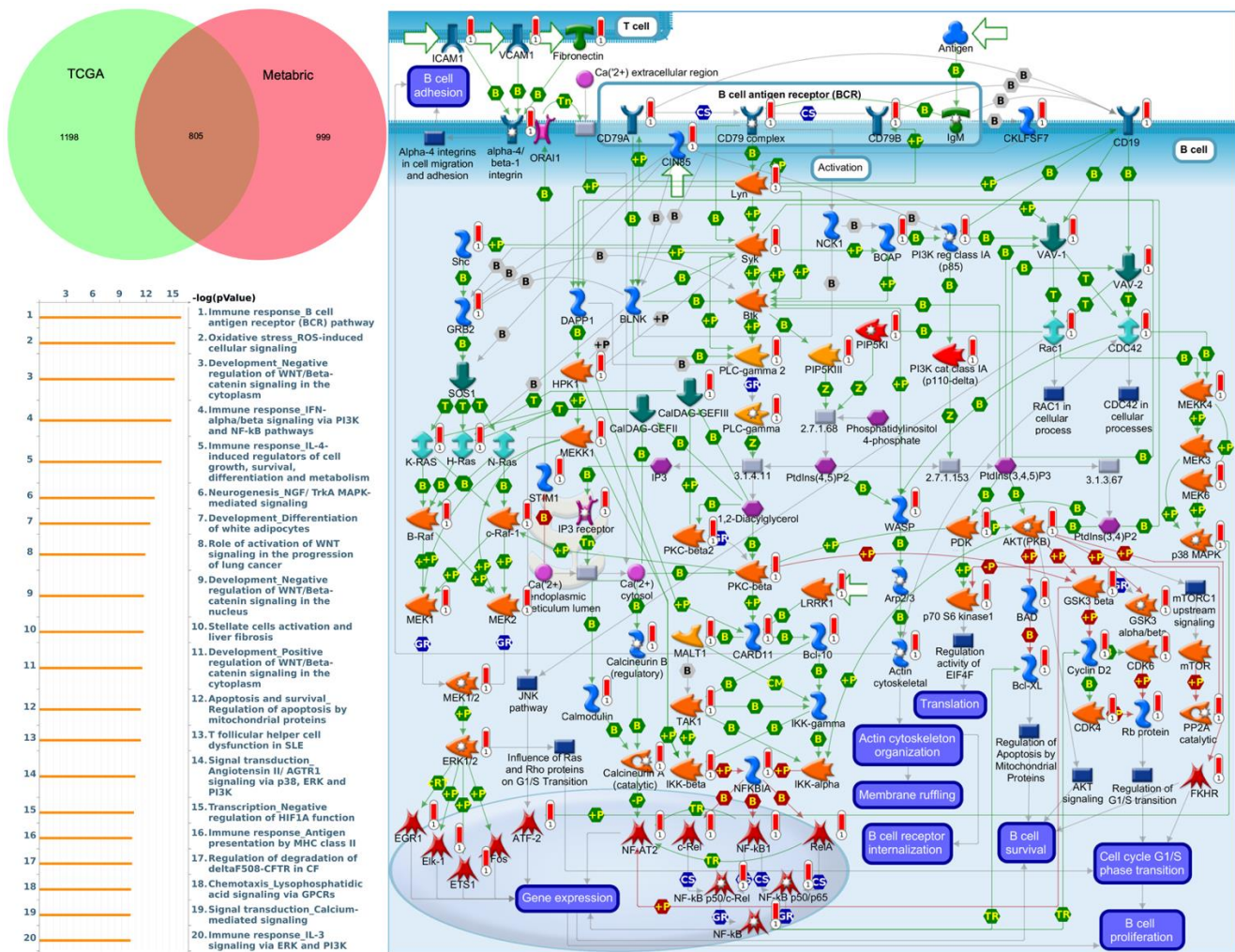


**Figure 8. MetaCore enrichment pathway analysis of genes coexpressed with cadherin 1 (*CDH1*).** The top 10% of expressed genes coexpressed with *CDH1* from both Metabric (1804 genes) and TCGA (2003 genes) were extracted. Overlapping (805) genes were integrated to implement a pathway analysis, which formed a pathway list ordered by the  $-\log p$  value. “Immune response B cell antigen receptor (BCR) pathway” was at the top of the pathway list when performing the “biological process” analysis. The figure demonstrates interactions between genes and proteins. Symbols represent proteins. Arrows depict protein interactions (green, activation; red, inhibition). Thermometer-like histograms indicate microarray gene expressions (blue, downregulated; red, upregulated).

protein secretion, estrogen response\_early, and mammalian target of rapamycin C1 (mTORC1) signaling (Supplementary Figure 9B in Supplementary Materials). Yet the EMT revealed negative correlations with *CDH1*. The Hallmark pathway analysis of *CDH2* revealed that it was significantly associated with the EMT, mTORC1 signaling, the G<sub>2</sub>M checkpoint, and E2F targets (Supplementary Figure 10B). The Hallmark pathway analysis of *CDH4* showed that it was significantly associated with the EMT, myogenesis, and apical junctions (Supplementary Figure 11B). The Hallmark pathway analysis of *CDH11* indicated that it was significantly associated with the EMT, UV response\_DN, coagulation, and angiogenesis (Supplementary Figure 12B). The Hallmark pathway analysis of *CDH12* revealed that it was significantly associated with the EMT, tumor necrosis factor (TNF)- $\alpha$  signaling via nuclear factor (NF)- $\kappa$ B, and UV response\_DN (Supplementary Figure 13B). The Hallmark pathway analysis of *CDH13* showed that it was significantly associated with UV response\_DN, DNA repair, adipogenesis, and IL-2-signal transduction and activator of transcription 5 (STAT5) signaling (Supplementary Figure 14B). *CDH2/4/11/12* were all associated with EMT signaling in the GSEA and were seen to be important inflammation- and immune-related gene sets and cancer-related gene sets in tumor metastasis.

#### **Micro-(mi)RNA-regulated network analysis of *CDH1/2/4/11/12/13***

We used the miRWalk database to identify associations with *CDH1/2/4/11/12/13*, and network regulation was analyzed by an IPA. Analysis of miRNA-regulated networks with *CDHs* (Supplementary Figure 15) indicated that hsa-miR-219a-2-3p regulated *CDH1* and was thus associated with breast cancer development; hsa-miR-330-3p, has-miR-4429, and hsa-miR-199a-5p regulated *CDH2*; hsa-miR-4644, hsa-miR-211-5p, hsa-miR-520f-3p, hsa-miR-34e-5p, and hsa-miR-34a-5p regulated *CDH4*; hsa-miR-486-5p, hsa-miR-200c-3p, hsa-miR-200b-3p, hsa-miR-26a-5p, hsa-miR-140-5p, hsa-miR-128-3p, and hsa-miR-19a-3p regulated *CDH11*; and hsa-miR-30c-5p regulated *CDH13*. In a previous study, the miRNA hsa-miR-200 family was identified as being a definitive factor of the epithelial phenotype of malignant cells, which targeted the E-cadherin repressors, zinc finger E-box-binding homeobox 1 (ZEB1) and ZEB2 [88–90]. Meanwhile, hsa-miR-200 was identified as a repressor of the EMT and was downregulated in more-aggressive molecular subtypes of breast tumors such as HER2 and triple-negative [91]. Our results of miRNA-regulated networks that hsa-miR-200c-3p and hsa-miR-200b-3p regulated *CDH11* were consistent with previous studies.

#### **Levels of immune infiltration in breast cancer were related to *CDH1/2/4/7/11/12/13/15* Expressions**

The TIMER database was utilized to investigate the immunological microenvironment. We identified correlations of immune infiltration levels with expressions of *CDH* gene family members in breast cancer (Figure 9). Results of the analysis showed significant correlations of *CDH1* with cluster of differentiation 4-positive (CD4<sup>+</sup>) T cells; *CDH2* with CD4<sup>+</sup> T cells, macrophages, neutrophils, and dendritic cells (DCs); *CDH4* with CD8<sup>+</sup> T cells, CD4<sup>+</sup> T cells, macrophages, neutrophils, and DCs; *CDH7* with CD8<sup>+</sup> T cells; *CDH11* with CD8<sup>+</sup> T cells, CD4<sup>+</sup> T cells, macrophages, neutrophils, and DCs; *CDH12* with B cells and DCs; *CDH13* with CD8<sup>+</sup> T cells, CD4<sup>+</sup> T cells, macrophages, neutrophils, and DCs; and *CDH15* with CD8<sup>+</sup> T cells.

#### **Drug target network analysis of *CDH1/2/4/11/12/13***

After comprehensive research on *CDH* family members, we were curious about drug targets and related mechanisms of drug resistance. Hence, drug target networks of *CDH1/2/4/11/12/13* were analyzed by the MetaCore and MetaDrug system (Supplementary Figure 16 in Supplementary Materials). We found that “Signal transduction\_c-myc, CREB1 signaling” was the top drug target of *CDH1*; “Cell adhesion\_Fibrinogen, collagen signaling” was the top drug target of *CDH2*; “Metabolism\_PPAR, RXR, VDR regulation of metabolism” was the top drug target of *CDH4*; “Cell adhesion\_Fibrinogen, collagen signaling” was the top drug target of *CDH11*; “Transport\_Potassium transport (core work 1)” was the top drug target of *CDH12*; and “Cell adhesion\_Intergrin signaling” was the top drug target of *CDH13*.

## **DISCUSSION**

In previous studies, the *CDH* family was proven to be associated with invasiveness and metastasis [92–95]. The cadherin family as transmembrane glycoproteins mediate calcium-dependent cell-cell adhesion and regulates cell growth and differentiation. In the process of cell adhesion, cadherins act as essential factors to maintain stable homeostasis of tissue structures [96–98]. Once cell-cell adhesion is disturbed, adhesion-related pathways are subsequently interfered with. Disruption of cadherin signaling has determining influence on tumor progression and tumor immune responses [99–104].

In the present study, to determine whether *CDH* family members can serve as suitable biomarkers for breast cancer and pathways related to the EMT and metastasi



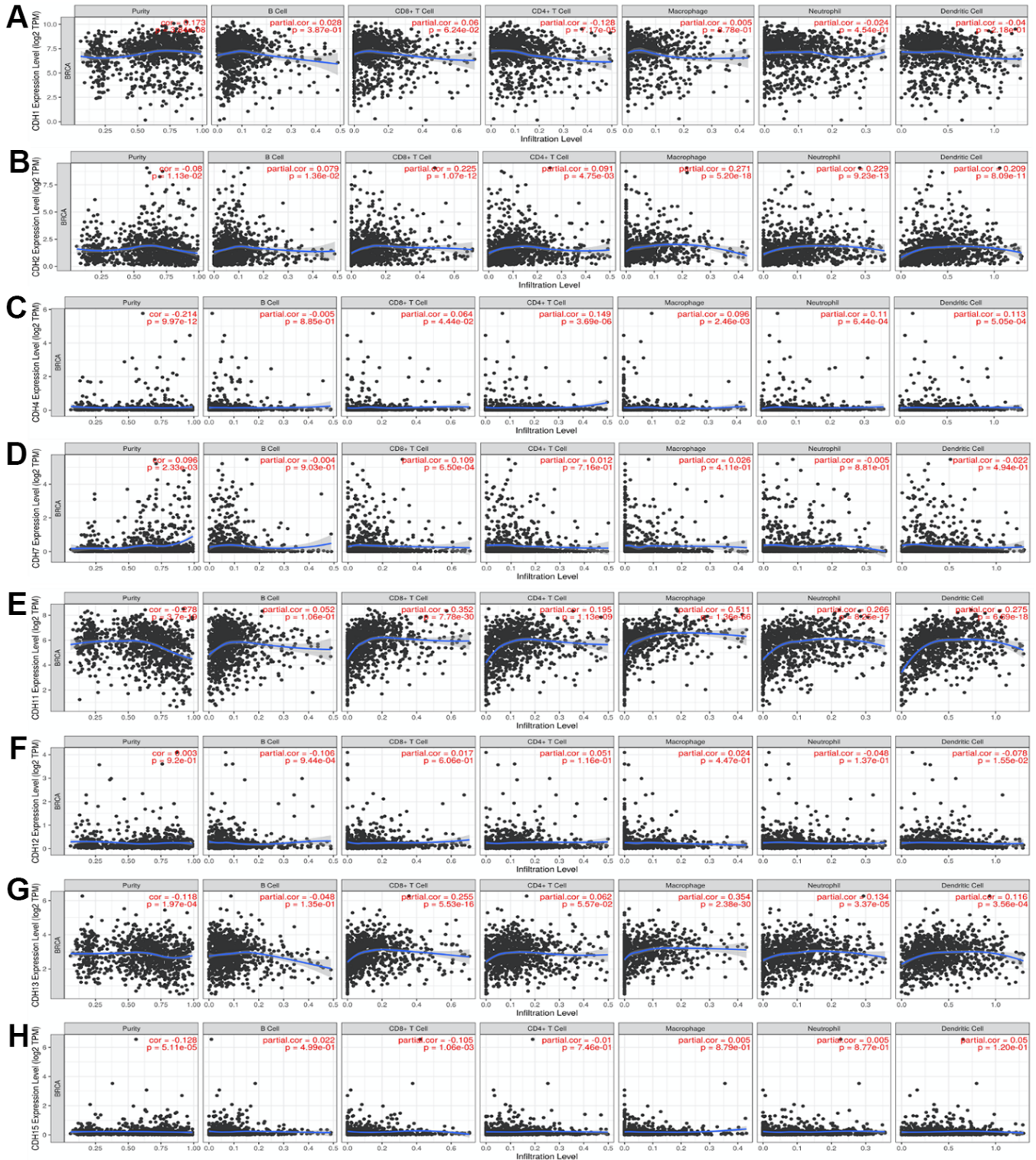


**Figure 9.** (A–H) Correlations between differentially expressed cadherin 1 (CDH1)/2/4/7/11/12/13/15 genes and immune cell infiltration in breast cancer. The figure showed that CDH1 (A); CDH2 (B); CDH4 (C); CDH7 (D); CDH11 (E); CDH12 (F); CDH13 (G); CDH15 (H) gene expressions were associated with tumor purity and tumor-infiltrating immune cell markers, such as cluster of differentiation 8-positive (CD8<sup>+</sup>) T cells, B cells, CD4<sup>+</sup> T cells, neutrophils, macrophages, and dendritic cells. Spearman correlations were applied to describe correlations between the CDH1/2/4/7/11/12/13/15 genes and the abovementioned immune cells ( $p < 0.05$  was accepted as statistically significant).

comprehensive integrative data mining was utilized, including gene expressions, survival analyses, clinical and pathological factors, immune infiltration, and enrichment pathway analyses. In the OncoPrint, TIMER, and prognostic analyses, significantly high expression levels of *CDH1/2/4/7/11/12/13/15* were observed in breast cancer compared to normal tissue samples, and these were associated with poor DMFS outcomes. These results were confirmed by IHC staining in which *CDH1*, *CDH2*, and *CDH12* exhibited strong intensities. Furthermore, results of the bc-GenExMiner database demonstrated that increased *CDH4/12/13* expressions were associated with basal-like breast cancer, and increased *CDH1/2/11* expressions suggested a high SBR grade status in patients. Genetic mutations of *CDH1* and *CDH4* at frequencies of >10% showed higher possibilities of altering cell signaling pathways and promoting proliferation in malignancies. *CDH2*, *CDH4*, and *CDH11* had close relationships via the PPI network, and this was further confirmed by the MetaCore enrichment pathway analysis. These three *CDH* family genes, *CDH2*, *CDH4* and *CDH11*, and genes coexpressed with *CDH13* were correlated with the “Cell adhesion\_ECM remodeling” process. *CDH11* and *CDH13* were also found to be closely related to *CDH1* due to its roles in regulating of the EMT. The enrichment pathway results suggested that in addition to *CDH1*, genes coexpressed with *CDH11* and *CDH13* were also correlated with “Development\_Regulation of the epithelial-to-mesenchymal transition (EMT)”. These correlations of *CDH* family genes could lead to a better understanding of breast cancer development and metastasis.

The ability to infiltrate different tissues is a critical step in cancer because it defines the metastatic potential of tumor cells [105–108]. This capacity can be achieved by the EMT [109–111]. Previous studies reported that the EMT is featured by the loss of *CDH1* expression and the concomitant upregulation or de novo expression of *CDH2*, the so-called “cadherin switch”, which is associated with increased migration and invasiveness and thus poor prognoses [112–115]. The EMT causes disorganization of cell-cell adhesive junctions, thereby facilitating cancer metastasis. Irrespective of *CDH1* expression, the migratory and invasive capacities are present in tumor cells by *CDH2* expression. Therefore, *CDH2* seems to be the key factor in epithelial cancer metastasis and disease progression. Those studies demonstrated the key roles of *CDH2* in cancer metastasis, corresponding to our results with poor survival prognoses, strong intensities in pathological samples, and advanced SBR grading, indicating poor cell differentiation. Furthermore, we found that *CDH2/4/11* had similar signaling pathways with cell adhesion, which was further correlated with the EMT. In other words,

high expression levels of *CDH2/4/11* are crucial for the EMT and cancer metastasis. To validate our results of positive correlations between *CDH* genes and the EMT, Pearson’s correlations were utilized to calculate correlations between *CDH1/2/4/7/11/12/13/15* and EMT-regulated genes such as *TWIST* and *SNAI1* based on mRNA expression levels (Supplementary Figure 17 in Supplementary Materials). Other EMT-core genes associated with cell adhesion and migration were obtained from a previous study [116]. *CDH11* displayed the greatest correlations with *COL3A1*, *COL1A1*, *COL5A1*, and *ADAM12* with Spearman’s rank correlation coefficients of >0.5 among these eight genes. *CDH13* showed mild positive correlations with *COL3A1*, *COL1A1*, *COL5A1*, *ADAM12*, *SNAI2*, *COL6A1*, and *TWIST2*. Conversely, traditional EMT markers, *CDH1* and *CDH2*, demonstrated nearly no correlations with these common EMT-regulated genes. *CDH1* only showed mild negative correlations with *TWIST2* and *SNAI3*. Other genes otherwise showed relatively no correlations with EMT-core genes. It was interesting to discover that *CDH11/13* demonstrated greater correlations with EMT-core genes rather than the traditional EMT-related cadherins, E-cadherin and N-cadherin, as mentioned in previous research [117, 118]. Our results supported the roles of *CDH11* in inducing the EMT, which corresponded to other research not only in cancer [119] but in other diseases including melasma [120] and pulmonary fibrosis [121].

To understand drug targets of *CDH* family genes, we implemented a drug target network analysis (Supplementary Figure 16). Since drug target network analyses of the *CDH2*, *CDH11*, and *CDH13* genes were all targeted to cell adhesion, we thus discussed the roles of cell adhesion in drug resistance. Cancer cells attaching to microenvironment components such as collagen type 1 (COL1) weakens the sensitivity of chemotherapeutic drugs like mitoxantrone, which is called cell adhesion-mediated drug resistance (CAM-DR) [122]. In consideration of the extensive presence of COL1 in mammary glands, breast cancer appears to have a high probability of presenting CAM-DR. The importance of COL1 is proven that patients with high-density breast tissues have higher risks of breast cancer [123–125] and poorer outcomes due to metastatic processes [126]. Regarding CAM-DR, the EMT plays a crucial part in drug resistance to breast cancer as well. The epithelial cell adhesion molecule (EPCAM) was implicated in tumor progression and drug resistance in breast cancer [127]. It was proven that EPCAM-knockdown resulted in upregulation of *CDH1* and attenuation of *CDH2* expression, which reversed the EMT. This process demonstrated that the EPCAM might possess the capability to induce the EMT in breast cancer to promote multidrug resistance. In addition,

transcriptional silencing of *CDH1* was associated with the EMT in human breast cancer cells [128]. Previous research demonstrated that upregulation of E-cadherin by miR-200b and miR-200c via direct targeting the transcriptional repressors of E-cadherin, ZEB1 and ZEB2, inhibited the EMT [129]. In summary, *CDH1/2/11/13* were associated with the cell adhesion network on drug targets and were thus associated with important factors in drug resistance.

*CDH4* hypermethylation was significantly associated with increased risks for breast cancer in peripheral blood leukocyte DNA [130]. *CDH11* was also known as one of the mediators that interacted with malignant cells and normal cells and was detected in various cancers, especially in metastatic cancer cell lines [131–133]. In particular, *CDH11* was involved in the maintenance of high endogenous Rac activity and cytoskeletal reorganization in migratory breast cancer cells [134]. Moreover, because of the role of *CDH11* as an inducer of metastatic signaling, targeting *CDH11* triggered re-expression of the miR-335 tumor suppressor, which limited the *CDH11*-induced EMT. This phenomenon repressed cancer stem cell activities. *CDH11*-related pathways demonstrated the miR-335-mediated therapeutic value of anti-*CDH11* antibody treatment and provided a therapeutic option in patients with metastatic breast cancer. Downregulation of *CDH12* could inhibit the process of angiogenesis. Previous research implied that *CDH12* might be influential in colorectal tumor metastasis [135]. *CDH13* expression exhibited functions in cell adhesion and migration which were promoted by DNA polymerase beta (Pol  $\beta$ ) by augmenting DNA demethylation of the *CDH13* promoter [136]. Abnormal methylation of *CDH13* promoter was observed in breast, colorectal, cervical and lung cancers, and chronic myeloid leukemia [137–139]. Those studies supported our results of the importance of *CDH4/11/12/13* in tumorigenesis. We supposed that high mRNA expression levels of *CDH4/11/12/13* were associated with breast cancer and poor survival.

As the tumor microenvironment plays important roles in tumorigenesis, we conducted an immune infiltration analysis in Figure 9. Previous studies also supported the associations between cadherin and immune pathways [140–142]. One of the most important pathways related to cadherin in immune responses is the Wnt pathway, which regulates cellular signaling by a canonical pathway with  $\beta$ -catenin [143].  $\beta$ -Catenin plays a fundamental role in the cadherin protein complex, whose stabilization is crucial to activate the Wnt/ $\beta$ -catenin pathway. The WNT/ $\beta$ -catenin pathway mediates the self-renewal and relocation of cancer stem cells, promoting malignant progression and metastasis in

breast cancer [144]. Our results of the enrichment pathway analysis were consistent with the importance of Wnt/ $\beta$ -catenin in breast cancer. Genes co-expressed with *CDH1/12/15* were correlated with the pathway of “Development negative regulation of WNT/Beta catenin signaling in the cytoplasm”. Induction of Wnt/ $\beta$ -catenin signaling was crucial in maintenance of stemness of memory CD8<sup>+</sup> T cells by blocking T-cell differentiation [145]. Clinical responses to immune checkpoint inhibitors were correlated with tumors in the immune cell microenvironment [146, 147]. The Wnt/ $\beta$ -catenin pathway is considered to be a potential target for cancer treatment. In pancreatic cancer, effective immunotherapy is likely to require upregulation of *CDH1* expression [148]. The roles of cadherin and Wnt/ $\beta$ -catenin signaling in regulating immune cell infiltrations of the tumor microenvironment aroused interest in immunotherapy treatment.

This study performed a comprehensive and systematic review of the genetic expressions, prognostic values, mutation levels, immune infiltration, and enrichment pathways of the CDH family. *CDH1/2/4/11/12/13* expressions are significantly increased in breast cancer and are associated with poor clinical prognoses of DMFS. We concluded that *CDH1/2/4/11/12/13* may be crucial for breast cancer tumorigenesis, providing novel insights into developing detection biomarkers or targeted therapies for breast cancer. Nevertheless, evidence from clinical applications such as *in vitro* data or large patient cohorts should be produced to validate associations between *CDH1/2/4/11/12/13* and breast cancer.

## CONCLUSIONS

*CDH1/2/4/11/12/13* were overexpressed in breast cancer and were associated with poor prognoses in the distant metastasis-free survival analysis. Genes coexpressed with these *CDH* family members were correlated with regulation of the EMT and cell adhesion ECM remodeling, which were validated as playing critical roles in tumor metastasis. Although further evidence of clinical correlations for validation in the future should be determined to support our hypothesis, *CDH1/2/4/11/12/13* are expected to be potential biomarkers for breast cancer progression and metastasis.

## AUTHOR CONTRIBUTIONS

S.C.K., H.L.L., W.J.W., and C.Y.W. conceived the project and performed the bioinformatics analysis. S.C.K., H.L.L., C.Y.S., I.J.Y., M.C.Y., and wrote the manuscript. G.A., H.D.K.T., C.C.C., D.T.M.X., and F.B.P. performed the data analysis. W.J.W. and C.Y.W.

were responsible for manuscript editing and revised the manuscript. All authors have read and agreed to the published version of the manuscript.

## ACKNOWLEDGMENTS

The authors acknowledge the statistical/computational/technical support of the Clinical Data Center, Office of Data Science, Taipei Medical University, Taipei, Taiwan. The authors also give special thanks to Daniel P. Chamberlin for his professional English editing from the Office of Research and Development at Taipei Medical University.

## CONFLICTS OF INTEREST

The authors declare that no conflicts of interest exist.

## FUNDING

This research was supported by grants from the Ministry of Science and Technology (MOST) of Taiwan (MOST-110-2320-B-039-068 to W-J.W. and 109-2320-B-038-009-MY2 to C-Y.W.), China Medical University (CMU110-MF-47 to W-J.W.), Taipei Medical University (TMU-108-AE1-B16), Taipei Medical University Hospital (111TMU-TMUH-08), and this work was financially supported by the “TMU Research Center of Cancer Translational Medicine” from The Featured Areas Research Center Program within the framework of the Higher Education Sprout Project by the Ministry of Education (MOE) in Taiwan.

## REFERENCES

1. Gulmez A. Breast cancer after multiple myeloma treatment. *Curr Probl Cancer*. 2019; 43:100463. <https://doi.org/10.1016/j.currproblcancer.2019.01.004> PMID:[30738577](https://pubmed.ncbi.nlm.nih.gov/30738577/)
2. Bray F, Ferlay J, Soerjomataram I, Siegel RL, Torre LA, Jemal A. Global cancer statistics 2018: GLOBOCAN estimates of incidence and mortality worldwide for 36 cancers in 185 countries. *CA Cancer J Clin*. 2018; 68:394–424. <https://doi.org/10.3322/caac.21492> PMID:[30207593](https://pubmed.ncbi.nlm.nih.gov/30207593/)
3. Falzone L, Grimaldi M, Celentano E, Augustin LS, Libra M. Identification of Modulated MicroRNAs Associated with Breast Cancer, Diet, and Physical Activity. *Cancers (Basel)*. 2020; 12:2555. <https://doi.org/10.3390/cancers12092555> PMID:[32911851](https://pubmed.ncbi.nlm.nih.gov/32911851/)
4. Wu M, Li Q, Wang H. Identification of Novel Biomarkers Associated With the Prognosis and Potential Pathogenesis of Breast Cancer via Integrated Bioinformatics Analysis. *Technol Cancer Res Treat*. 2021. <https://doi.org/10.1177/1533033821992081> PMID:[33550915](https://pubmed.ncbi.nlm.nih.gov/33550915/)
5. Pan Y, Liu G, Yuan Y, Zhao J, Yang Y, Li Y. Analysis of differential gene expression profile identifies novel biomarkers for breast cancer. *Oncotarget*. 2017; 8:114613–25. <https://doi.org/10.18632/oncotarget.23061> PMID:[29383106](https://pubmed.ncbi.nlm.nih.gov/29383106/)
6. Li CJ, Chen HM, Lai JC. Diagnostic, Prognostic, and Predictive Biomarkers in Breast Cancer. *J Oncol*. 2020; 2020:1835691. <https://doi.org/10.1155/2020/1835691> PMID:[32256579](https://pubmed.ncbi.nlm.nih.gov/32256579/)
7. Paul A, Paul S. The breast cancer susceptibility genes (BRCA) in breast and ovarian cancers. *Front Biosci (Landmark Ed)*. 2014; 19:605–18. <https://doi.org/10.2741/4230> PMID:[24389207](https://pubmed.ncbi.nlm.nih.gov/24389207/)
8. van de Vijver MJ, He YD, van't Veer LJ, Dai H, Hart AA, Voskuil DW, Schreiber GJ, Peterse JL, Roberts C, Marton MJ, Parrish M, Atsma D, Witteveen A, et al. A gene-expression signature as a predictor of survival in breast cancer. *N Engl J Med*. 2002; 347:1999–2009. <https://doi.org/10.1056/NEJMoa021967> PMID:[12490681](https://pubmed.ncbi.nlm.nih.gov/12490681/)
9. Sultan G, Zubair S, Tayubi IA, Dahms HU, Madar IH. Towards the early detection of ductal carcinoma (a common type of breast cancer) using biomarkers linked to the PPAR( $\gamma$ ) signaling pathway. *Bioinformation*. 2019; 15:799–805. <https://doi.org/10.6026/97320630015799> PMID:[31902979](https://pubmed.ncbi.nlm.nih.gov/31902979/)
10. Fahad Ullah M. Breast Cancer: Current Perspectives on the Disease Status. *Adv Exp Med Biol*. 2019; 1152:51–64. [https://doi.org/10.1007/978-3-030-20301-6\\_4](https://doi.org/10.1007/978-3-030-20301-6_4) PMID:[31456179](https://pubmed.ncbi.nlm.nih.gov/31456179/)
11. Sever R, Brugge JS. Signal transduction in cancer. *Cold Spring Harb Perspect Med*. 2015; 5:a006098. <https://doi.org/10.1101/cshperspect.a006098> PMID:[25833940](https://pubmed.ncbi.nlm.nih.gov/25833940/)
12. Chakravarthi BV, Nepal S, Varambally S. Genomic and Epigenomic Alterations in Cancer. *Am J Pathol*. 2016; 186:1724–35. <https://doi.org/10.1016/j.ajpath.2016.02.023> PMID:[27338107](https://pubmed.ncbi.nlm.nih.gov/27338107/)
13. Herceg Z, Hainaut P. Genetic and epigenetic alterations as biomarkers for cancer detection, diagnosis and prognosis. *Mol Oncol*. 2007; 1:26–41. <https://doi.org/10.1016/j.molonc.2007.01.004> PMID:[19383285](https://pubmed.ncbi.nlm.nih.gov/19383285/)

14. Kaszak I, Witkowska-Piłaszewicz O, Niewiadomska Z, Dworecka-Kaszak B, Ngosa Toka F, Jurka P. Role of Cadherins in Cancer-A Review. *Int J Mol Sci.* 2020; 21:7624.  
<https://doi.org/10.3390/ijms21207624>  
PMID:[33076339](https://pubmed.ncbi.nlm.nih.gov/33076339/)
15. de Agustín-Durán D, Mateos-White I, Fabra-Beser J, Gil-Sanz C. Stick around: Cell-Cell Adhesion Molecules during Neocortical Development. *Cells.* 2021; 10:118.  
<https://doi.org/10.3390/cells10010118>  
PMID:[33435191](https://pubmed.ncbi.nlm.nih.gov/33435191/)
16. Stelzer G, Rosen N, Plaschkes I, Zimmerman S, Twik M, Fishilevich S, Stein TI, Nudel R, Lieder I, Mazor Y, Kaplan S, Dahary D, Warshawsky D, et al. The GeneCards Suite: From Gene Data Mining to Disease Genome Sequence Analyses. *Curr Protoc Bioinformatics.* 2016; 54:1.30.  
<https://doi.org/10.1002/cpbi.5> PMID:[27322403](https://pubmed.ncbi.nlm.nih.gov/27322403/)
17. Takeichi M. Cadherin cell adhesion receptors as a morphogenetic regulator. *Science.* 1991; 251:1451–5.  
<https://doi.org/10.1126/science.2006419>  
PMID:[2006419](https://pubmed.ncbi.nlm.nih.gov/2006419/)
18. Yu W, Yang L, Li T, Zhang Y. Cadherin Signaling in Cancer: Its Functions and Role as a Therapeutic Target. *Front Oncol.* 2019; 9:989.  
<https://doi.org/10.3389/fonc.2019.00989>  
PMID:[31637214](https://pubmed.ncbi.nlm.nih.gov/31637214/)
19. Thiery JP. Epithelial-mesenchymal transitions in tumour progression. *Nat Rev Cancer.* 2002; 2:442–54.  
<https://doi.org/10.1038/nrc822> PMID:[12189386](https://pubmed.ncbi.nlm.nih.gov/12189386/)
20. Kalluri R, Neilson EG. Epithelial-mesenchymal transition and its implications for fibrosis. *J Clin Invest.* 2003; 112:1776–84.  
<https://doi.org/10.1172/JCI20530>  
PMID:[14679171](https://pubmed.ncbi.nlm.nih.gov/14679171/)
21. de Vasconcelos Azevedo FVP, Zóia MAP, Lopes DS, Gimenes SN, Vecchi L, Alves PT, Rodrigues RS, Silva ACA, Yoneyama KAG, Goulart LR, de Melo Rodrigues V. Antitumor and antimetastatic effects of PLA<sub>2</sub>-BthTX-II from Bothrops jararacussu venom on human breast cancer cells. *Int J Biol Macromol.* 2019; 135:261–73.  
<https://doi.org/10.1016/j.ijbiomac.2019.05.164>  
PMID:[31128190](https://pubmed.ncbi.nlm.nih.gov/31128190/)
22. Fujii R, Imanishi Y, Shibata K, Sakai N, Sakamoto K, Shigetomi S, Habu N, Otsuka K, Sato Y, Watanabe Y, Ozawa H, Tomita T, Kameyama K, et al. Restoration of E-cadherin expression by selective Cox-2 inhibition and the clinical relevance of the epithelial-to-mesenchymal transition in head and neck squamous cell carcinoma. *J Exp Clin Cancer Res.* 2014; 33:40.  
<https://doi.org/10.1186/1756-9966-33-40>  
PMID:[24887090](https://pubmed.ncbi.nlm.nih.gov/24887090/)
23. Ribatti D, Tamma R, Annese T. Epithelial-Mesenchymal Transition in Cancer: A Historical Overview. *Transl Oncol.* 2020; 13:100773.  
<https://doi.org/10.1016/j.tranon.2020.100773>  
PMID:[32334405](https://pubmed.ncbi.nlm.nih.gov/32334405/)
24. Chu K, Boley KM, Moraes R, Barsky SH, Robertson FM. The paradox of E-cadherin: role in response to hypoxia in the tumor microenvironment and regulation of energy metabolism. *Oncotarget.* 2013; 4:446–62.  
<https://doi.org/10.18632/oncotarget.872>  
PMID:[23530113](https://pubmed.ncbi.nlm.nih.gov/23530113/)
25. Kemler R, Hierholzer A, Kanzler B, Kuppig S, Hansen K, Taketo MM, de Vries WN, Knowles BB, Solter D. Stabilization of beta-catenin in the mouse zygote leads to premature epithelial-mesenchymal transition in the epiblast. *Development.* 2004; 131:5817–24.  
<https://doi.org/10.1242/dev.01458> PMID:[15525667](https://pubmed.ncbi.nlm.nih.gov/15525667/)
26. Klymkowsky MW. beta-catenin and its regulatory network. *Hum Pathol.* 2005; 36:225–7.  
<https://doi.org/10.1016/j.humpath.2005.02.002>  
PMID:[15791565](https://pubmed.ncbi.nlm.nih.gov/15791565/)
27. Thorat MA, Balasubramanian R. Breast cancer prevention in high-risk women. *Best Pract Res Clin Obstet Gynaecol.* 2020; 65:18–31.  
<https://doi.org/10.1016/j.bpobgyn.2019.11.006>  
PMID:[31862315](https://pubmed.ncbi.nlm.nih.gov/31862315/)
28. Lin CY, Lee CH, Chuang YH, Lee JY, Chiu YY, Wu Lee YH, Jong YJ, Hwang JK, Huang SH, Chen LC, Wu CH, Tu SH, Ho YS, Yang JM. Membrane protein-regulated networks across human cancers. *Nat Commun.* 2019; 10:3131.  
<https://doi.org/10.1038/s41467-019-10920-8>  
PMID:[31311925](https://pubmed.ncbi.nlm.nih.gov/31311925/)
29. Tsai HT, Huang CS, Tu CC, Liu CY, Huang CJ, Ho YS, Tu SH, Tseng LM, Huang CC. Multi-gene signature of microcalcification and risk prediction among Taiwanese breast cancer. *Sci Rep.* 2020; 10:18276.  
<https://doi.org/10.1038/s41598-020-74982-1>  
PMID:[33106505](https://pubmed.ncbi.nlm.nih.gov/33106505/)
30. Nguyen HD, Liao YC, Ho YS, Chen LC, Chang HW, Cheng TC, Liu D, Lee WR, Shen SC, Wu CH, Tu SH. The  $\alpha 9$  Nicotinic Acetylcholine Receptor Mediates Nicotine-Induced PD-L1 Expression and Regulates Melanoma Cell Proliferation and Migration. *Cancers (Basel).* 2019; 11:1991.  
<https://doi.org/10.3390/cancers11121991>  
PMID:[31835799](https://pubmed.ncbi.nlm.nih.gov/31835799/)
31. Lee KL, Kuo YC, Ho YS, Huang YH. Triple-Negative Breast Cancer: Current Understanding and Future Therapeutic Breakthrough Targeting Cancer Stemness. *Cancers (Basel).* 2019; 11:1334.  
<https://doi.org/10.3390/cancers11091334>

PMID:[31505803](#)

32. Rhodes DR, Yu J, Shanker K, Deshpande N, Varambally R, Ghosh D, Barrette T, Pandey A, Chinnaiyan AM. ONCOMINE: a cancer microarray database and integrated data-mining platform. *Neoplasia*. 2004; 6:1–6.  
[https://doi.org/10.1016/s1476-5586\(04\)80047-2](https://doi.org/10.1016/s1476-5586(04)80047-2)  
PMID:[15068665](#)
33. Kao TJ, Wu CC, Phan NN, Liu YH, Ta HD, Anuraga G, Wu YF, Lee KH, Chuang JY, Wang CY. Prognoses and genomic analyses of proteasome 26S subunit, ATPase (PSMC) family genes in clinical breast cancer. *Aging (Albany NY)*. 2021; 13:17970.  
<https://doi.org/10.18632/aging.203345>  
PMID:[34329194](#)
34. Wu PS, Yen JH, Wang CY, Chen PY, Hung JH, Wu MJ. 8-Hydroxydaidzein, an Isoflavone from Fermented Soybean, Induces Autophagy, Apoptosis, Differentiation, and Degradation of Oncoprotein BCR-ABL in K562 Cells. *Biomedicines*. 2020; 8:506.  
<https://doi.org/10.3390/biomedicines8110506>  
PMID:[33207739](#)
35. Wu CC, Ekanem TI, Phan NN, Loan DT, Hou SY, Lee KH, Wang CY. Gene signatures and prognostic analyses of the Tob/BTG pituitary tumor-transforming gene (PTTG) family in clinical breast cancer patients. *Int J Med Sci*. 2020; 17:3112–24.  
<https://doi.org/10.7150/ijms.49652> PMID:[33173433](#)
36. Lin YY, Wang CY, Phan NN, Chiao CC, Li CY, Sun Z, Hung JH, Chen YL, Yen MC, Weng TY, Hsu HP, Lai MD. PODXL2 maintains cellular stemness and promotes breast cancer development through the Rac1/Akt pathway. *Int J Med Sci*. 2020; 17:1639–51.  
<https://doi.org/10.7150/ijms.46125>  
PMID:[32669966](#)
37. Hsu HP, Wang CY, Hsieh PY, Fang JH, Chen YL. Knockdown of serine/threonine-protein kinase 24 promotes tumorigenesis and myeloid-derived suppressor cell expansion in an orthotopic immunocompetent gastric cancer animal model. *J Cancer*. 2020; 11:213–28.  
<https://doi.org/10.7150/jca.35821>  
PMID:[31892988](#)
38. Tang Z, Kang B, Li C, Chen T, Zhang Z. GEPIA2: an enhanced web server for large-scale expression profiling and interactive analysis. *Nucleic Acids Res*. 2019; 47:W556–60.  
<https://doi.org/10.1093/nar/gkz430>  
PMID:[31114875](#)
39. Barrett T, Wilhite SE, Ledoux P, Evangelista C, Kim IF, Tomashevsky M, Marshall KA, Phillippy KH, Sherman PM, Holko M, Yefanov A, Lee H, Zhang N, et al. NCBI GEO: archive for functional genomics data sets—update. *Nucleic Acids Res*. 2013; 41:D991–5.  
<https://doi.org/10.1093/nar/gks1193> PMID:[23193258](#)
40. Lin JC, Liu TP, Yang PM. CDKN2A-Inactivated Pancreatic Ductal Adenocarcinoma Exhibits Therapeutic Sensitivity to Paclitaxel: A Bioinformatics Study. *J Clin Med*. 2020; 9:4019.  
<https://doi.org/10.3390/jcm9124019> PMID:[33322698](#)
41. Lin TY, Wang PW, Huang CH, Yang PM, Pan TL. Characterizing the Relapse Potential in Different Luminal Subtypes of Breast Cancers with Functional Proteomics. *Int J Mol Sci*. 2020; 21:6077.  
<https://doi.org/10.3390/ijms21176077>  
PMID:[32846884](#)
42. Liu LW, Hsieh YY, Yang PM. Bioinformatics Data Mining Repurposes the JAK2 (Janus Kinase 2) Inhibitor Fedratinib for Treating Pancreatic Ductal Adenocarcinoma by Reversing the KRAS (Kirsten Rat Sarcoma 2 Viral Oncogene Homolog)-Driven Gene Signature. *J Pers Med*. 2020; 10:130.  
<https://doi.org/10.3390/jpm10030130>  
PMID:[32947833](#)
43. Yang PM, Hsieh YY, Du JL, Yen SC, Hung CF. Sequential Interferon  $\beta$ -Cisplatin Treatment Enhances the Surface Exposure of Calreticulin in Cancer Cells via an Interferon Regulatory Factor 1-Dependent Manner. *Biomolecules*. 2020; 10:643.  
<https://doi.org/10.3390/biom10040643>  
PMID:[32326356](#)
44. Yang PM, Lin LS, Liu TP. Sorafenib Inhibits Ribonucleotide Reductase Regulatory Subunit M2 (RRM2) in Hepatocellular Carcinoma Cells. *Biomolecules*. 2020; 10:117.  
<https://doi.org/10.3390/biom10010117>  
PMID:[31936661](#)
45. Nagy Á, Munkácsy G, Gyórfy B. Pancancer survival analysis of cancer hallmark genes. *Sci Rep*. 2021; 11:6047.  
<https://doi.org/10.1038/s41598-021-84787-5>  
PMID:[33723286](#)
46. Lánckzy A, Nagy Á, Bottai G, Munkácsy G, Szabó A, Santarpia L, Gyórfy B. miRpower: a web-tool to validate survival-associated miRNAs utilizing expression data from 2178 breast cancer patients. *Breast Cancer Res Treat*. 2016; 160:439–46.  
<https://doi.org/10.1007/s10549-016-4013-7>  
PMID:[27744485](#)
47. Gao J, Aksoy BA, Dogrusoz U, Dresdner G, Gross B, Sumer SO, Sun Y, Jacobsen A, Sinha R, Larsson E, Cerami E, Sander C, Schultz N. Integrative analysis of complex cancer genomics and clinical profiles using the cBioPortal. *Sci Signal*. 2013; 6:pl1.

- <https://doi.org/10.1126/scisignal.2004088>  
PMID:23550210
48. Sun CC, Li SJ, Hu W, Zhang J, Zhou Q, Liu C, Li LL, Songyang YY, Zhang F, Chen ZL, Li G, Bi ZY, Bi YY, et al. RETRACTED: Comprehensive Analysis of the Expression and Prognosis for E2Fs in Human Breast Cancer. *Mol Ther*. 2019; 27:1153–65.  
<https://doi.org/10.1016/j.ymthe.2019.03.019>  
PMID:31010740
49. Hagerling C, Owyong M, Sitarama V, Wang CY, Lin C, van den Bijgaart RJ, Koopman CD, Brenot A, Nanjaraj A, Wärnberg F, Jirström K, Klein OD, Werb Z, Plaks V. LGR5 in breast cancer and ductal carcinoma *in situ*: a diagnostic and prognostic biomarker and a therapeutic target. *BMC Cancer*. 2020; 20:542.  
<https://doi.org/10.1186/s12885-020-06986-z>  
PMID:32522170
50. Phan NN, Liu S, Wang CY, Hsu HP, Lai MD, Li CY, Chen CF, Chiao CC, Yen MC, Sun Z, Jiang JZ. Overexpressed gene signature of EPH receptor A/B family in cancer patients-comprehensive analyses from the public high-throughput database. *Int J Clin Exp Pathol*. 2020; 13:1220–42.  
PMID:32509099
51. Uhlén M, Fagerberg L, Hallström BM, Lindskog C, Oksvold P, Mardinoglu A, Sivertsson Å, Kampf C, Sjöstedt E, Asplund A, Olsson I, Edlund K, Lundberg E, et al. Proteomics. Tissue-based map of the human proteome. *Science*. 2015; 347:1260419.  
<https://doi.org/10.1126/science.1260419>  
PMID:25613900
52. Jézéquel P, Gouraud W, Ben Azzouz F, Guérin-Charbonnel C, Juin PP, Lasla H, Campone M. bc-GenExMiner 4.5: new mining module computes breast cancer differential gene expression analyses. *Database (Oxford)*. 2021; 2021:baab007.  
<https://doi.org/10.1093/database/baab007>  
PMID:33599248
53. Barretina J, Caponigro G, Stransky N, Venkatesan K, Margolin AA, Kim S, Wilson CJ, Lehár J, Kryukov GV, Sonkin D, Reddy A, Liu M, Murray L, et al. The Cancer Cell Line Encyclopedia enables predictive modelling of anticancer drug sensitivity. *Nature*. 2012; 483:603–7.  
<https://doi.org/10.1038/nature11003>  
PMID:22460905
54. Lawal B, Liu YL, Mokgautsi N, Khedkar H, Sumitra MR, Wu AT, Huang HS. Pharmacoinformatics and Preclinical Studies of NSC765690 and NSC765599, Potential STAT3/CDK2/4/6 Inhibitors with Antitumor Activities against NCI60 Human Tumor Cell Lines. *Biomedicines*. 2021; 9:92.  
<https://doi.org/10.3390/biomedicines9010092>  
PMID:33477856
55. Lawal B, Lee CY, Mokgautsi N, Sumitra MR, Khedkar H, Wu AT, Huang HS. mTOR/EGFR/iNOS/MAP2K1/FGFR/TGFB1 Are Druggable Candidates for N-(2,4-Difluorophenyl)-2',4'-Difluoro-4-Hydroxybiphenyl-3-Carboxamide (NSC765598), With Consequent Anticancer Implications. *Front Oncol*. 2021; 11:656738.  
<https://doi.org/10.3389/fonc.2021.656738>  
PMID:33842373
56. Lawal B, Kuo YC, Sumitra MR, Wu AT, Huang HS. *In vivo* Pharmacokinetic and Anticancer Studies of HH-N25, a Selective Inhibitor of Topoisomerase I, and Hormonal Signaling for Treating Breast Cancer. *J Inflamm Res*. 2021; 14:4901–13.  
<https://doi.org/10.2147/JIR.S329401> PMID:34588796
57. Lawal B, Kuo YC, Wu AT, Huang HS. BC-N102 suppress breast cancer tumorigenesis by interfering with cell cycle regulatory proteins and hormonal signaling, and induction of time-course arrest of cell cycle at G1/G0 phase. *Int J Biol Sci*. 2021; 17:3224–38.  
<https://doi.org/10.7150/ijbs.62808> PMID:34421361
58. Modhukur V, Iljasenko T, Metsalu T, Lokk K, Laisk-Podar T, Vilo J. MethSurv: a web tool to perform multivariable survival analysis using DNA methylation data. *Epigenomics*. 2018; 10:277–88.  
<https://doi.org/10.2217/epi-2017-0118>  
PMID:29264942
59. Curtis C, Shah SP, Chin SF, Turashvili G, Rueda OM, Dunning MJ, Speed D, Lynch AG, Samarajiwa S, Yuan Y, Gräf S, Ha G, Haffari G, et al, and METABRIC Group. The genomic and transcriptomic architecture of 2,000 breast tumours reveals novel subgroups. *Nature*. 2012; 486:346–52.  
<https://doi.org/10.1038/nature10983>  
PMID:22522925
60. Cancer Genome Atlas Network. Comprehensive molecular portraits of human breast tumours. *Nature*. 2012; 490:61–70.  
<https://doi.org/10.1038/nature11412> PMID:23000897
61. Anuraga G, Wang WJ, Phan NN, An Ton NT, Ta HD, Berenice Prayugo F, Minh Xuan DT, Ku SC, Wu YF, Andriani V, Athoillah M, Lee KH, Wang CY. Potential Prognostic Biomarkers of NIMA (Never in Mitosis, Gene A)-Related Kinase (NEK) Family Members in Breast Cancer. *J Pers Med*. 2021; 11:1089.  
<https://doi.org/10.3390/jpm11111089>  
PMID:34834441
62. Khoa Ta HD, Tang WC, Phan NN, Anuraga G, Hou SY, Chiao CC, Liu YH, Wu YF, Lee KH, Wang CY. Analysis of LAGEs Family Gene Signature and Prognostic Relevance in Breast Cancer. *Diagnostics (Basel)*. 2021; 11:726.  
<https://doi.org/10.3390/diagnostics11040726>

- PMID:[33921749](#)
63. Ta HD, Wang WJ, Phan NN, An Ton NT, Anuraga G, Ku SC, Wu YF, Wang CY, Lee KH. Potential Therapeutic and Prognostic Values of LSM Family Genes in Breast Cancer. *Cancers (Basel)*. 2021; 13:4902. <https://doi.org/10.3390/cancers13194902> PMID:[34638387](#)
64. Wu YH, Yeh IJ, Phan NN, Yen MC, Liu HL, Wang CY, Hsu HP. Severe acute respiratory syndrome coronavirus (SARS-CoV)-2 infection induces dysregulation of immunity: *in silico* gene expression analysis. *Int J Med Sci*. 2021; 18:1143–52. <https://doi.org/10.7150/ijms.52256> PMID:[33526974](#)
65. Liu HL, Yeh IJ, Phan NN, Wu YH, Yen MC, Hung JH, Chiao CC, Chen CF, Sun Z, Jiang JZ, Hsu HP, Wang CY, Lai MD. Gene signatures of SARS-CoV/SARS-CoV-2-infected ferret lungs in short- and long-term models. *Infect Genet Evol*. 2020; 85:104438. <https://doi.org/10.1016/j.meegid.2020.104438> PMID:[32615317](#)
66. Liu CH, Lu CH, Lin LT. Pandemic strategies with computational and structural biology against COVID-19: A retrospective. *Comput Struct Biotechnol J*. 2021; 20:187–92. <https://doi.org/10.1016/j.csbj.2021.11.040> PMID:[34900126](#)
67. Lim HG, Hsiao SH, Fann YC, Lee YG. Robust Mutation Profiling of SARS-CoV-2 Variants from Multiple Raw Illumina Sequencing Data with Cloud Workflow. *Genes (Basel)*. 2022; 13:686. <https://doi.org/10.3390/genes13040686> PMID:[35456492](#)
68. Yu WL, Toh HS, Liao CT, Chang WT. A Double-Edged Sword-Cardiovascular Concerns of Potential Anti-COVID-19 Drugs. *Cardiovasc Drugs Ther*. 2021; 35:205–14. <https://doi.org/10.1007/s10557-020-07024-7> PMID:[32557011](#)
69. Poly TN, Islam MM, Li YJ, Alsinglawi B, Hsu MH, Jian WS, Yang HC. Application of Artificial Intelligence for Screening COVID-19 Patients Using Digital Images: Meta-analysis. *JMIR Med Inform*. 2021; 9:e21394. <https://doi.org/10.2196/21394> PMID:[33764884](#)
70. Yu CS, Chang SS, Chang TH, Wu JL, Lin YJ, Chien HF, Chen RJ. A COVID-19 Pandemic Artificial Intelligence-Based System With Deep Learning Forecasting and Automatic Statistical Data Acquisition: Development and Implementation Study. *J Med Internet Res*. 2021; 23:e27806. <https://doi.org/10.2196/27806> PMID:[33900932](#)
71. Boyle EI, Weng S, Gollub J, Jin H, Botstein D, Cherry JM, Sherlock G. GO::TermFinder--open source software for accessing Gene Ontology information and finding significantly enriched Gene Ontology terms associated with a list of genes. *Bioinformatics*. 2004; 20:3710–5. <https://doi.org/10.1093/bioinformatics/bth456> PMID:[15297299](#)
72. Wang CY, Chiao CC, Phan NN, Li CY, Sun ZD, Jiang JZ, Hung JH, Chen YL, Yen MC, Weng TY, Chen WC, Hsu HP, Lai MD. Gene signatures and potential therapeutic targets of amino acid metabolism in estrogen receptor-positive breast cancer. *Am J Cancer Res*. 2020; 10:95–113. PMID:[32064155](#)
73. Xuan DT, Yeh IJ, Wu CC, Su CY, Liu HL, Chiao CC, Ku SC, Jiang JZ, Sun Z, Ta HD, Anuraga G, Wang CY, Yen MC. Comparison of Transcriptomic Signatures between Monkeypox-Infected Monkey and Human Cell Lines. *J Immunol Res*. 2022; 2022:3883822. <https://doi.org/10.1155/2022/3883822> PMID:[36093436](#)
74. Sergushichev A. An algorithm for fast preranked gene set enrichment analysis using cumulative statistic calculation. *BioRxiv*. 2016. [Epub ahead of print].
75. Korotkevich G, Sukhov V, Budin N, Shpak B, Artyomov MN, Sergushichev A. Fast gene set enrichment analysis. *BioRxiv*. 2021. [Epub ahead of print]. <https://doi.org/10.1101/060012>
76. Chen PS, Hsu HP, Phan NN, Yen MC, Chen FW, Liu YW, Lin FP, Feng SY, Cheng TL, Yeh PH, Omar HA, Sun Z, Jiang JZ, et al. CCDC167 as a potential therapeutic target and regulator of cell cycle-related networks in breast cancer. *Aging (Albany NY)*. 2021; 13:4157–81. <https://doi.org/10.18632/aging.202382> PMID:[33461170](#)
77. Bakre A, Andersen LE, Meliopoulos V, Coleman K, Yan X, Brooks P, Crabtree J, Tompkins SM, Tripp RA. Identification of Host Kinase Genes Required for Influenza Virus Replication and the Regulatory Role of MicroRNAs. *PLoS One*. 2013; 8:e66796. <https://doi.org/10.1371/journal.pone.0066796> PMID:[23805279](#)
78. Fujiwara Y, Saito M, Robles AI, Nishida M, Takeshita F, Watanabe M, Ochiya T, Yokota J, Kohno T, Harris CC, Tsuchiya N. A Nucleolar Stress-Specific p53-miR-101 Molecular Circuit Functions as an Intrinsic Tumor-Suppressor Network. *EBioMedicine*. 2018; 33:33–48. <https://doi.org/10.1016/j.ebiom.2018.06.031> PMID:[30049386](#)
79. Wu YH, Yeh IJ, Phan NN, Yen MC, Hung JH, Chiao CC, Chen CF, Sun Z, Hsu HP, Wang CY, Lai MD. Gene signatures and potential therapeutic targets of Middle



- East respiratory syndrome coronavirus (MERS-CoV)-infected human lung adenocarcinoma epithelial cells. *J Microbiol Immunol Infect.* 2021; 54:845–57.  
<https://doi.org/10.1016/j.jmii.2021.03.007>  
PMID:34176764
80. Li T, Fan J, Wang B, Traugh N, Chen Q, Liu JS, Li B, Liu XS. TIMER: A Web Server for Comprehensive Analysis of Tumor-Infiltrating Immune Cells. *Cancer Res.* 2017; 77:e108–10.  
<https://doi.org/10.1158/0008-5472.CAN-17-0307>  
PMID:29092952
81. Li B, Severson E, Pignon JC, Zhao H, Li T, Novak J, Jiang P, Shen H, Aster JC, Rodig S, Signoretti S, Liu JS, Liu XS. Comprehensive analyses of tumor immunity: implications for cancer immunotherapy. *Genome Biol.* 2016; 17:174.  
<https://doi.org/10.1186/s13059-016-1028-7>  
PMID:27549193
82. Amat S, Penault-Llorca F, Cure H, Le Bouedec G, Achard JL, Van Praagh I, Feillel V, Mouret-Reynier MA, Dauplat J, Chollet P. Scarff-Bloom-Richardson (SBR) grading: a pleiotropic marker of chemosensitivity in invasive ductal breast carcinomas treated by neoadjuvant chemotherapy. *Int J Oncol.* 2002; 20:791–6.  
PMID:11894126
83. Galea MH, Blamey RW, Elston CE, Ellis IO. The Nottingham Prognostic Index in primary breast cancer. *Breast Cancer Res Treat.* 1992; 22:207–19.  
<https://doi.org/10.1007/BF01840834> PMID:1391987
84. Chava S, Gupta R. Identification of the Mutational Landscape of Gynecological Malignancies. *J Cancer.* 2020; 11:4870–83.  
<https://doi.org/10.7150/jca.46174>  
PMID:32626534
85. Yang SY, Lheureux S, Karakasis K, Burnier JV, Bruce JP, Clouthier DL, Danesh A, Quevedo R, Dowar M, Hanna Y, Li T, Lu L, Xu W, et al. Landscape of genomic alterations in high-grade serous ovarian cancer from exceptional long- and short-term survivors. *Genome Med.* 2018; 10:81.  
<https://doi.org/10.1186/s13073-018-0590-x>  
PMID:30382883
86. Ciriello G, Gatza ML, Beck AH, Wilkerson MD, Rhie SK, Pastore A, Zhang H, McLellan M, Yau C, Kandoth C, Bowlby R, Shen H, Hayat S, et al, and TCGA Research Network. Comprehensive Molecular Portraits of Invasive Lobular Breast Cancer. *Cell.* 2015; 163:506–19.  
<https://doi.org/10.1016/j.cell.2015.09.033>  
PMID:26451490
87. Dabbs DJ, Schnitt SJ, Geyer FC, Weigelt B, Baehner FL, Decker T, Eusebi V, Fox SB, Ichihara S, Lakhani SR, Palacios J, Rakha E, Richardson AL, et al. Lobular neoplasia of the breast revisited with emphasis on the role of E-cadherin immunohistochemistry. *Am J Surg Pathol.* 2013; 37:e1–11.  
<https://doi.org/10.1097/PAS.0b013e3182918a2b>  
PMID:23759937
88. Gregory PA, Bert AG, Paterson EL, Barry SC, Tsykin A, Farshid G, Vadas MA, Khew-Goodall Y, Goodall GJ. The miR-200 family and miR-205 regulate epithelial to mesenchymal transition by targeting ZEB1 and SIP1. *Nat Cell Biol.* 2008; 10:593–601.  
<https://doi.org/10.1038/ncb1722> PMID:18376396
89. Park SM, Gaur AB, Lengyel E, Peter ME. The miR-200 family determines the epithelial phenotype of cancer cells by targeting the E-cadherin repressors ZEB1 and ZEB2. *Genes Dev.* 2008; 22:894–907.  
<https://doi.org/10.1101/gad.1640608>  
PMID:18381893
90. Korpala M, Lee ES, Hu G, Kang Y. The miR-200 family inhibits epithelial-mesenchymal transition and cancer cell migration by direct targeting of E-cadherin transcriptional repressors ZEB1 and ZEB2. *J Biol Chem.* 2008; 283:14910–4.  
<https://doi.org/10.1074/jbc.C800074200>  
PMID:18411277
91. Fontana A, Barbano R, Dama E, Pasculli B, Rendina M, Morrilli MG, Melocchi V, Castelvetero M, Valori VM, Ravaioli S, Bravaccini S, Ciuffreda L, Graziano P, et al. Combined analysis of miR-200 family and its significance for breast cancer. *Sci Rep.* 2021; 11:2980.  
<https://doi.org/10.1038/s41598-021-82286-1>  
PMID:33536459
92. Thiery JP. Epithelial-mesenchymal transitions in development and pathologies. *Curr Opin Cell Biol.* 2003; 15:740–6.  
<https://doi.org/10.1016/j.ceb.2003.10.006>  
PMID:14644200
93. Nakajima S, Doi R, Toyoda E, Tsuji S, Wada M, Koizumi M, Tulachan SS, Ito D, Kami K, Mori T, Kawaguchi Y, Fujimoto K, Hosotani R, Imamura M. N-cadherin expression and epithelial-mesenchymal transition in pancreatic carcinoma. *Clin Cancer Res.* 2004; 10:4125–33.  
<https://doi.org/10.1158/1078-0432.CCR-0578-03>  
PMID:15217949
94. Hazan RB, Qiao R, Keren R, Badano I, Suyama K. Cadherin switch in tumor progression. *Ann N Y Acad Sci.* 2004; 1014:155–63.  
<https://doi.org/10.1196/annals.1294.016>  
PMID:15153430
95. Bartolomé RA, Torres S, Isern de Val S, Escudero-Paniagua B, Calviño E, Teixidó J, Casal JI. VE-cadherin

- RGD motifs promote metastasis and constitute a potential therapeutic target in melanoma and breast cancers. *Oncotarget*. 2017; 8:215–27.  
<https://doi.org/10.18632/oncotarget.13832>  
PMID:[27966446](https://pubmed.ncbi.nlm.nih.gov/27966446/)
96. Huang TH, Mokgautsi N, Huang YJ, Wu AT, Huang HS. Comprehensive Omics Analysis of a Novel Small-Molecule Inhibitor of Chemoresistant Oncogenic Signatures in Colorectal Cancer Cell with Antitumor Effects. *Cells*. 2021; 10:1970.  
<https://doi.org/10.3390/cells10081970>  
PMID:[34440739](https://pubmed.ncbi.nlm.nih.gov/34440739/)
97. Yadav VK, Huang YJ, George TA, Wei PL, Sumitra MR, Ho CL, Chang TH, Wu AT, Huang HS. Preclinical Evaluation of the Novel Small-Molecule MSI-N1014 for Treating Drug-Resistant Colon Cancer via the LGR5/ $\beta$ -catenin/miR-142-3p Network and Reducing Cancer-Associated Fibroblast Transformation. *Cancers (Basel)*. 2020; 12:1590.  
<https://doi.org/10.3390/cancers12061590>  
PMID:[32560222](https://pubmed.ncbi.nlm.nih.gov/32560222/)
98. Lawal B, Wang YC, Wu AT, Huang HS. Pro-Oncogenic c-Met/EGFR, Biomarker Signatures of the Tumor Microenvironment are Clinical and Therapy Response Prognosticators in Colorectal Cancer, and Therapeutic Targets of 3-Phenyl-2H-benzo[e][1,3]-Oxazine-2,4(3H)-Dione Derivatives. *Front Pharmacol*. 2021; 12:691234.  
<https://doi.org/10.3389/fphar.2021.691234>  
PMID:[34512327](https://pubmed.ncbi.nlm.nih.gov/34512327/)
99. Chung CC, Huang TY, Chu HR, De Luca R, Candelotti E, Huang CH, Yang YS, Incerpi S, Pedersen JZ, Lin CY, Huang HM, Lee SY, Li ZL, et al. Heteronemin and tetrac derivatives suppress non-small cell lung cancer growth via ERK1/2 inhibition. *Food Chem Toxicol*. 2022; 161:112850.  
<https://doi.org/10.1016/j.fct.2022.112850>  
PMID:[35151786](https://pubmed.ncbi.nlm.nih.gov/35151786/)
100. Hsiao SH, Chen WT, Chung CL, Chou YT, Lin SE, Hong SY, Chang JH, Chang TH, Chien LN. Comparative survival analysis of platinum-based adjuvant chemotherapy for early-stage squamous cell carcinoma and adenocarcinoma of the lung. *Cancer Med*. 2022; 11:2067–78.  
<https://doi.org/10.1002/cam4.4570>  
PMID:[35274494](https://pubmed.ncbi.nlm.nih.gov/35274494/)
101. Kuo KT, Lin CH, Wang CH, Pikatan NW, Yadav VK, Fong IH, Yeh CT, Lee WH, Huang WC. HNMT Upregulation Induces Cancer Stem Cell Formation and Confers Protection against Oxidative Stress through Interaction with HER2 in Non-Small-Cell Lung Cancer. *Int J Mol Sci*. 2022; 23:1663.  
<https://doi.org/10.3390/ijms23031663>  
PMID:[35163585](https://pubmed.ncbi.nlm.nih.gov/35163585/)
102. Tseng PC, Chen CL, Lee KY, Feng PH, Wang YC, Satria RD, Lin CF. Epithelial-to-mesenchymal transition hinders interferon- $\gamma$ -dependent immunosurveillance in lung cancer cells. *Cancer Lett*. 2022; 539:215712.  
<https://doi.org/10.1016/j.canlet.2022.215712>  
PMID:[35490920](https://pubmed.ncbi.nlm.nih.gov/35490920/)
103. Lee HC, Lu YH, Huang YL, Huang SL, Chuang HC. Air Pollution Effects to the Subtype and Severity of Lung Cancers. *Front Med (Lausanne)*. 2022; 9:835026.  
<https://doi.org/10.3389/fmed.2022.835026>  
PMID:[35433740](https://pubmed.ncbi.nlm.nih.gov/35433740/)
104. Chen YL, Lee KT, Wang CY, Shen CH, Chen SC, Chung WP, Hsu YT, Kuo YL, Chen PS, Cheung CH, Chang CP, Shen MR, Hsu HP. Low expression of cytosolic NOTCH1 predicts poor prognosis of breast cancer patients. *Am J Cancer Res*. 2022; 12:2084–101.  
PMID:[35693094](https://pubmed.ncbi.nlm.nih.gov/35693094/)
105. Hagerling C, Gonzalez H, Salari K, Wang CY, Lin C, Robles I, van Gogh M, Dejmeek A, Jirström K, Werb Z. Immune effector monocyte-neutrophil cooperation induced by the primary tumor prevents metastatic progression of breast cancer. *Proc Natl Acad Sci USA*. 2019; 116:21704–14.  
<https://doi.org/10.1073/pnas.1907660116>  
PMID:[31591235](https://pubmed.ncbi.nlm.nih.gov/31591235/)
106. Wang WJ, Lai HY, Zhang F, Shen WJ, Chu PY, Liang HY, Liu YB, Wang JM. MCL1 participates in leptin-promoted mitochondrial fusion and contributes to drug resistance in gallbladder cancer. *JCI Insight*. 2021; 6:e135438.  
<https://doi.org/10.1172/jci.insight.135438>  
PMID:[34156978](https://pubmed.ncbi.nlm.nih.gov/34156978/)
107. Chou CW, Hsieh YH, Ku SC, Shen WJ, Anuraga G, Khoa Ta HD, Lee KH, Lee YC, Lin CH, Wang CY, Wang WJ. Potential Prognostic Biomarkers of OSBPL Family Genes in Patients with Pancreatic Ductal Adenocarcinoma. *Biomedicines*. 2021; 9:1601.  
<https://doi.org/10.3390/biomedicines9111601>  
PMID:[34829830](https://pubmed.ncbi.nlm.nih.gov/34829830/)
108. Ramezani M, Baharzadeh F, Almasi A, Sadeghi M. A Systematic Review and Meta-Analysis: Evaluation of the  $\beta$ -Human Papillomavirus in Immunosuppressed Individuals with Cutaneous Squamous Cell Carcinoma. *Biomedicine (Taipei)*. 2020; 10:1–10.  
<https://doi.org/10.37796/2211-8039.1110>  
PMID:[33854928](https://pubmed.ncbi.nlm.nih.gov/33854928/)
109. Lindsey S, Langhans SA. Crosstalk of Oncogenic Signaling Pathways during Epithelial-Mesenchymal

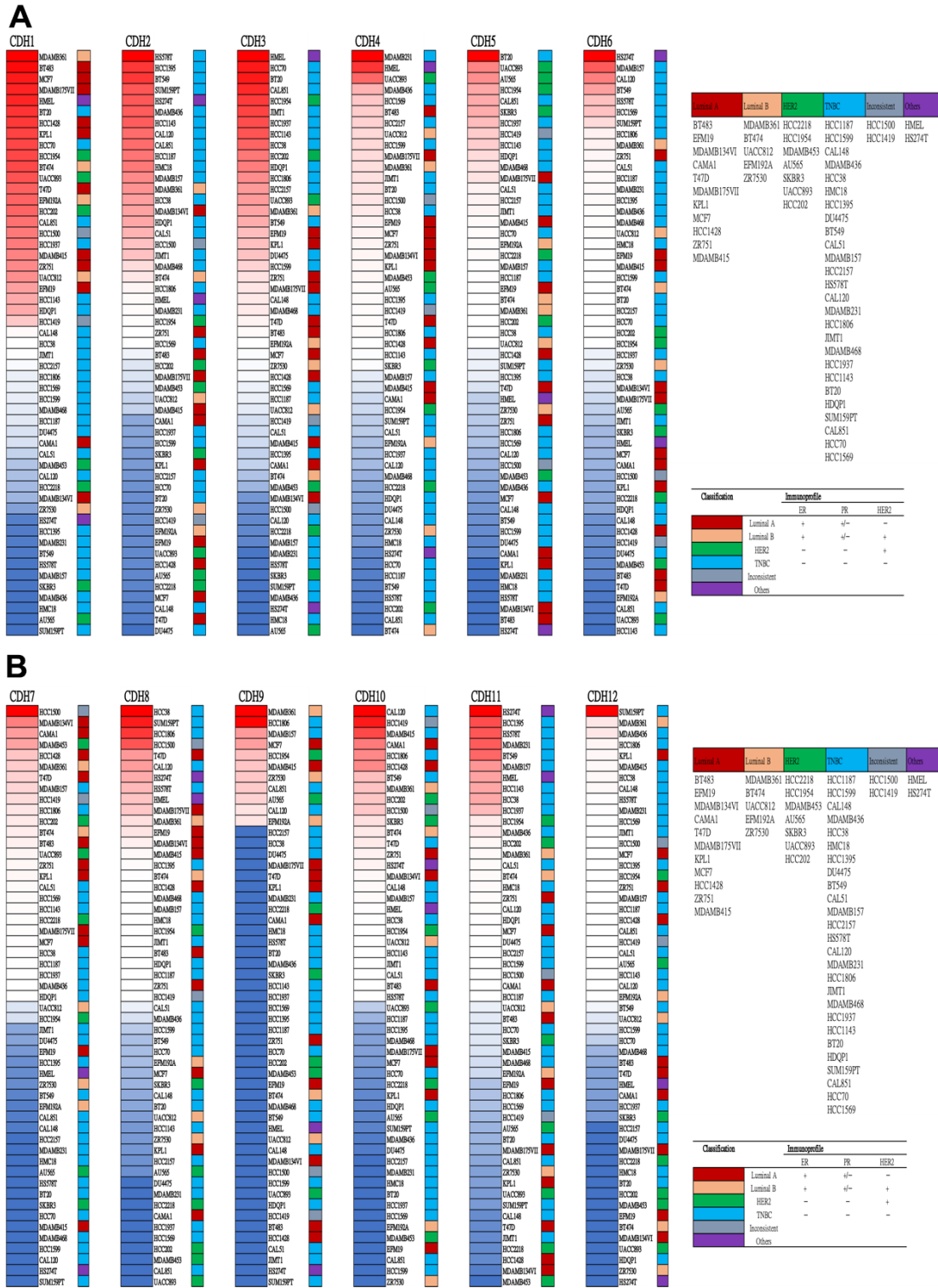
- Transition. *Front Oncol.* 2014; 4:358.  
<https://doi.org/10.3389/fonc.2014.00358>  
PMID:[25566498](https://pubmed.ncbi.nlm.nih.gov/25566498/)
110. Falzone L, Candido S, Salemi R, Basile MS, Scalisi A, McCubrey JA, Torino F, Signorelli SS, Montella M, Libra M. Computational identification of microRNAs associated to both epithelial to mesenchymal transition and NGAL/MMP-9 pathways in bladder cancer. *Oncotarget.* 2016; 7:72758–66.  
<https://doi.org/10.18632/oncotarget.11805>  
PMID:[27602581](https://pubmed.ncbi.nlm.nih.gov/27602581/)
111. McCubrey JA, Fitzgerald TL, Yang LV, Lertpiriyapong K, Steelman LS, Abrams SL, Montalto G, Cervello M, Neri LM, Cocco L, Martelli AM, Laidler P, Dulińska-Litewka J, et al. Roles of GSK-3 and microRNAs on epithelial mesenchymal transition and cancer stem cells. *Oncotarget.* 2017; 8:14221–50.  
<https://doi.org/10.18632/oncotarget.13991>  
PMID:[27999207](https://pubmed.ncbi.nlm.nih.gov/27999207/)
112. Lade-Keller J, Riber-Hansen R, Guldborg P, Schmidt H, Hamilton-Dutoit SJ, Steiniche T. E- to N-cadherin switch in melanoma is associated with decreased expression of phosphatase and tensin homolog and cancer progression. *Br J Dermatol.* 2013; 169:618–28.  
<https://doi.org/10.1111/bjd.12426> PMID:[23662813](https://pubmed.ncbi.nlm.nih.gov/23662813/)
113. Araki K, Shimura T, Suzuki H, Tsutsumi S, Wada W, Yajima T, Kobayahi T, Kubo N, Kuwano H. E/N-cadherin switch mediates cancer progression via TGF- $\beta$ -induced epithelial-to-mesenchymal transition in extrahepatic cholangiocarcinoma. *Br J Cancer.* 2011; 105:1885–93.  
<https://doi.org/10.1038/bjc.2011.452>  
PMID:[22068819](https://pubmed.ncbi.nlm.nih.gov/22068819/)
114. Aleskandarany MA, Negm OH, Green AR, Ahmed MA, Nolan CC, Tighe PJ, Ellis IO, Rakha EA. Epithelial mesenchymal transition in early invasive breast cancer: an immunohistochemical and reverse phase protein array study. *Breast Cancer Res Treat.* 2014; 145:339–48.  
<https://doi.org/10.1007/s10549-014-2927-5>  
PMID:[24771047](https://pubmed.ncbi.nlm.nih.gov/24771047/)
115. Gravdal K, Halvorsen OJ, Haukaas SA, Akslen LA. A switch from E-cadherin to N-cadherin expression indicates epithelial to mesenchymal transition and is of strong and independent importance for the progress of prostate cancer. *Clin Cancer Res.* 2007; 13:7003–11.  
<https://doi.org/10.1158/1078-0432.CCR-07-1263>  
PMID:[18056176](https://pubmed.ncbi.nlm.nih.gov/18056176/)
116. Gröger CJ, Grubinger M, Waldhör T, Vierlinger K, Mikulits W. Meta-analysis of gene expression signatures defining the epithelial to mesenchymal transition during cancer progression. *PLoS One.* 2012; 7:e51136.  
<https://doi.org/10.1371/journal.pone.0051136>  
PMID:[23251436](https://pubmed.ncbi.nlm.nih.gov/23251436/)
117. Thiery JP, Acloque H, Huang RY, Nieto MA. Epithelial-mesenchymal transitions in development and disease. *Cell.* 2009; 139:871–90.  
<https://doi.org/10.1016/j.cell.2009.11.007>  
PMID:[19945376](https://pubmed.ncbi.nlm.nih.gov/19945376/)
118. Peinado H, Olmeda D, Cano A. Snail, Zeb and bHLH factors in tumour progression: an alliance against the epithelial phenotype? *Nat Rev Cancer.* 2007; 7:415–28.  
<https://doi.org/10.1038/nrc2131>  
PMID:[17508028](https://pubmed.ncbi.nlm.nih.gov/17508028/)
119. Chen JH, Huang WC, Bamodu OA, Chang PM, Chao TY, Huang TH. Monospecific antibody targeting of CDH11 inhibits epithelial-to-mesenchymal transition and represses cancer stem cell-like phenotype by up-regulating miR-335 in metastatic breast cancer, *in vitro* and *in vivo*. *BMC Cancer.* 2019; 19:634.  
<https://doi.org/10.1186/s12885-019-5811-1>  
PMID:[31248373](https://pubmed.ncbi.nlm.nih.gov/31248373/)
120. Kim NH, Choi SH, Lee TR, Lee CH, Lee AY. Cadherin 11, a miR-675 target, induces N-cadherin expression and epithelial-mesenchymal transition in melasma. *J Invest Dermatol.* 2014; 134:2967–76.  
<https://doi.org/10.1038/jid.2014.257> PMID:[24940649](https://pubmed.ncbi.nlm.nih.gov/24940649/)
121. Schneider DJ, Wu M, Le TT, Cho SH, Brenner MB, Blackburn MR, Agarwal SK. Cadherin-11 contributes to pulmonary fibrosis: potential role in TGF- $\beta$  production and epithelial to mesenchymal transition. *FASEB J.* 2012; 26:503–12.  
<https://doi.org/10.1096/fj.11-186098> PMID:[21990376](https://pubmed.ncbi.nlm.nih.gov/21990376/)
122. Jakubzig B, Baltes F, Henze S, Schlesinger M, Bendas G. Mechanisms of Matrix-Induced Chemoresistance of Breast Cancer Cells-Deciphering Novel Potential Targets for a Cell Sensitization. *Cancers (Basel).* 2018; 10:495.  
<https://doi.org/10.3390/cancers10120495>  
PMID:[30563275](https://pubmed.ncbi.nlm.nih.gov/30563275/)
123. McCormack VA, dos Santos Silva I. Breast density and parenchymal patterns as markers of breast cancer risk: a meta-analysis. *Cancer Epidemiol Biomarkers Prev.* 2006; 15:1159–69.  
<https://doi.org/10.1158/1055-9965.EPI-06-0034>  
PMID:[16775176](https://pubmed.ncbi.nlm.nih.gov/16775176/)
124. Boyd NF, Martin LJ, Yaffe MJ, Minkin S. Mammographic density and breast cancer risk: current understanding and future prospects. *Breast Cancer Res.* 2011; 13:223.  
<https://doi.org/10.1186/bcr2942>  
PMID:[22114898](https://pubmed.ncbi.nlm.nih.gov/22114898/)

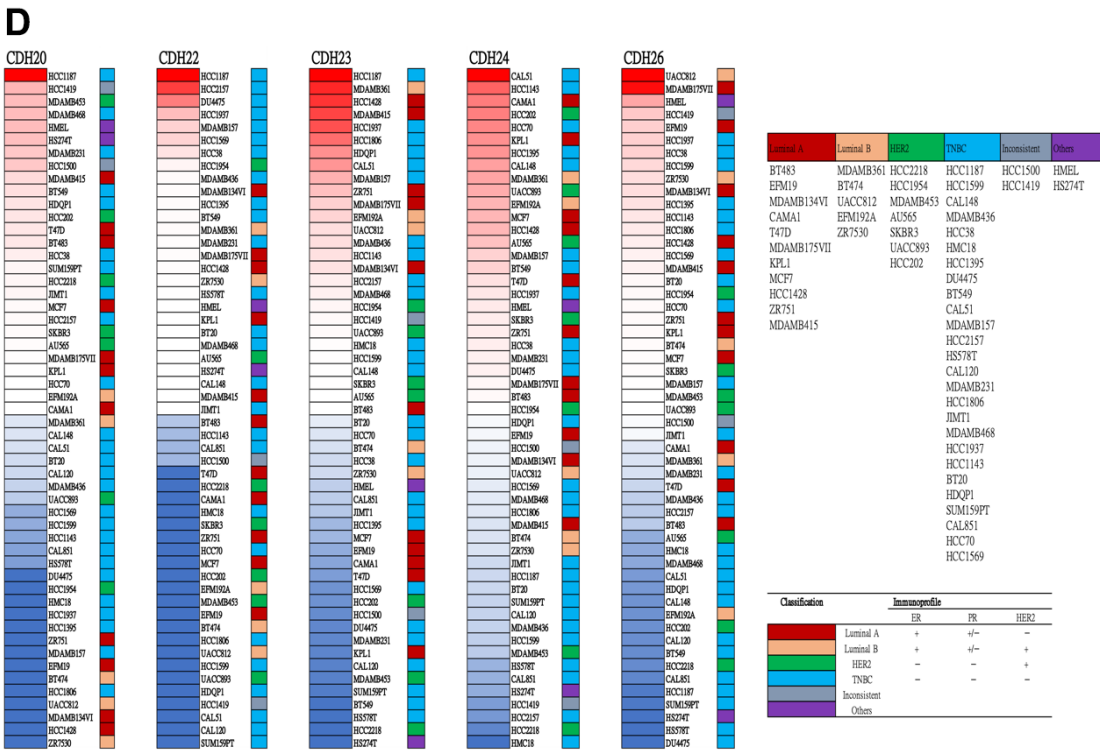
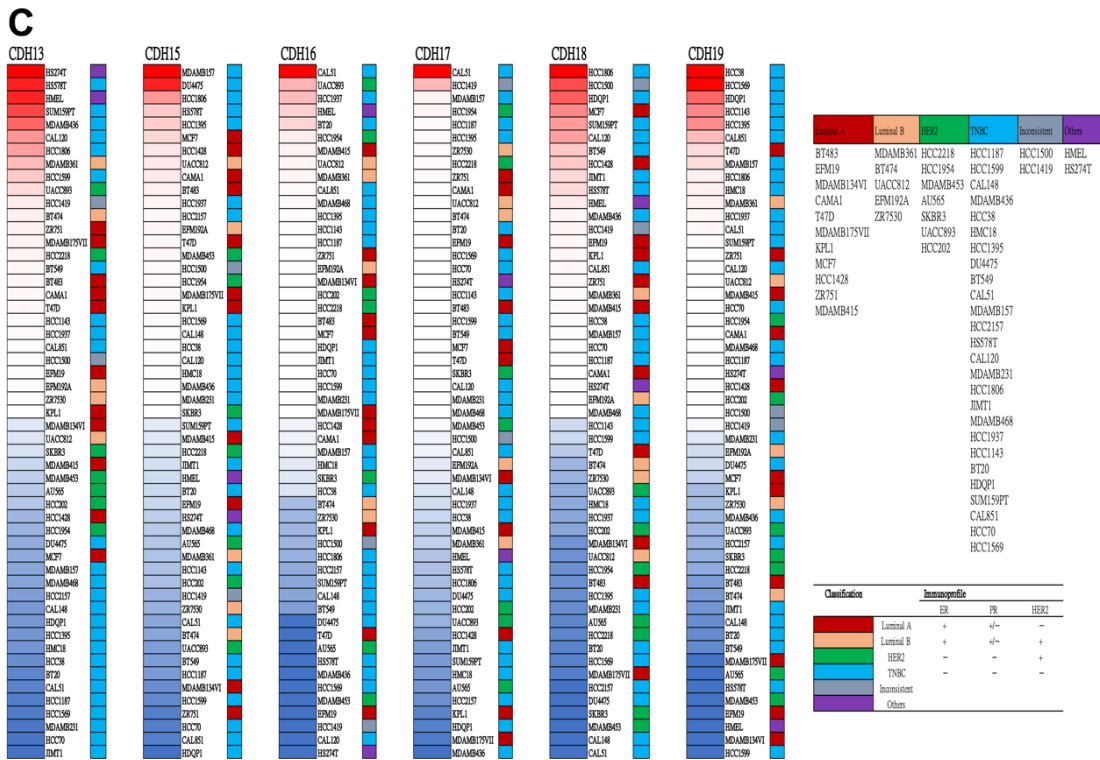
125. Nazari SS, Mukherjee P. An overview of mammographic density and its association with breast cancer. *Breast Cancer*. 2018; 25:259–67. <https://doi.org/10.1007/s12282-018-0857-5> PMID:[29651637](https://pubmed.ncbi.nlm.nih.gov/29651637/)
126. Liu J, Shen JX, Wu HT, Li XL, Wen XF, Du CW, Zhang GJ. Collagen 1A1 (COL1A1) promotes metastasis of breast cancer and is a potential therapeutic target. *Discov Med*. 2018; 25:211–23. PMID:[29906404](https://pubmed.ncbi.nlm.nih.gov/29906404/)
127. Shi RZ, He YF, Wen J, Niu YN, Gao Y, Liu LH, Zhang XP, Wang Y, Zhang XL, Zhang HF, Chen M, Hu XL. Epithelial cell adhesion molecule promotes breast cancer resistance protein-mediated multidrug resistance in breast cancer by inducing partial epithelial-mesenchymal transition. *Cell Biol Int*. 2021; 45:1644–53. <https://doi.org/10.1002/cbin.11598> PMID:[33760350](https://pubmed.ncbi.nlm.nih.gov/33760350/)
128. Tryndyak VP, Beland FA, Pogribny IP. E-cadherin transcriptional down-regulation by epigenetic and microRNA-200 family alterations is related to mesenchymal and drug-resistant phenotypes in human breast cancer cells. *Int J Cancer*. 2010; 126:2575–83. <https://doi.org/10.1002/ijc.24972> PMID:[19839049](https://pubmed.ncbi.nlm.nih.gov/19839049/)
129. Burk U, Schubert J, Wellner U, Schmalhofer O, Vincan E, Spaderna S, Brabletz T. A reciprocal repression between ZEB1 and members of the miR-200 family promotes EMT and invasion in cancer cells. *EMBO Rep*. 2008; 9:582–9. <https://doi.org/10.1038/embor.2008.74> PMID:[18483486](https://pubmed.ncbi.nlm.nih.gov/18483486/)
130. Miotto E, Sabbioni S, Veronese A, Calin GA, Gullini S, Liboni A, Gramantieri L, Bolondi L, Ferrazzi E, Gafà R, Lanza G, Negrini M. Frequent aberrant methylation of the CDH4 gene promoter in human colorectal and gastric cancer. *Cancer Res*. 2004; 64:8156–9. <https://doi.org/10.1158/0008-5472.CAN-04-3000> PMID:[15548679](https://pubmed.ncbi.nlm.nih.gov/15548679/)
131. Li L, Ying J, Li H, Zhang Y, Shu X, Fan Y, Tan J, Cao Y, Tsao SW, Srivastava G, Chan AT, Tao Q. The human cadherin 11 is a pro-apoptotic tumor suppressor modulating cell stemness through Wnt/ $\beta$ -catenin signaling and silenced in common carcinomas. *Oncogene*. 2012; 31:3901–12. <https://doi.org/10.1038/onc.2011.541> PMID:[22139084](https://pubmed.ncbi.nlm.nih.gov/22139084/)
132. Sarrió D, Rodríguez-Pinilla SM, Hardisson D, Cano A, Moreno-Bueno G, Palacios J. Epithelial-mesenchymal transition in breast cancer relates to the basal-like phenotype. *Cancer Res*. 2008; 68:989–97. <https://doi.org/10.1158/0008-5472.CAN-07-2017> PMID:[18281472](https://pubmed.ncbi.nlm.nih.gov/18281472/)
133. Tomita K, van Bokhoven A, van Leenders GJ, Ruijter ET, Jansen CF, Bussemakers MJ, Schalken JA. Cadherin switching in human prostate cancer progression. *Cancer Res*. 2000; 60:3650–4. PMID:[10910081](https://pubmed.ncbi.nlm.nih.gov/10910081/)
134. Li Y, Guo Z, Chen H, Dong Z, Pan ZK, Ding H, Su SB, Huang S. HOXC8-Dependent Cadherin 11 Expression Facilitates Breast Cancer Cell Migration through Trio and Rac. *Genes Cancer*. 2011; 2:880–8. <https://doi.org/10.1177/1947601911433129> PMID:[22593800](https://pubmed.ncbi.nlm.nih.gov/22593800/)
135. Zhao J, Li P, Feng H, Wang P, Zong Y, Ma J, Zhang Z, Chen X, Zheng M, Zhu Z, Lu A. Cadherin-12 contributes to tumorigenicity in colorectal cancer by promoting migration, invasion, adhesion and angiogenesis. *J Transl Med*. 2013; 11:288. <https://doi.org/10.1186/1479-5876-11-288> PMID:[24237488](https://pubmed.ncbi.nlm.nih.gov/24237488/)
136. Wang M, Long K, Li E, Li L, Li B, Ci S, He L, Pan F, Hu Z, Guo Z. DNA polymerase beta modulates cancer progression via enhancing CDH13 expression by promoter demethylation. *Oncogene*. 2020; 39:5507–19. <https://doi.org/10.1038/s41388-020-1386-1> PMID:[32641859](https://pubmed.ncbi.nlm.nih.gov/32641859/)
137. Krishnamachary B, Zagzag D, Nagasawa H, Rainey K, Okuyama H, Baek JH, Semenza GL. Hypoxia-inducible factor-1-dependent repression of E-cadherin in von Hippel-Lindau tumor suppressor-null renal cell carcinoma mediated by TCF3, ZFH1A, and ZFH1B. *Cancer Res*. 2006; 66:2725–31. <https://doi.org/10.1158/0008-5472.CAN-05-3719> PMID:[16510593](https://pubmed.ncbi.nlm.nih.gov/16510593/)
138. Toyooka S, Toyooka KO, Harada K, Miyajima K, Makarla P, Sathyanarayana UG, Yin J, Sato F, Shivapurkar N, Meltzer SJ, Gazdar AF. Aberrant methylation of the CDH13 (H-cadherin) promoter region in colorectal cancers and adenomas. *Cancer Res*. 2002; 62:3382–6. PMID:[12067979](https://pubmed.ncbi.nlm.nih.gov/12067979/)
139. Takeuchi T, Misaki A, Sonobe H, Liang SB, Ohtsuki Y. Is T-cadherin (CDH13, H-cadherin) expression related to lung metastasis of osteosarcoma? *Histopathology*. 2000; 37:193–4. <https://doi.org/10.1046/j.1365-2559.2000.00985-5.x> PMID:[10931247](https://pubmed.ncbi.nlm.nih.gov/10931247/)
140. Cali B, Molon B, Viola A. Tuning cancer fate: the unremitting role of host immunity. *Open Biol*. 2017; 7:170006.

- <https://doi.org/10.1098/rsob.170006> PMID:[28404796](https://pubmed.ncbi.nlm.nih.gov/28404796/)
141. Nawijn MC, Hackett TL, Postma DS, van Oosterhout AJ, Heijink IH. E-cadherin: gatekeeper of airway mucosa and allergic sensitization. *Trends Immunol.* 2011; 32:248–55.  
<https://doi.org/10.1016/j.it.2011.03.004>  
PMID:[21493142](https://pubmed.ncbi.nlm.nih.gov/21493142/)
142. Jiang Y, Wan T, Chen G, Xiu F, Xia D, Zhang W, Zhou X, Cao X. DC-CLM, a cadherin-like molecule cloned from human dendritic cells, inhibits growth of breast cancer cells. *J Cancer Res Clin Oncol.* 2003; 129:57–64.  
<https://doi.org/10.1007/s00432-002-0404-8>  
PMID:[12618902](https://pubmed.ncbi.nlm.nih.gov/12618902/)
143. Pai SG, Carneiro BA, Mota JM, Costa R, Leite CA, Barroso-Sousa R, Kaplan JB, Chae YK, Giles FJ. Wnt/beta-catenin pathway: modulating anticancer immune response. *J Hematol Oncol.* 2017; 10:101.  
<https://doi.org/10.1186/s13045-017-0471-6>  
PMID:[28476164](https://pubmed.ncbi.nlm.nih.gov/28476164/)
144. Jang GB, Kim JY, Cho SD, Park KS, Jung JY, Lee HY, Hong IS, Nam JS. Blockade of Wnt/ $\beta$ -catenin signaling suppresses breast cancer metastasis by inhibiting CSC-like phenotype. *Sci Rep.* 2015; 5:12465.  
<https://doi.org/10.1038/srep12465>  
PMID:[26202299](https://pubmed.ncbi.nlm.nih.gov/26202299/)
145. Gattinoni L, Zhong XS, Palmer DC, Ji Y, Hinrichs CS, Yu Z, Wrzesinski C, Boni A, Cassard L, Garvin LM, Paulos CM, Muranski P, Restifo NP. Wnt signaling arrests effector T cell differentiation and generates CD8+ memory stem cells. *Nat Med.* 2009; 15:808–13.  
<https://doi.org/10.1038/nm.1982>  
PMID:[19525962](https://pubmed.ncbi.nlm.nih.gov/19525962/)
146. Iglesia MD, Parker JS, Hoadley KA, Serody JS, Perou CM, Vincent BG. Genomic Analysis of Immune Cell Infiltrates Across 11 Tumor Types. *J Natl Cancer Inst.* 2016; 108:djw144.  
<https://doi.org/10.1093/jnci/djw144>  
PMID:[27335052](https://pubmed.ncbi.nlm.nih.gov/27335052/)
147. Meng X, Huang Z, Teng F, Xing L, Yu J. Predictive biomarkers in PD-1/PD-L1 checkpoint blockade immunotherapy. *Cancer Treat Rev.* 2015; 41:868–76.  
<https://doi.org/10.1016/j.ctrv.2015.11.001>  
PMID:[26589760](https://pubmed.ncbi.nlm.nih.gov/26589760/)
148. French JJ, Cresswell J, Wong WK, Seymour K, Charnley RM, Kirby JA. T cell adhesion and cytolysis of pancreatic cancer cells: a role for E-cadherin in immunotherapy? *Br J Cancer.* 2002; 87:1034–41.  
<https://doi.org/10.1038/sj.bjc.6600597>  
PMID:[12434297](https://pubmed.ncbi.nlm.nih.gov/12434297/)

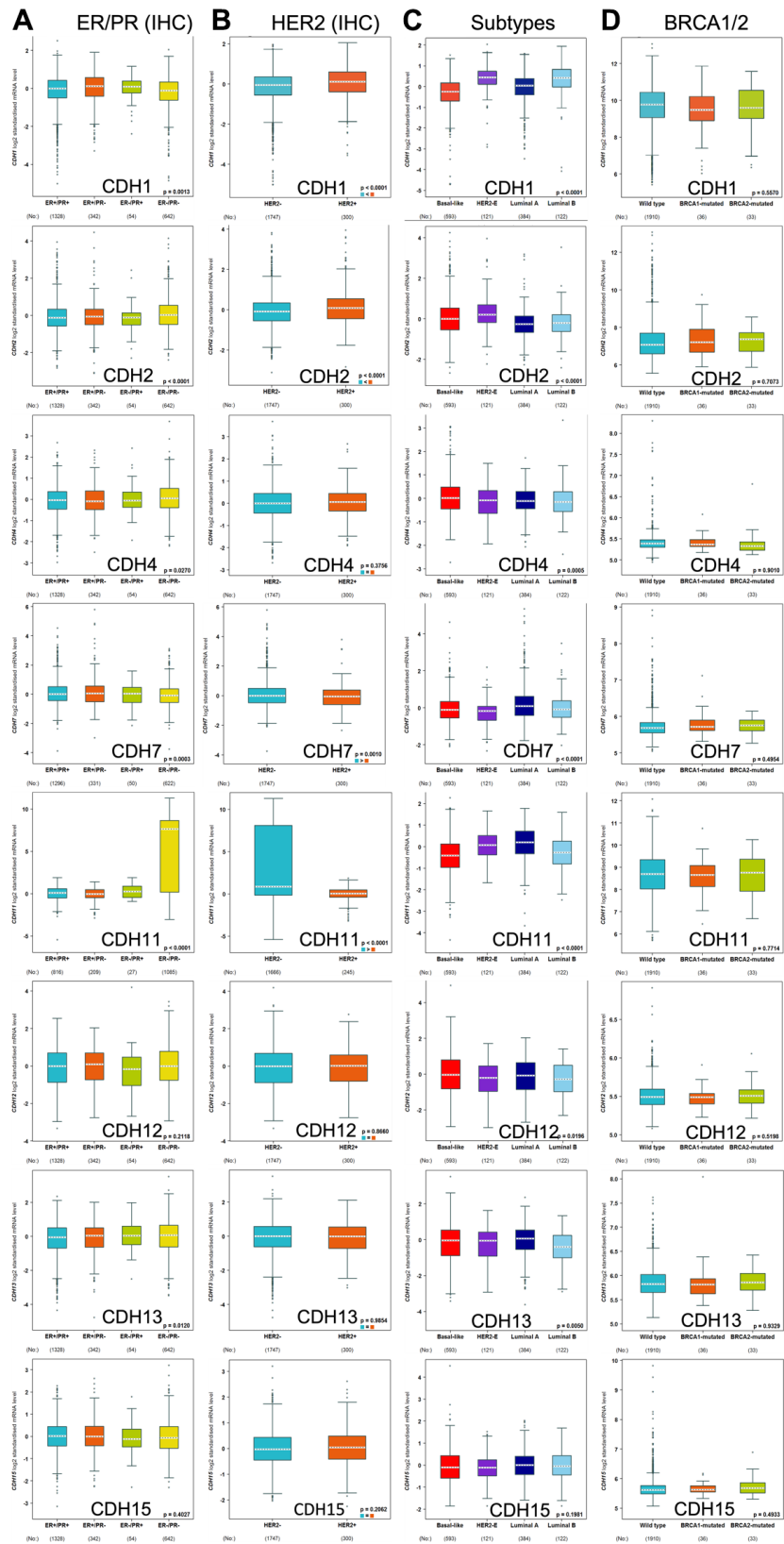
# SUPPLEMENTARY MATERIALS

## Supplementary Figures



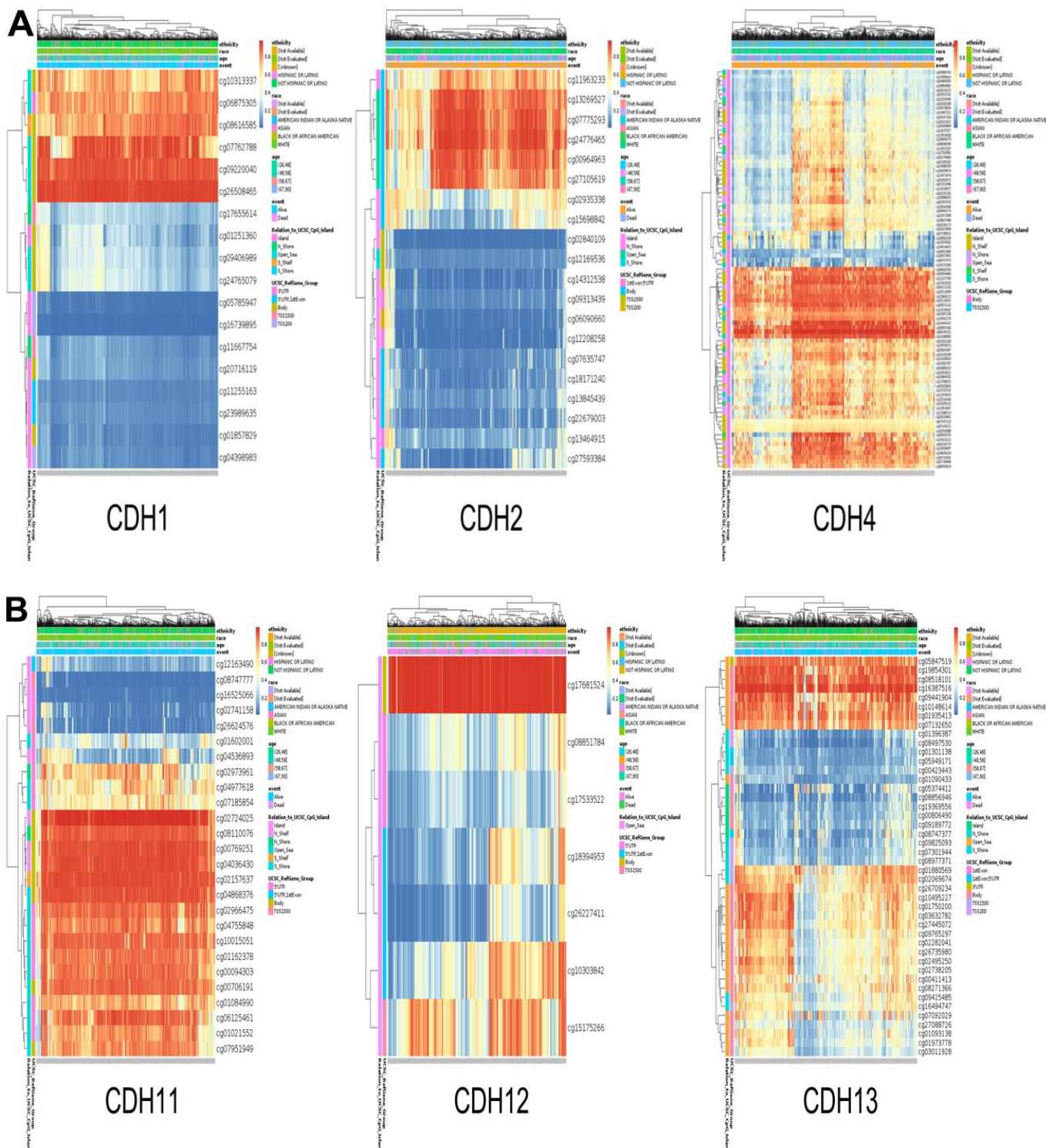


**Supplementary Figure 1. (A–D)** Molecular subtypes of breast cancer cell lines with expressions of CDH family. Colored columns on the right side displayed the molecular subtypes of each cell line. “Inconsistent” denoted cell lines that are inconsistently annotated regarding the status of markers. “Others” included two cell lines that were not breast cancers (HMEL, engineered breast; HS274T, breast fibroblast). TNBC, triple negative breast cancer.

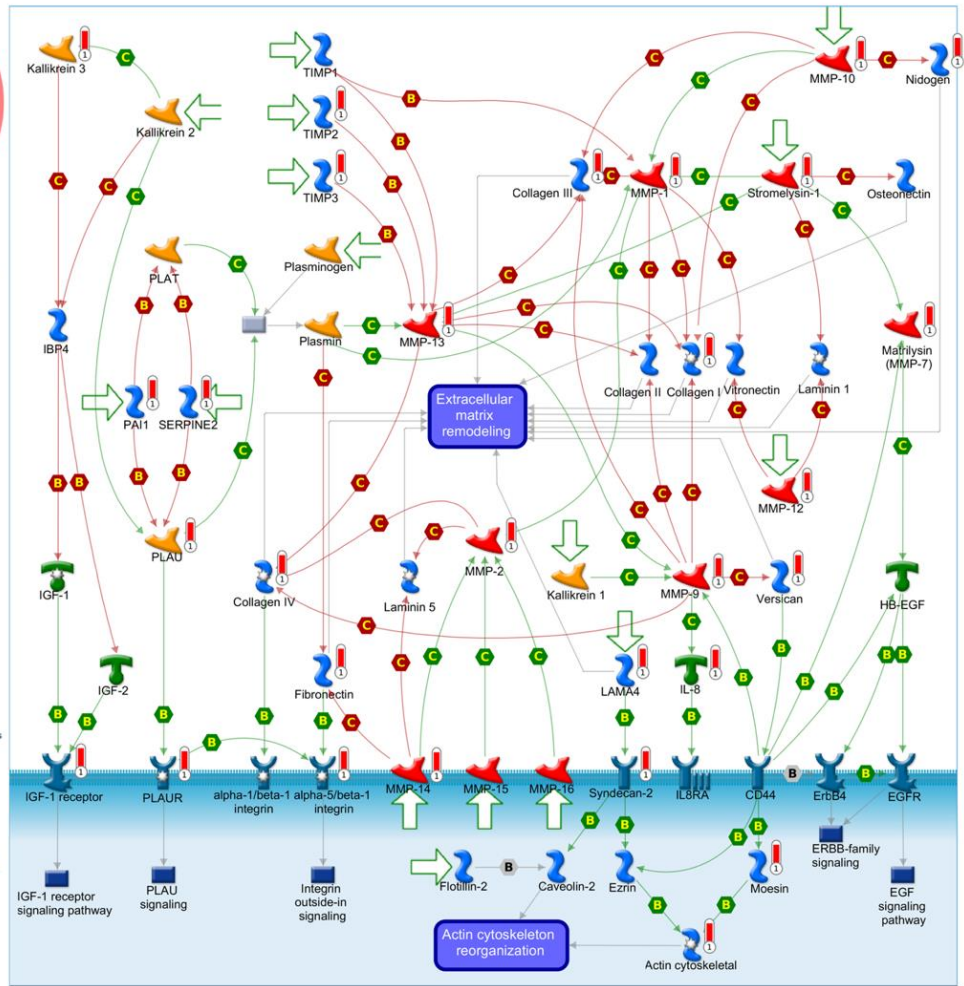
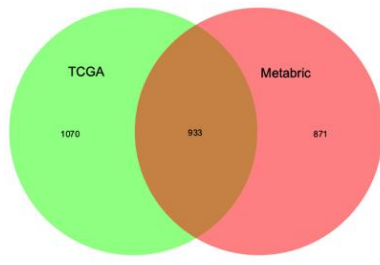


**Supplementary Figure 2. Clinical indicators for treatment and subtypes of breast invasive carcinoma patients with cadherin 1 (CDH1)/2/4/7/11/12/13/15 expressions. (A)** Estrogen receptor (ER)/progesterone (PR) expression with *CDH* family genes co-expression. **(B)** Human epidermal growth factor receptor-2 (HER2) expression with *CDH* family genes co-expression. **(C)** Subtypes of breast invasive carcinoma with *CDH* family genes co-expression. **(D)** Breast cancer gene-1 (*BRCA1*)/*BRCA2* mutations with *CDH* family genes co-expression.

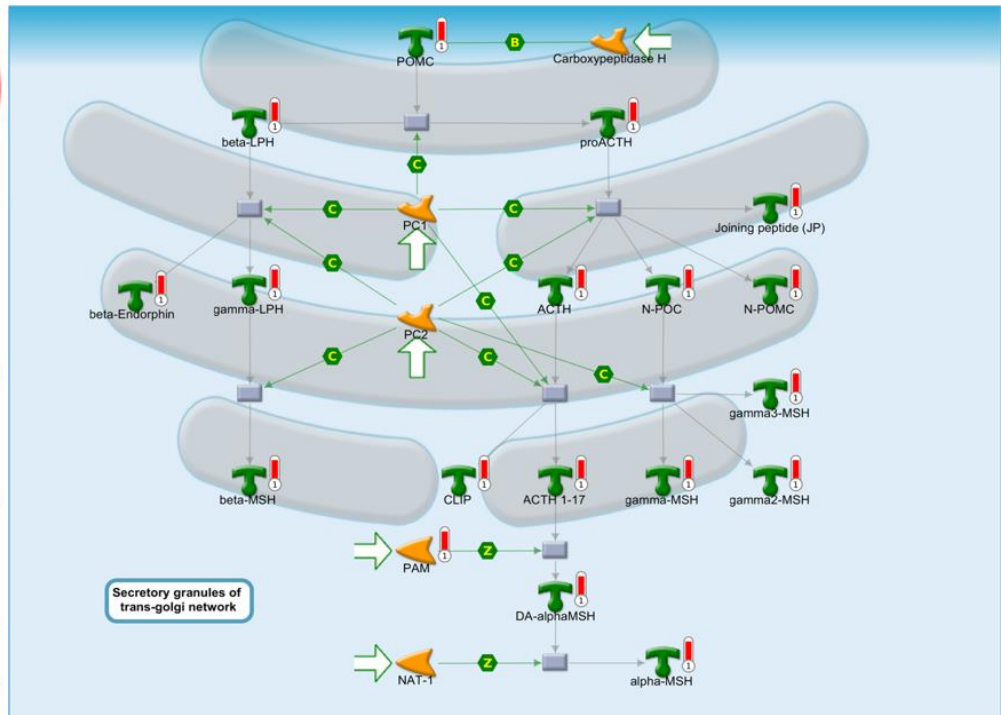
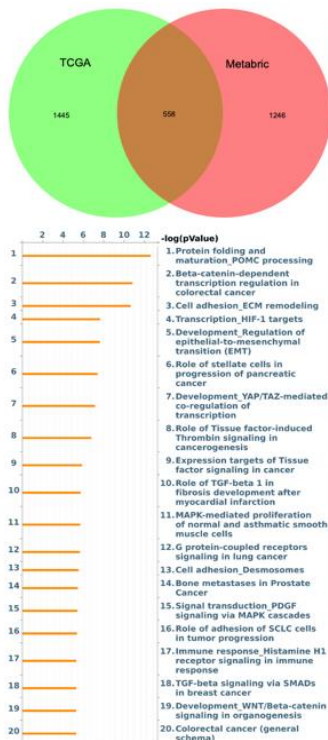




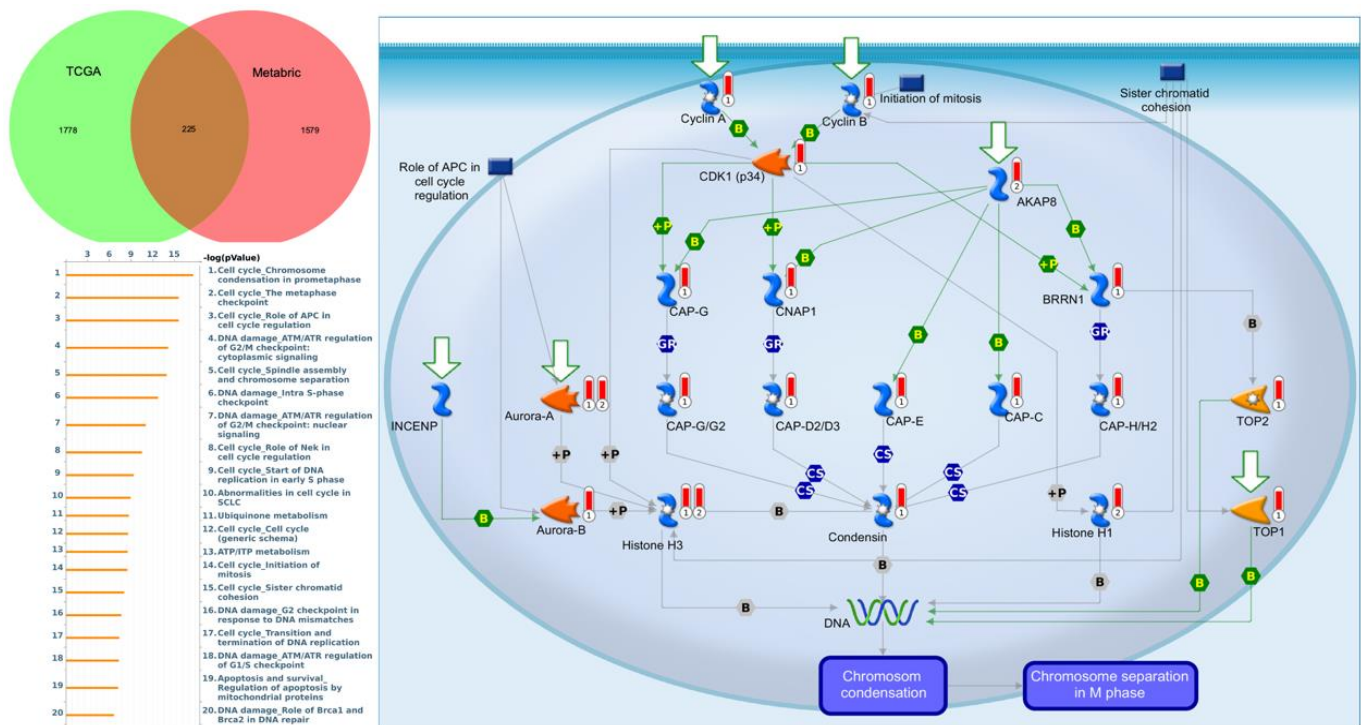
**Supplementary Figure 3. Heatmap of DNA methylation expression levels of *CDH1/2/4/11/12/13* in breast cancer by the MethSurv platform. Blue bars indicated low expressions, while red bars indicated high expressions. Different colored boxes indicated different ethnicities, races, ages, events, relation to UCSC CpG island and UCSC RefGene Groups. DNA methylation status was represented as  $\beta$ -values (ranging from 0 to 1). (A) Among *CDH1*, cg26508465 and cg09220040 showed the highest levels of DNA methylation; cg24776465 showed the highest level among *CDH2*; cg140152 showed the highest level among *CDH4*; (B) cg02724025 showed the highest level among *CDH11*; cg17681524 showed the highest level among *CDH12*; cg16387516 showed the highest level among *CDH13*.**



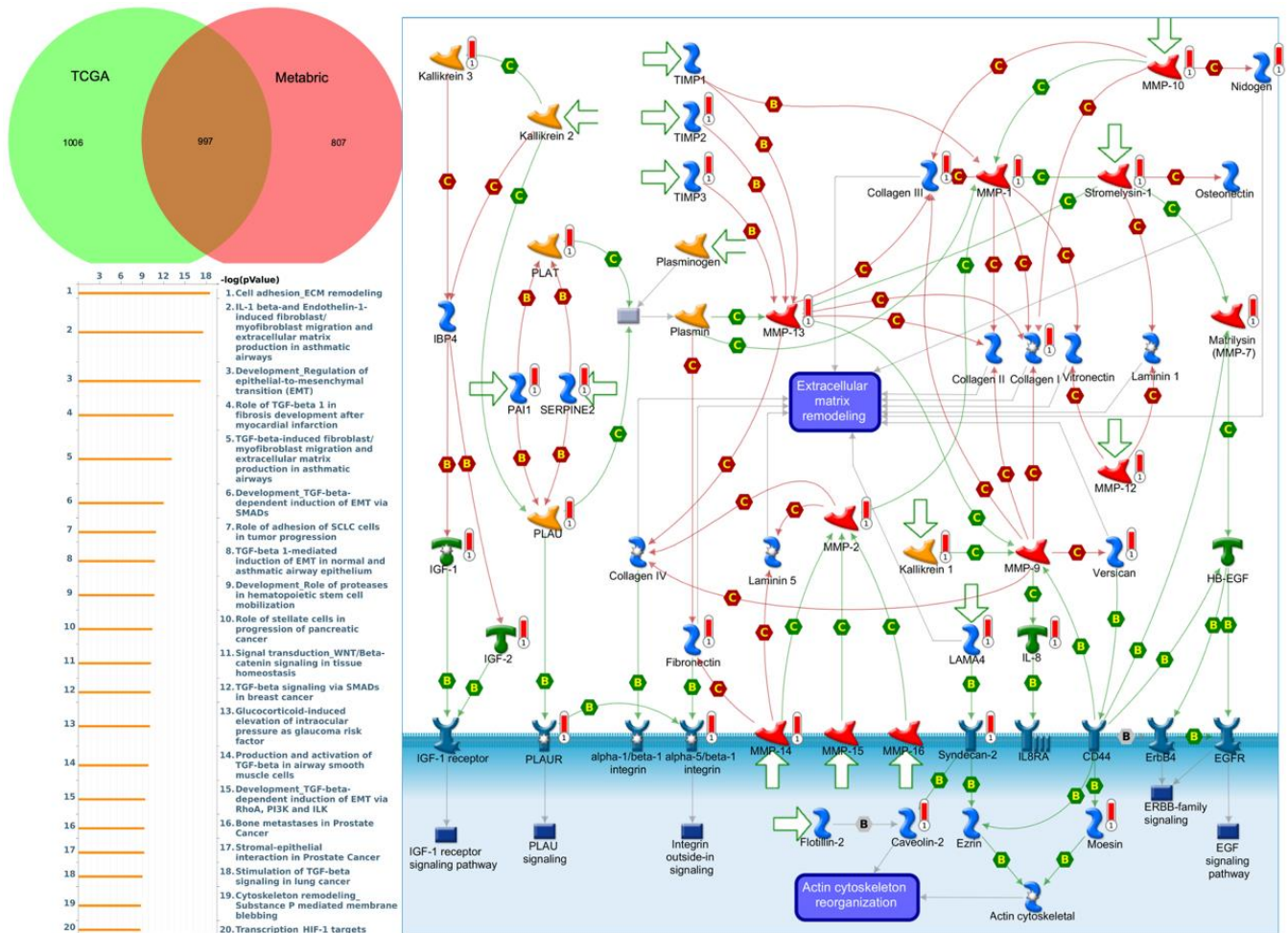
**Supplementary Figure 4. MetaCore enrichment pathway analysis of genes co-expressed with cadherin 2 (*CDH2*).** Top 10% of expression gene lists from both Metabric (1804 genes) and TCGA (2003 genes) were extracted. Overlapped (933) genes were integrated to implement pathway analysis, which formed a pathway list ordered by the  $-\log p$ -value. “Cell adhesion\_ECM remodeling” was at the top of the pathway list when performing the “biological process” analysis. The figure demonstrates the interactions between genes and proteins. Symbols represent proteins. Arrows depict protein interactions (green, activation; red, inhibition). Thermometer-like histograms indicate microarray gene expression (blue, down-regulation; red, up-regulation).



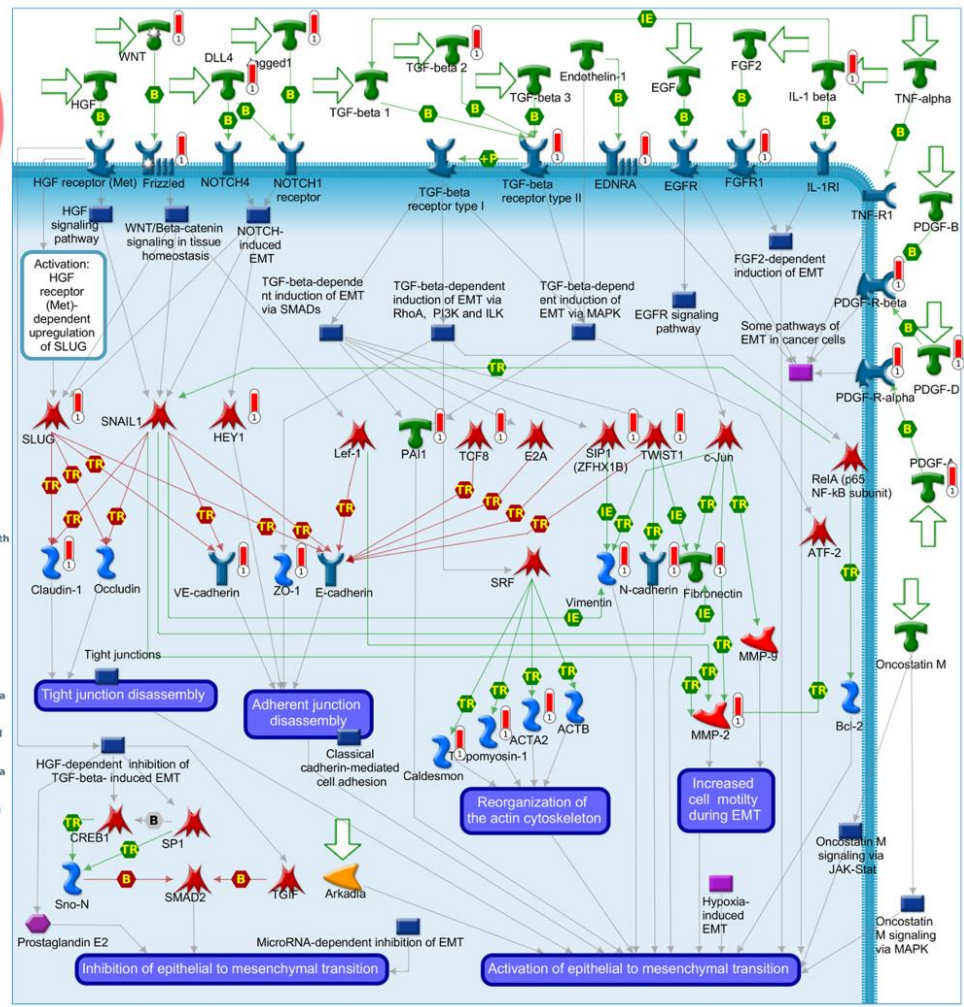
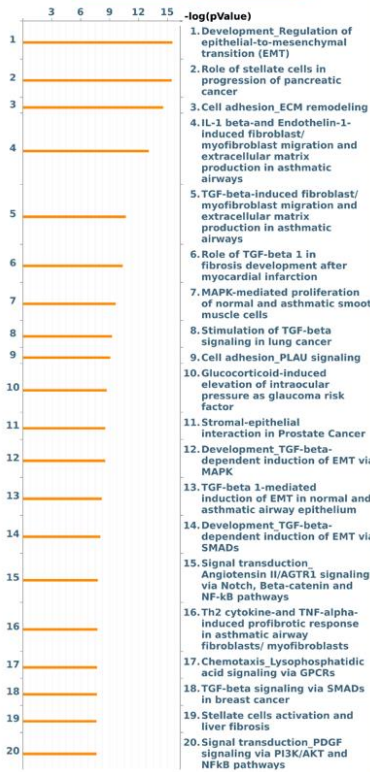
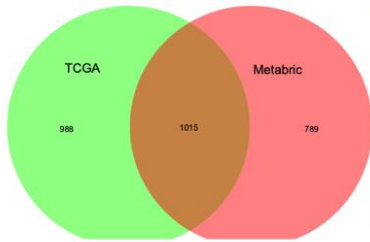
**Supplementary Figure 5. MetaCore enrichment pathway analysis of genes co-expressed with cadherin 4 (*CDH4*).** Top 10% of expression gene lists from both Metabric (1804 genes) and TCGA (2003 genes) were extracted. Overlapped (558) genes were integrated to implement pathway analysis, which formed a pathway list ordered by the  $-\log p$ -value. “Protein folding and maturation\_POMC processing” was at the top of the pathway list when performing the “biological process” analysis. The figure demonstrates the interactions between genes and proteins. Symbols represent proteins. Arrows depict protein interactions (green, activation; red, inhibition). Thermometer-like histograms indicate microarray gene expression (blue, down-regulation; red, up-regulation).



**Supplementary Figure 6. MetaCore enrichment pathway analysis of genes co-expressed with cadherin 7 (*CDH7*).** Top 10% of expression gene lists from both Metabric (1804 genes) and TCGA (2003 genes) were extracted. Overlapped (225) genes were integrated to implement pathway analysis, which formed a pathway list ordered by the  $-\log p$ -value. “Cell cycle\_Chromosome condensation in prometaphase” was at the top of the pathway list when performing the “biological process” analysis. The figure demonstrates the interactions between genes and proteins. Symbols represent proteins. Arrows depict protein interactions (green, activation; red, inhibition). Thermometer-like histograms indicate microarray gene expression (blue, down-regulation; red, up-regulation).



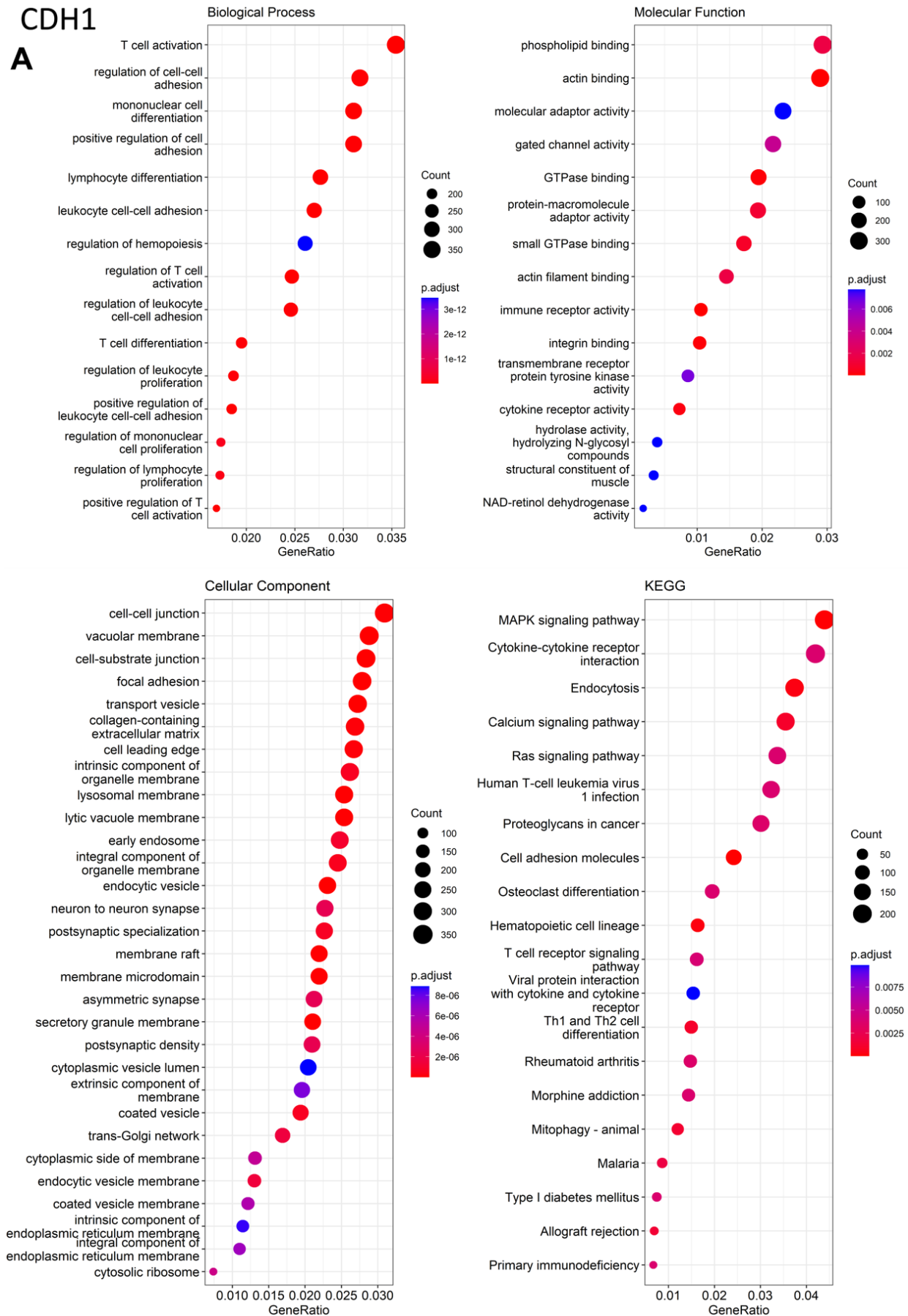
**Supplementary Figure 7. MetaCore enrichment pathway analysis of genes co-expressed with cadherin 11 (*CDH11*).** Top 10% of expression gene lists from both Metabric (1804 genes) and TCGA (2003 genes) were extracted. Overlapped (997) genes were integrated to implement pathway analysis, which formed a pathway list ordered by the  $-\log p$ -value. “Cell adhesion\_ECM remodeling” was at the top of the pathway list when performing the “biological process” analysis. The figure demonstrates the interactions between genes and proteins. Symbols represent proteins. Arrows depict protein interactions (green, activation; red, inhibition). Thermometer-like histograms indicate microarray gene expression (blue, down-regulation; red, up-regulation).

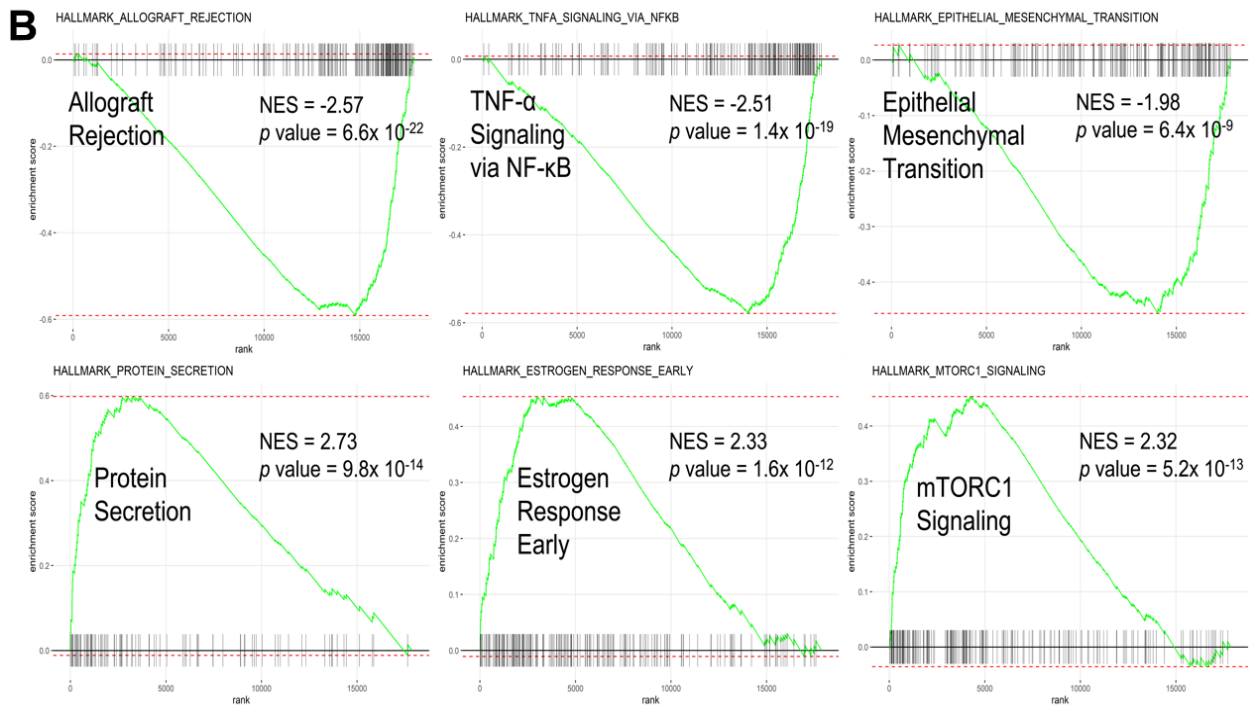


**Supplementary Figure 8. MetaCore enrichment pathway analysis of genes co-expressed with cadherin 13 (*CDH13*).** Top 10% of expression gene lists from both Metabric (1804 genes) and TCGA (2003 genes) were extracted. Overlapped (1015) genes were integrated to implement pathway analysis, which formed a pathway list ordered by the  $-\log p$ -value. “Development\_Regulation of epithelial-to-mesenchymal transition (EMT)” was at the top of the pathway list when performing the “biological process” analysis. The figure demonstrates the interactions between genes and proteins. Symbols represent proteins. Arrows depict protein interactions (green, activation; red, inhibition). Thermometer-like histograms indicate microarray gene expression (blue, down-regulation; red, up-regulation).

# CDH1

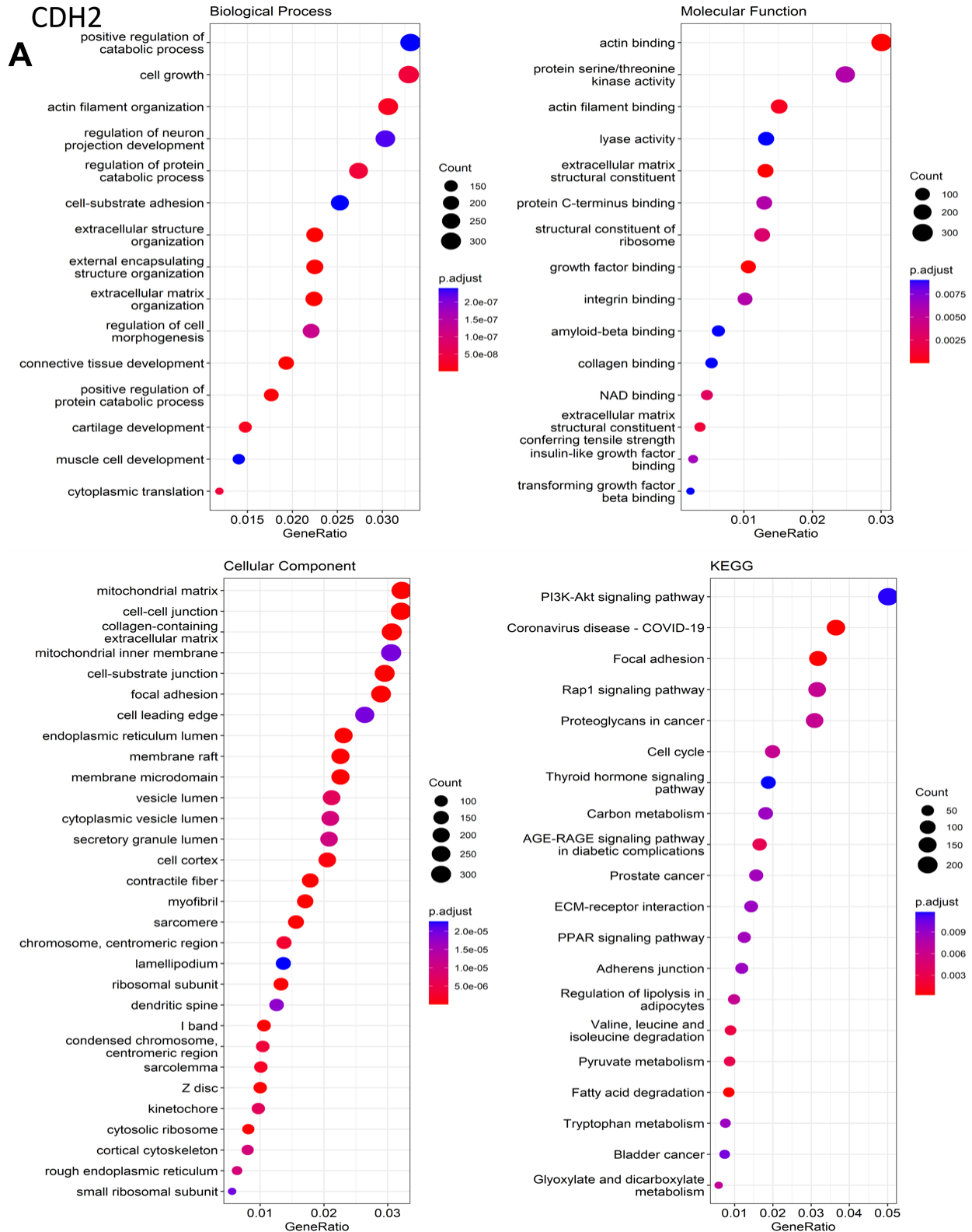
A

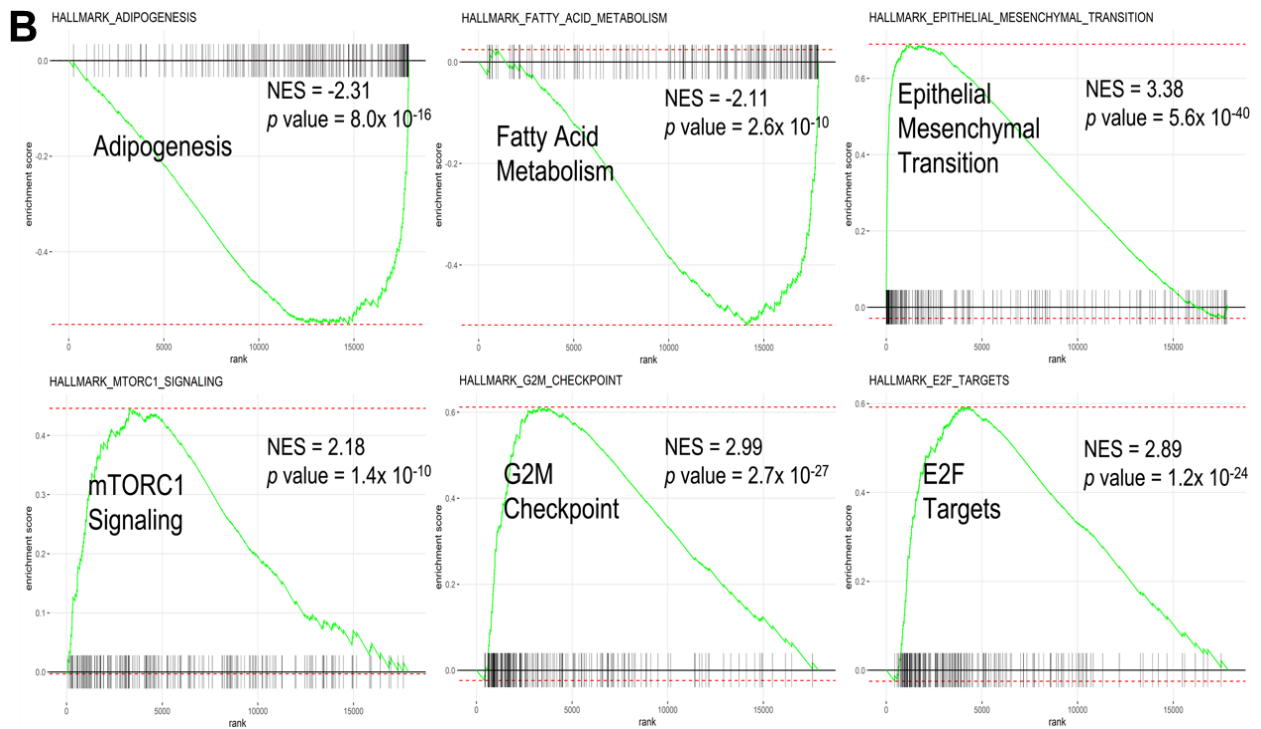




**Supplementary Figure 9. (A, B)** Gene Ontology (GO) analysis and Gene Set Enrichment Analysis (GSEA) based on genes co-expressed with *CDH1*. (A) Dot plots display biological processes, cellular components, molecular functions, and KEGG. The dot size is determined by the count of enriched genes in the pathway, and the color of the dots represents the significance of enrichment pathway. “clusterProfiler” package in R/Bioconductor was used to perform the GO analyses of dot plots. (B) Hallmark signaling pathway analysis of *CDH1* in breast cancer. Results of the analysis showed significant values of gene classes in the Hallmark database. Statistical significance was presented by  $p$  value, and the normalized enrichment score (NES) reflected the rank of gene classes.

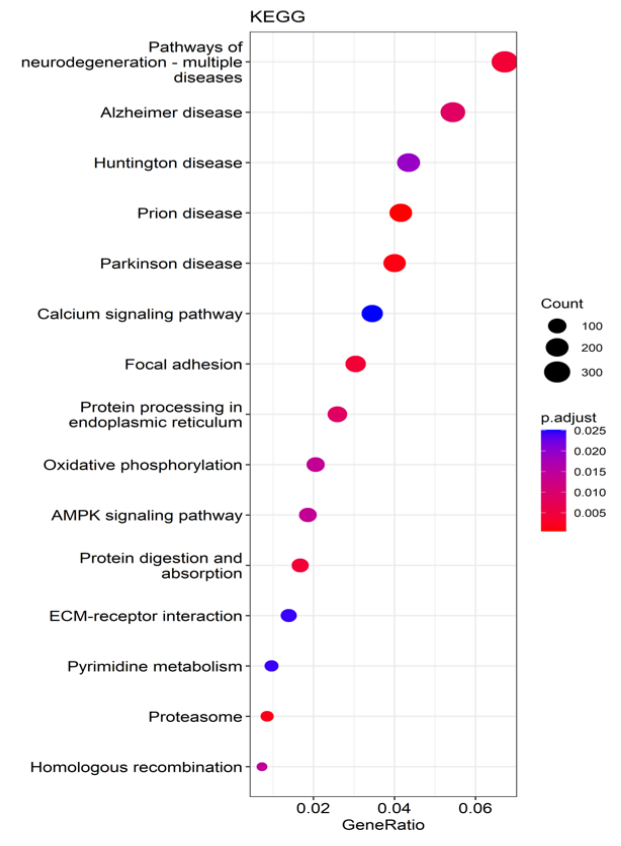
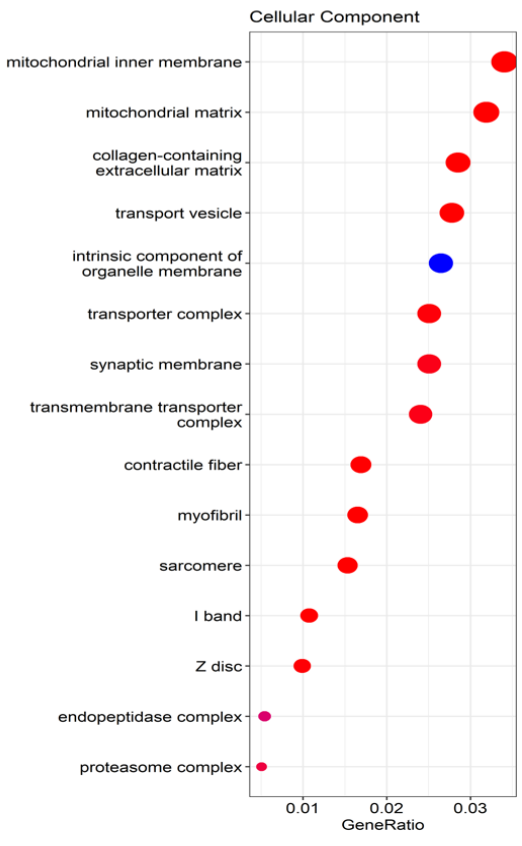
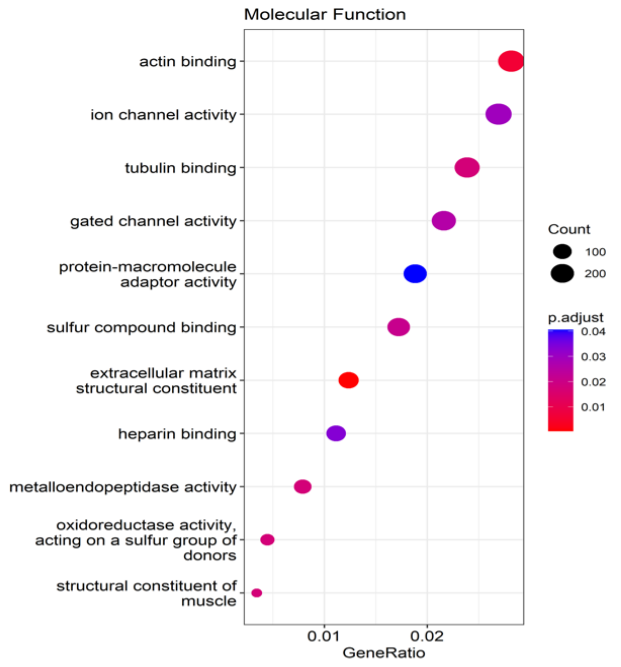
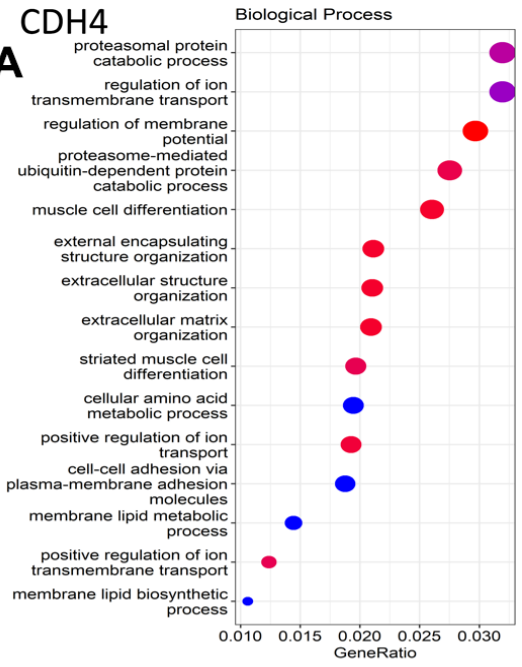


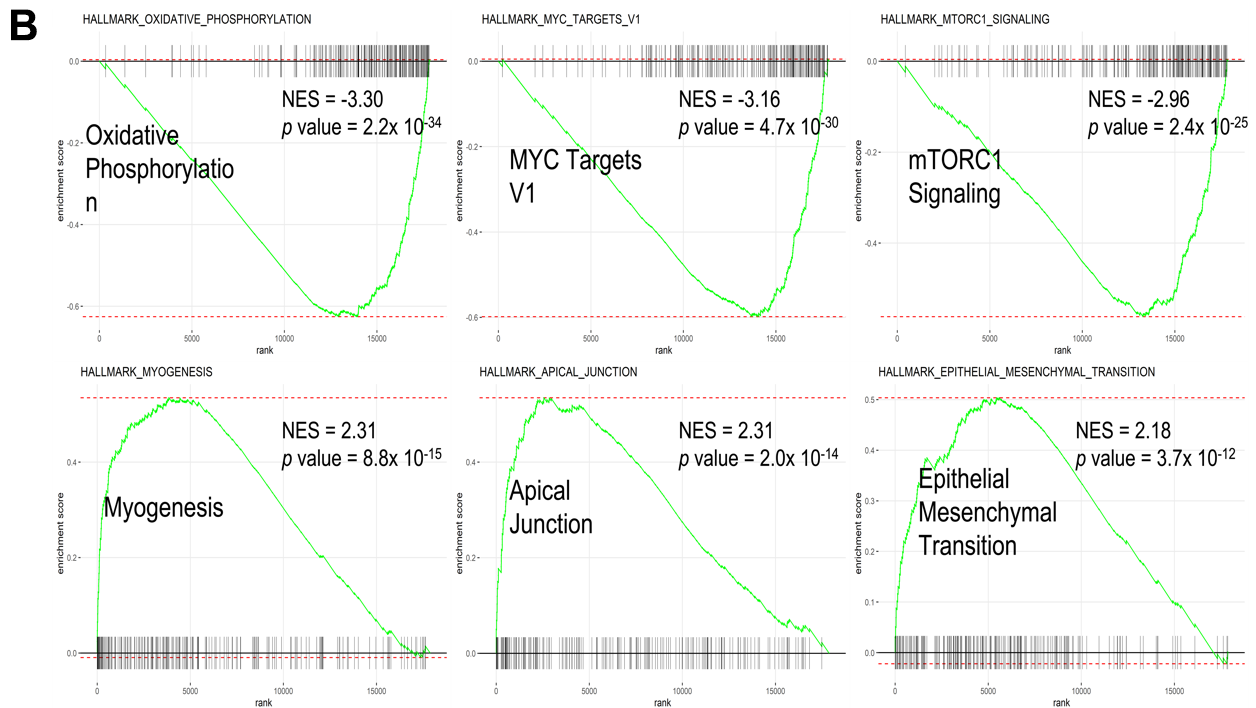




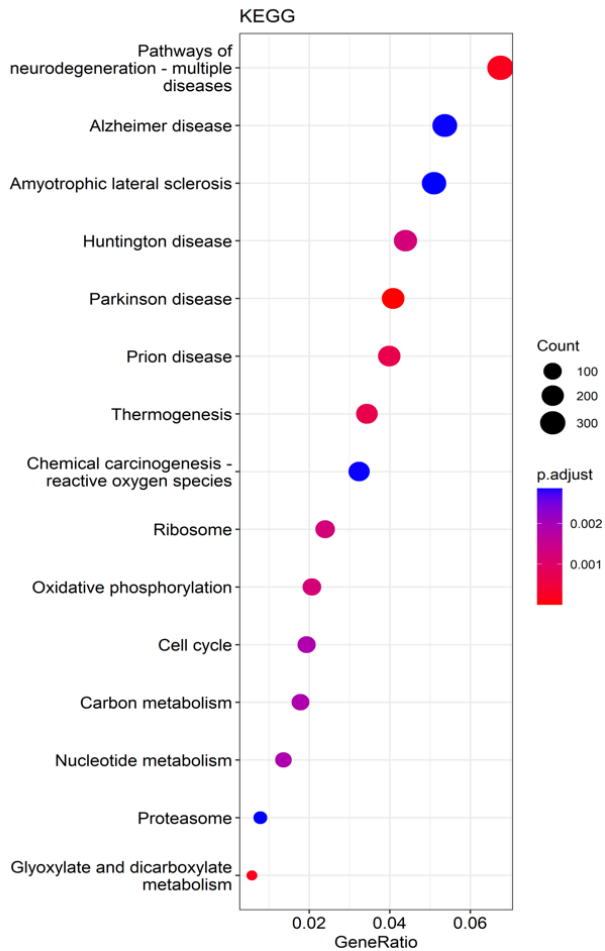
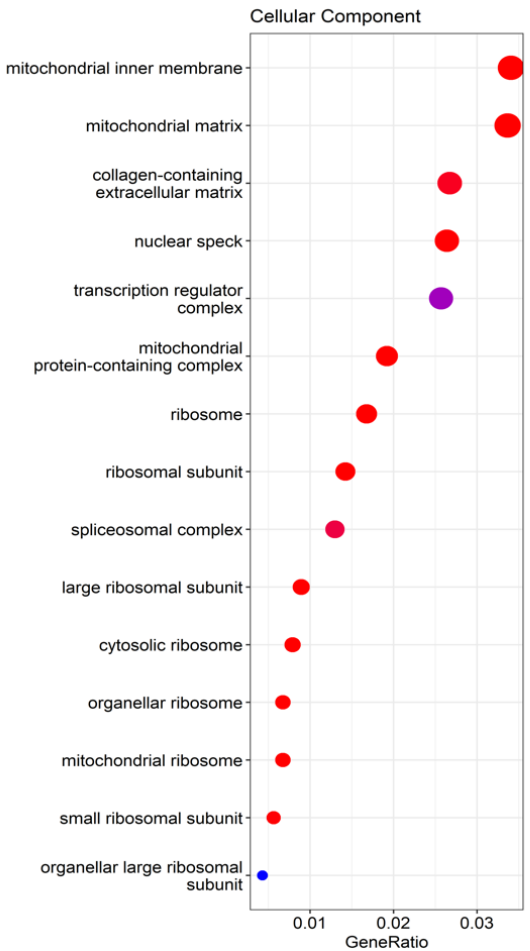
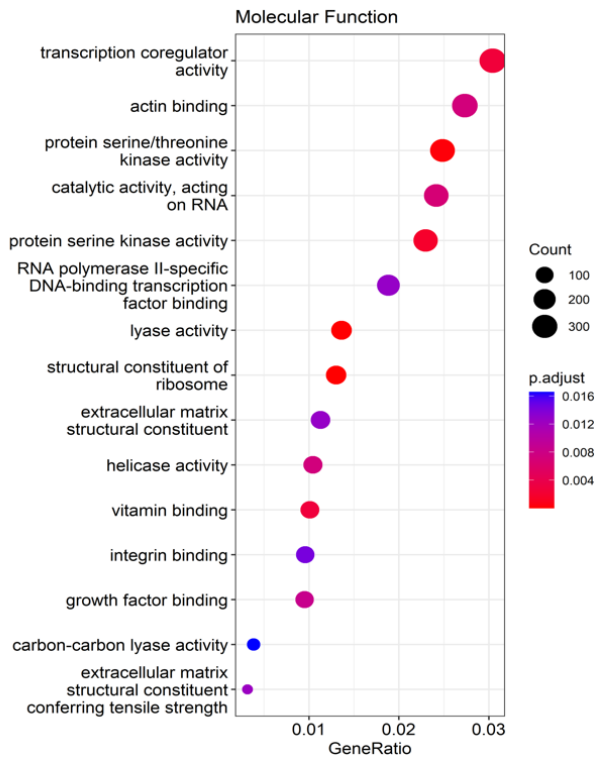
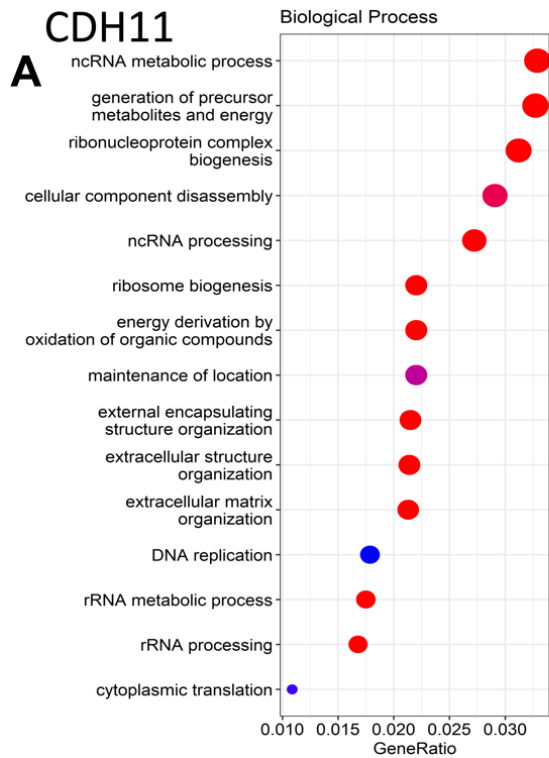
**Supplementary Figure 10. (A, B)** Gene Ontology (GO) analysis and Gene Set Enrichment Analysis (GSEA) based on genes co-expressed with *CDH2*. **(A)** Dot plots display biological processes, cellular components, molecular functions, and KEGG. The dot size is determined by the count of enriched genes in the pathway, and the color of the dots represents the significance of enrichment pathway. “clusterProfiler” package in R/Bioconductor was used to perform the GO analyses of dot plots. **(B)** Hallmark signaling pathway analysis of *CDH2* in breast cancer. Results of the analysis showed significant values of gene classes in the Hallmark database. Statistical significance was presented by  $p$  value, and the normalized enrichment score (NES) reflected the rank of gene classes.

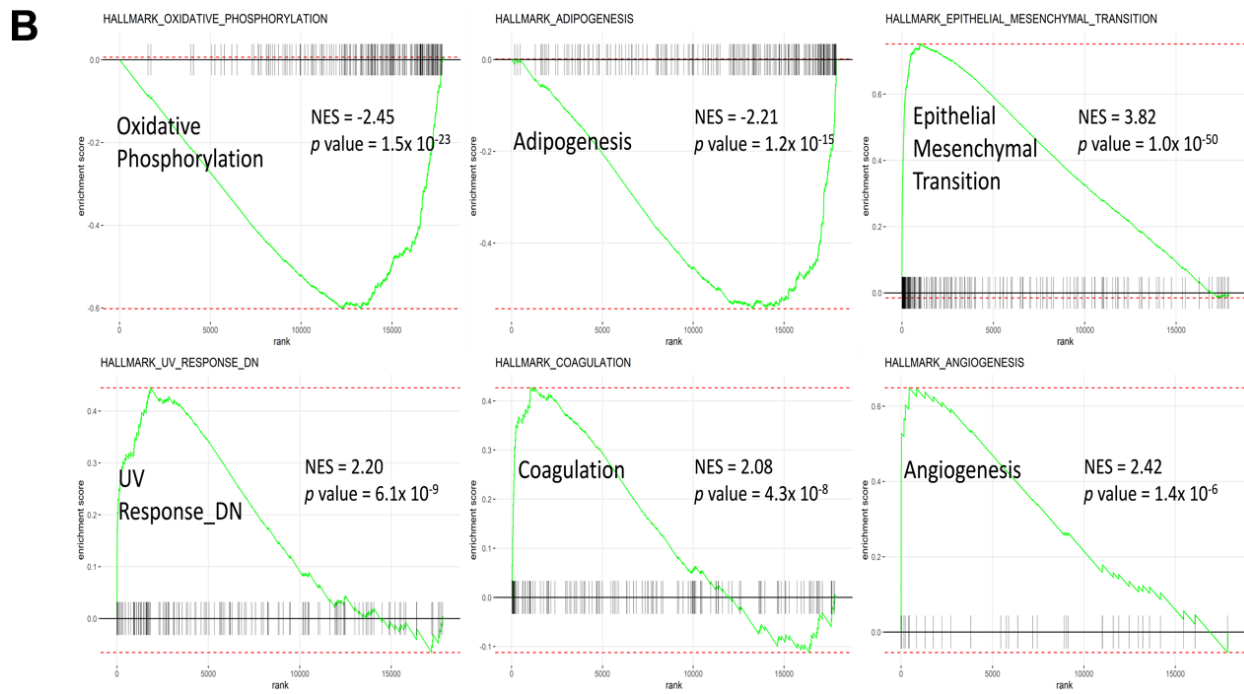
# A CDH4





**Supplementary Figure 11. (A, B)** Gene Ontology (GO) analysis and Gene Set Enrichment Analysis (GSEA) based on genes co-expressed with *CDH4*. (A) Dot plots display biological processes, cellular components, molecular functions, and KEGG. The dot size is determined by the count of enriched genes in the pathway, and the color of the dots represents the significance of enrichment pathway. “clusterProfiler” package in R/Bioconductor was used to perform the GO analyses of dot plots. (B) Hallmark signaling pathway analysis of *CDH4* in breast cancer. Results of the analysis showed significant values of gene classes in the Hallmark database. Statistical significance was presented by  $p$  value, and the normalized enrichment score (NES) reflected the rank of gene classes.

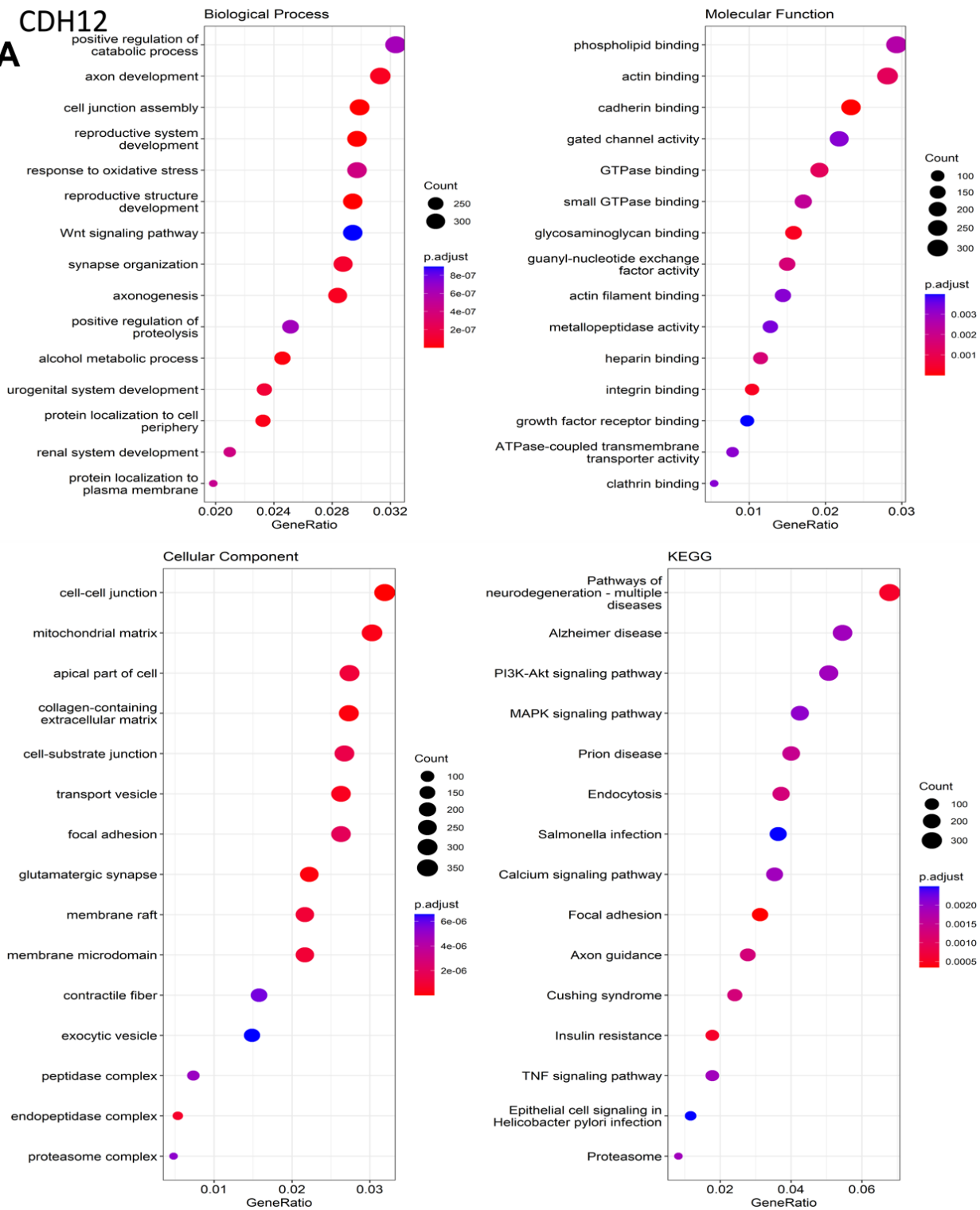


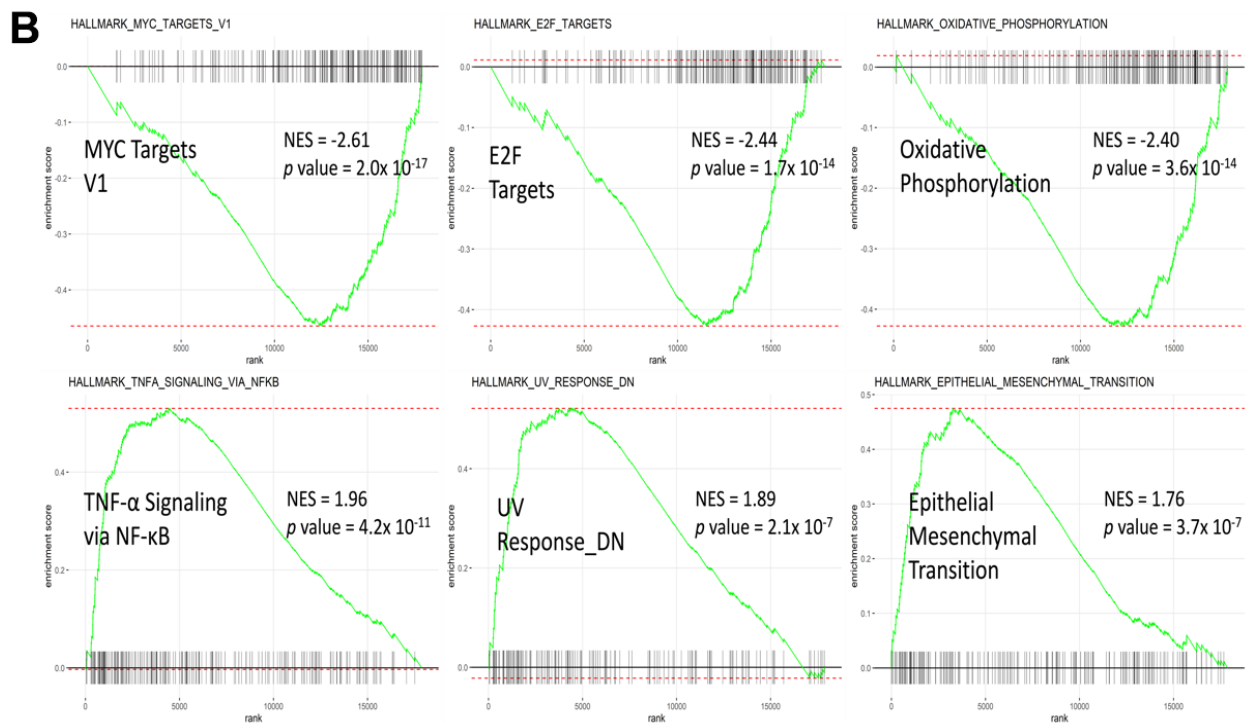


**Supplementary Figure 12. (A, B)** Gene Ontology (GO) analysis and Gene Set Enrichment Analysis (GSEA) based on genes co-expressed with *CDH11*. **(A)** Dot plots display biological processes, cellular components, molecular functions, and KEGG. The dot size is determined by the count of enriched genes in the pathway, and the color of the dots represents the significance of enrichment pathway. “clusterProfiler” package in R/Bioconductor was used to perform the GO analyses of dot plots. **(B)** Hallmark signaling pathway analysis of *CDH11* in breast cancer. Results of the analysis showed significant values of gene classes in the Hallmark database. Statistical significance was presented by *p* value, and the normalized enrichment score (NES) reflected the rank of gene classes.

# CDH12

A



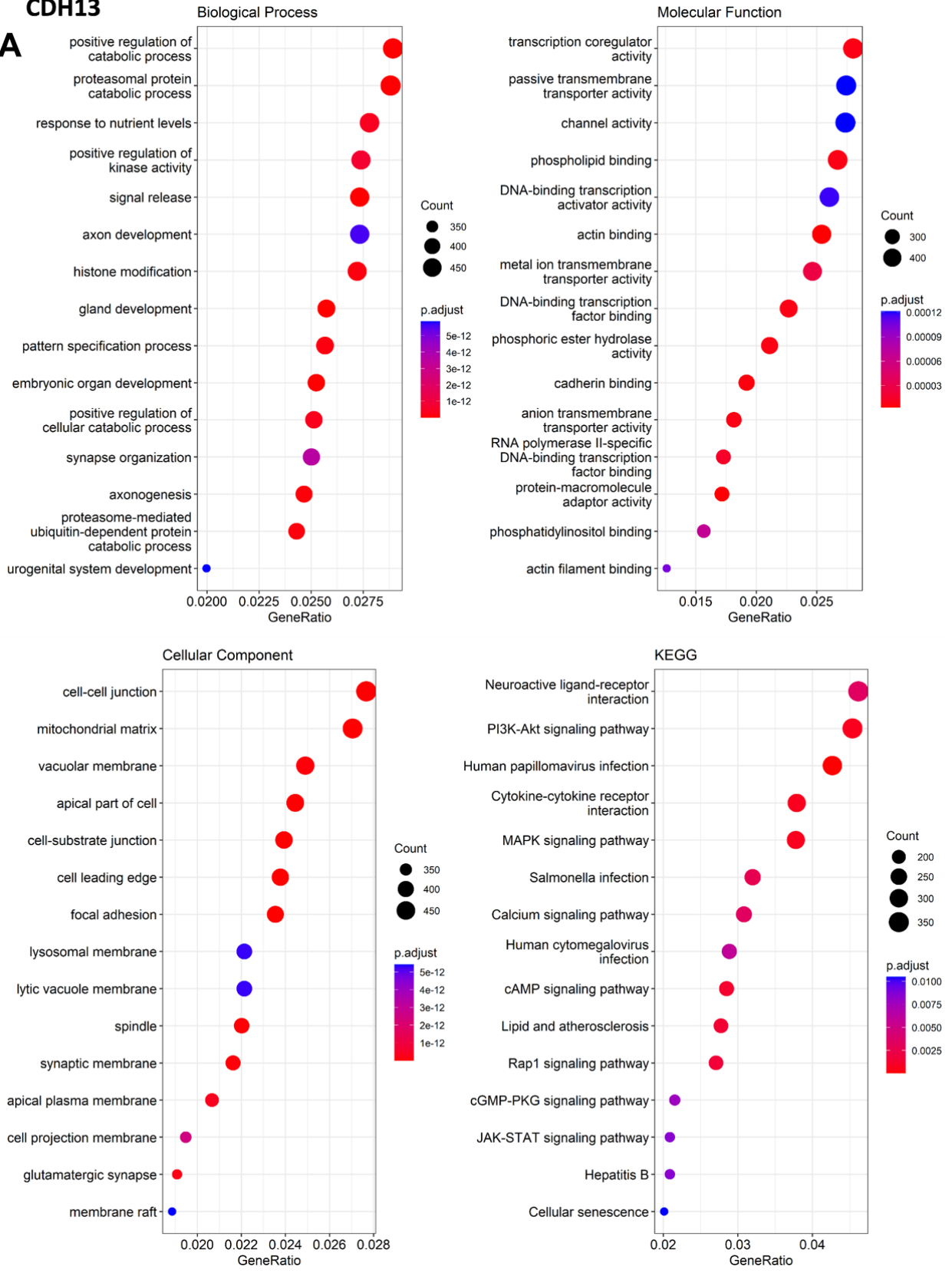


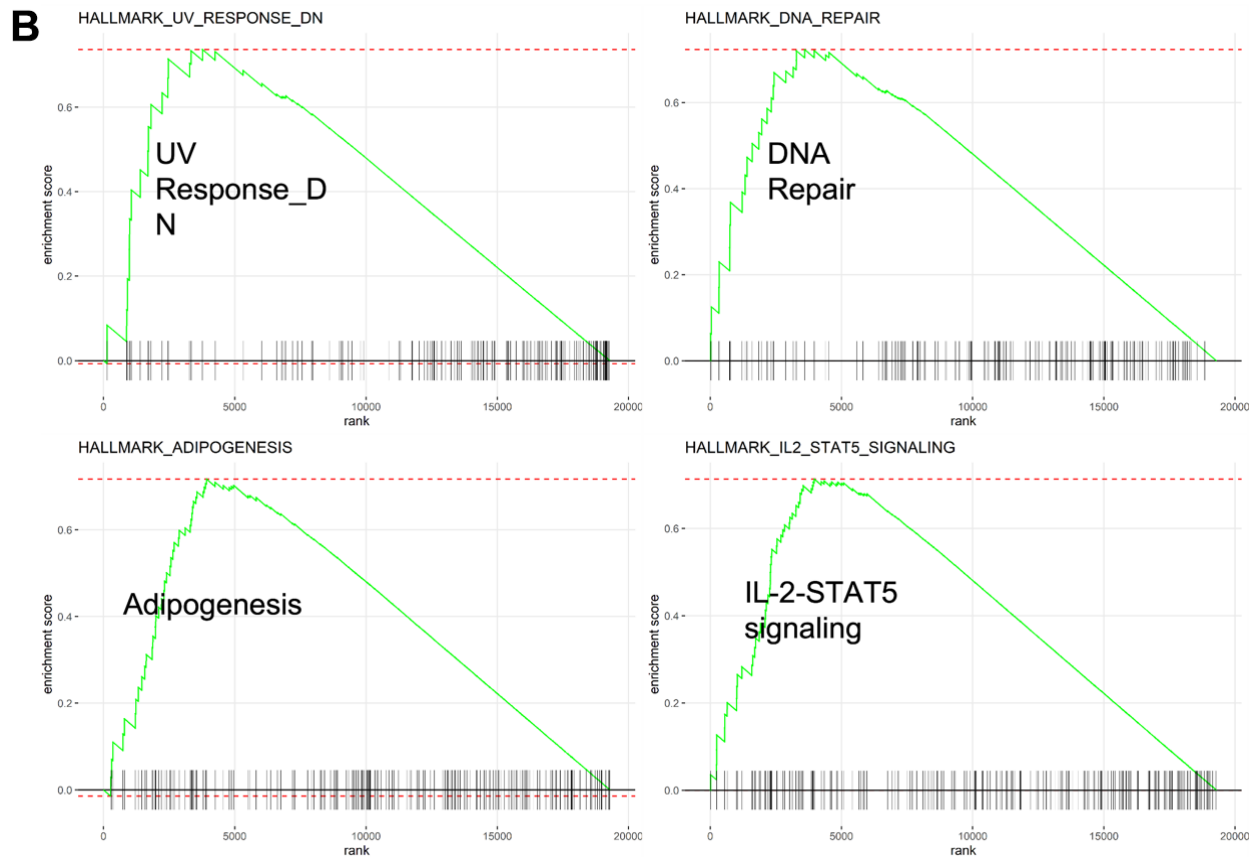
**Supplementary Figure 13. (A, B)** Gene Ontology (GO) analysis and Gene Set Enrichment Analysis (GSEA) based on genes co-expressed with *CDH12*. **(A)** Dot plots display biological processes, cellular components, molecular functions, and KEGG. The dot size is determined by the count of enriched genes in the pathway, and the color of the dots represents the significance of enrichment pathway. “clusterProfiler” package in R/Bioconductor was used to perform the GO analyses of dot plots. **(B)** Hallmark signaling pathway analysis of *CDH12* in breast cancer. Results of the analysis showed significant values of gene classes in the Hallmark database. Statistical significance was presented by  $p$  value, and the normalized enrichment score (NES) reflected the rank of gene classes.



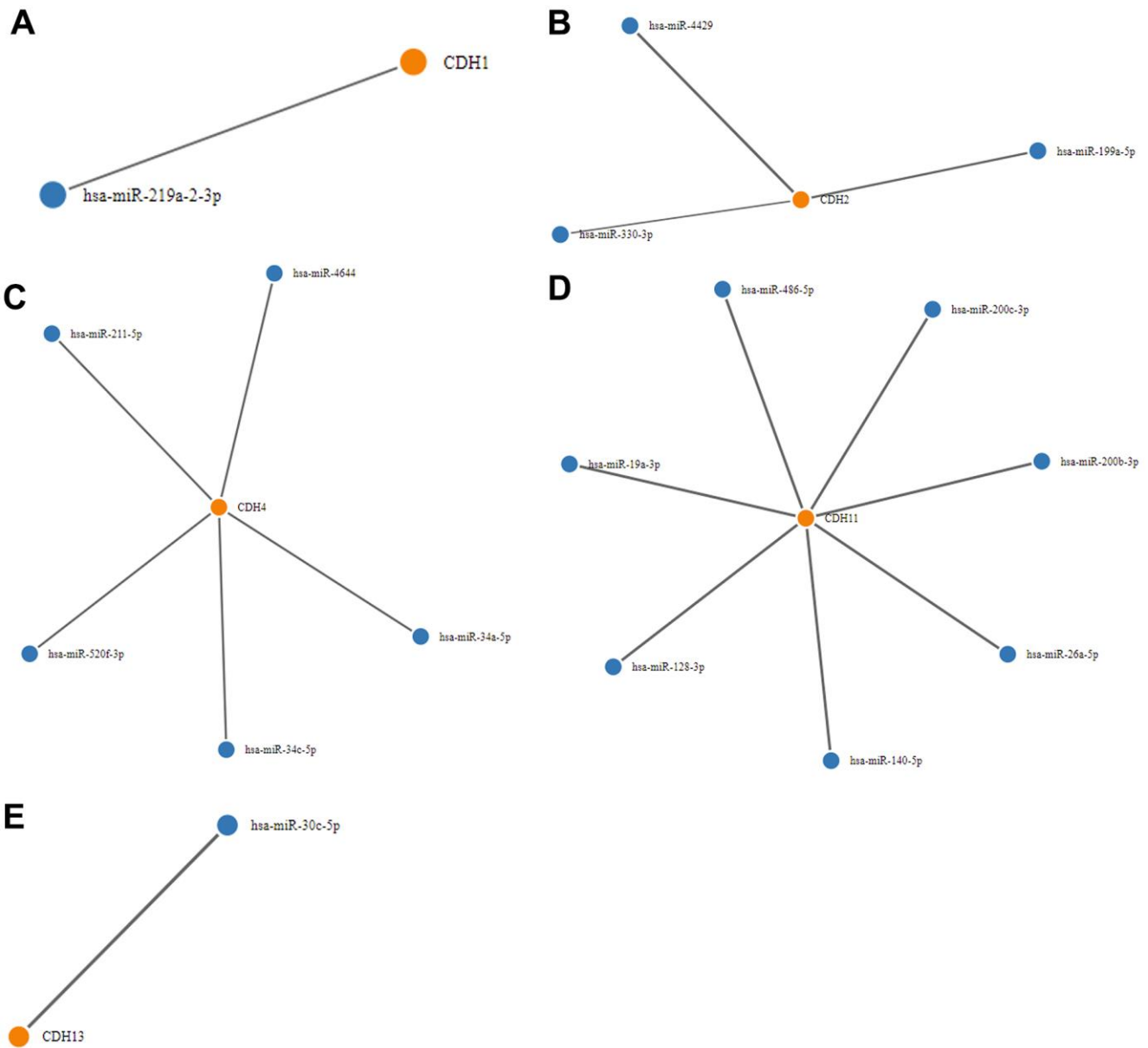
# CDH13

A



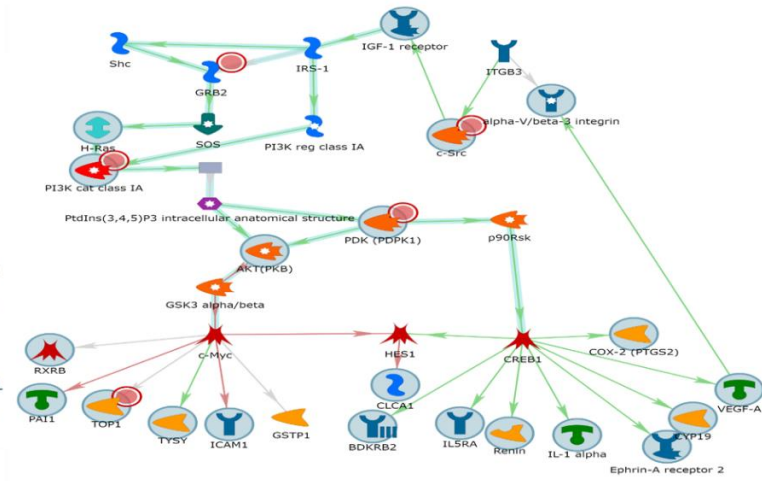
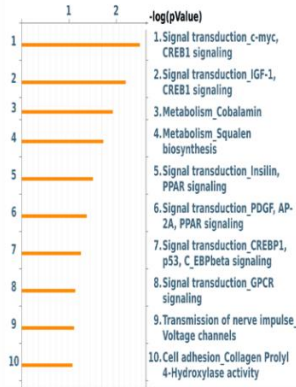


**Supplementary Figure 14. (A, B)** Gene Ontology (GO) analysis and Gene Set Enrichment Analysis (GSEA) based on genes co-expressed with *CDH13*. **(A)** Dot plots display biological processes, cellular components, molecular functions, and KEGG. The dot size is determined by the count of enriched genes in the pathway, and the color of the dots represents the significance of enrichment pathway. “clusterProfiler” package in R/Bioconductor was used to perform the GO analyses of dot plots. **(B)** Hallmark signaling pathway analysis of *CDH13* in breast cancer. Results of the analysis showed significant values of gene classes in the Hallmark database. Statistical significance was presented by *p* value, and the normalized enrichment score (NES) reflected the rank of gene classes.

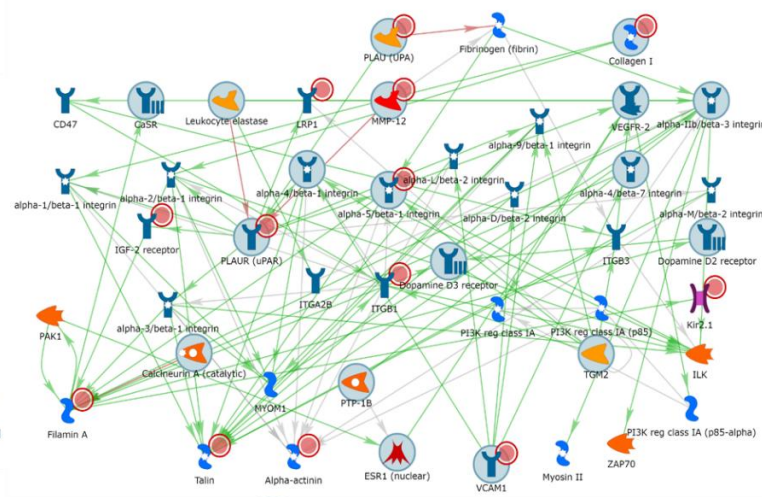
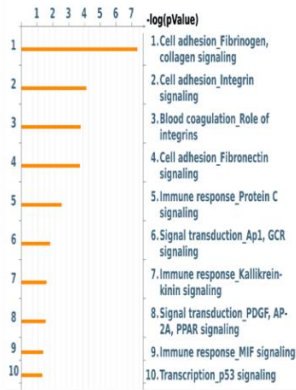


**Supplementary Figure 15. Analysis of micro-(mi)RNA networks with *CDH1/2/4/11/13* in breast cancer.** (A) *CDH1* demonstrated network interaction with hsa-miR-219a-2-3p in breast cancer development; (B) *CDH2* demonstrated network interaction with hsa-miR-330-3p, has-miR-4429, and hsa-miR-199a-5p; (C) *CDH4* demonstrated network interaction with hsa-miR-4644, hsa-miR-211-5p, hsa-miR-520f-3p, hsa-miR-34e-5p, and hsa-miR-34a-5p; (D) *CDH11* demonstrated network interaction with hsa-miR-486-5p, hsa-miR-200c-3p, hsa-miR-200b-3p, hsa-miR-26a-5p, hsa-miR-140-5p, hsa-miR-128-3p, and hsa-miR-19a-3p; (E) *CDH13* demonstrated network interaction with hsa-miR-30c-5p.

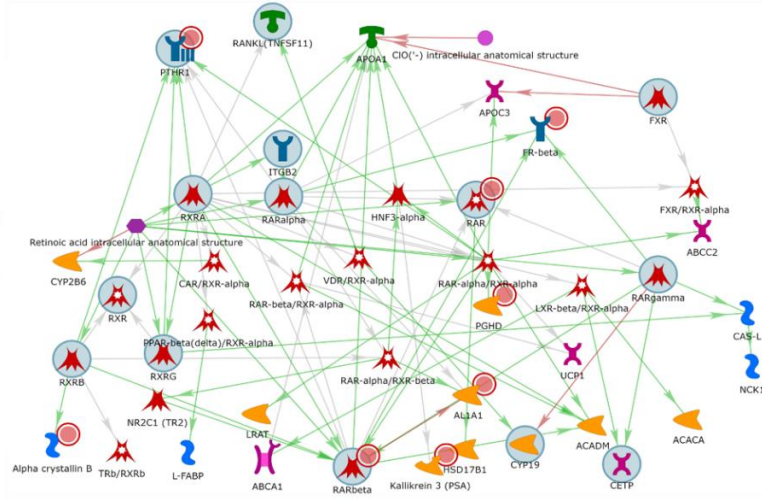
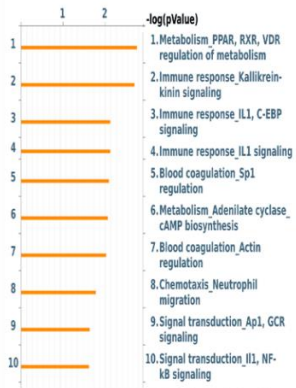
# A CDH1



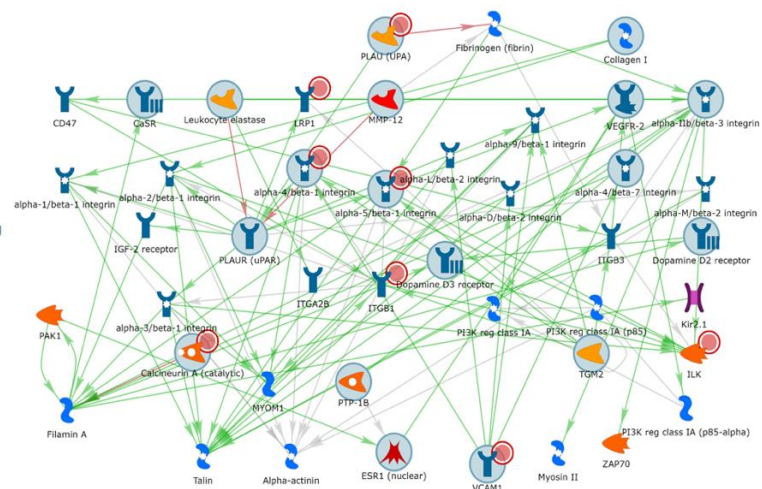
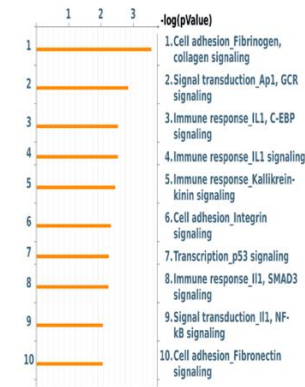
# CDH2



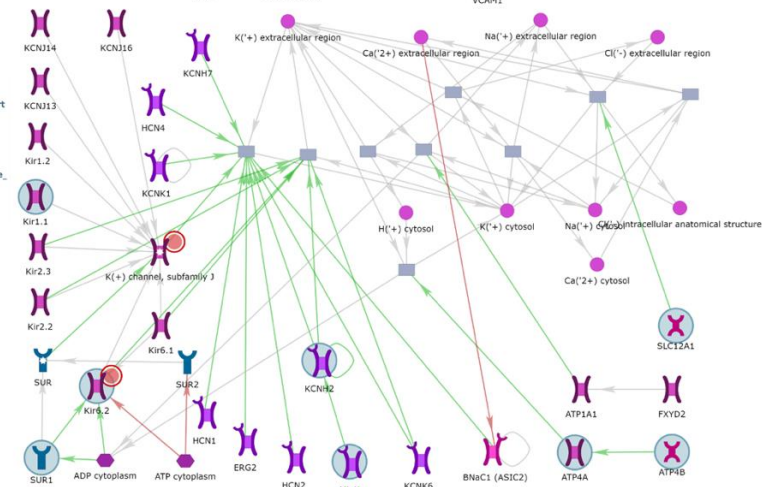
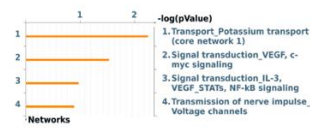
# CDH4



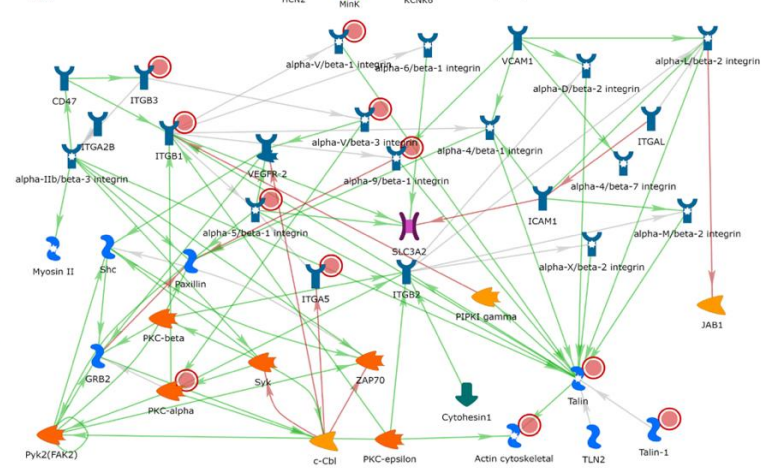
## B CDH11



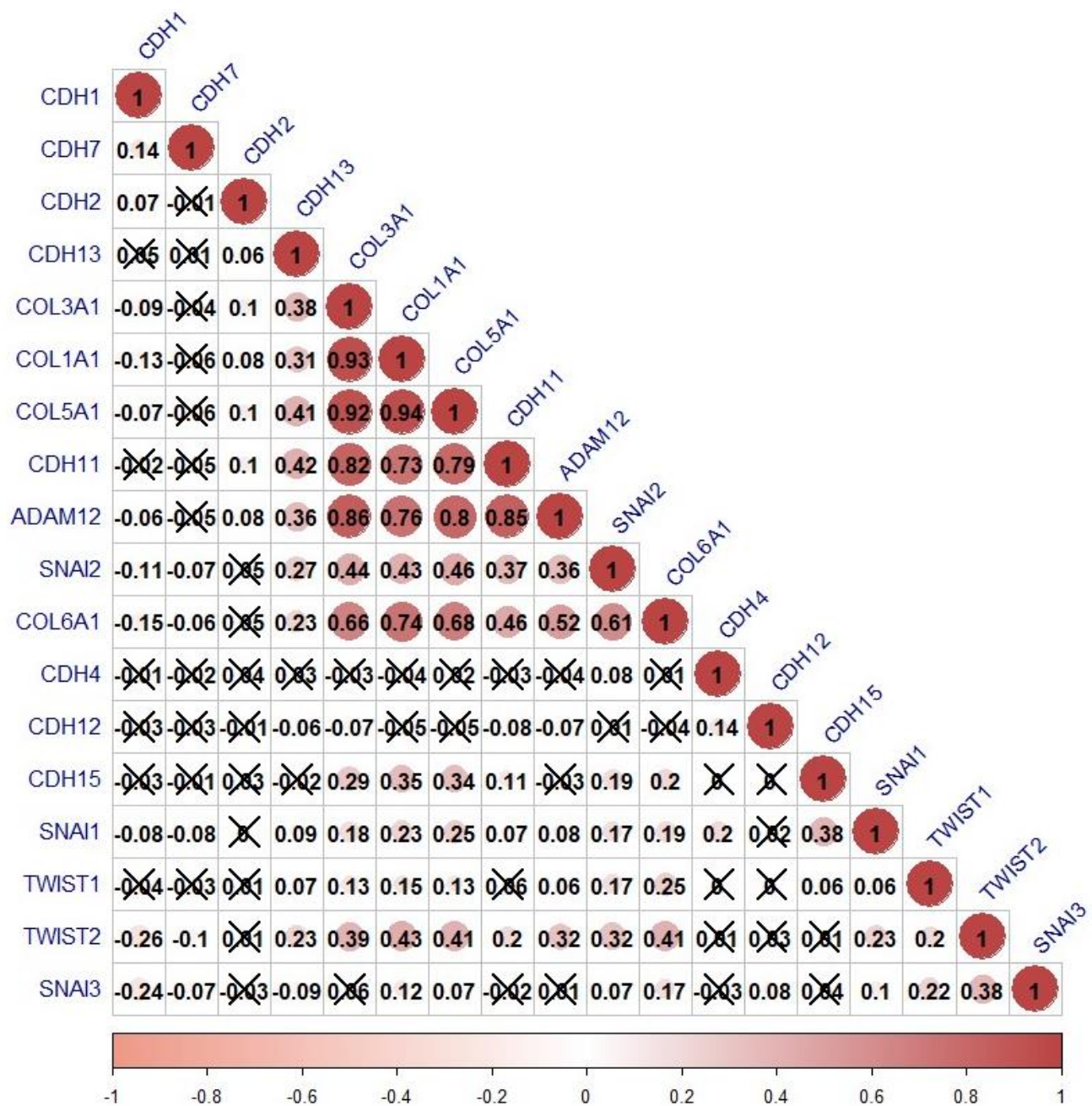
## CDH12



## CDH13



**Supplementary Figure 16. (A, B) Drug target networks analysis of genes co-expressed with cadherin (*CDH*) 1/2/4/11/12/13.** Genes co-expressed with CDH1/2/4/11/12/13 were integrated to implement drug target networks analysis, which formed a pathway list ordered by the  $-\log p$ -value on the left. (A) “Signal transduction\_c-myc, CREB1 signaling” was at the top of the drug target of CDH1; “Cell adhesion\_Fibrinogen, collagen signaling” was at the top of the drug target of CDH2; “Metabolism\_PPAR, RXR, VDR regulation of metabolism” was at the top of the drug target of CDH4; (B) “Cell adhesion\_Fibrinogen, collagen signaling” was at the top of the drug target of CDH11; “Transport\_Potassium transport (core work 1)” was at the top of the drug target of CDH12; “Cell adhesion\_Integrin signaling” was at the top of the drug target of CDH13. The figure demonstrates the interactions between genes and proteins. Symbols represent proteins. Arrows depict protein interactions (green, activation; red, inhibition).



**Supplementary Figure 17. Correlations between cadherin (CDH) family and epithelial-mesenchymal transition (EMT)-regulated genes in breast cancer using TCGA dataset.** The symmetric correlation matrix was created by the “corrplot” R package. The color represents the degree of pairwise correlation regarding Spearman’s rank correlation coefficient. Darker red and larger dot size mean stronger positive correlation, while orange indicates stronger negative correlation. The cross symbols represent non-significant correlation coefficient values ( $p$  value > 0.01).

## Supplementary Tables

**Supplementary Table 1A. Univariate Cox regression analysis of CDH1/2/4/11/12/13 and age, gender, tumor stage with overall survival in breast cancer (BRCA) patients.**

Univariate	BRCA			
	Overall survival			
	Coefficient	HR	(95% CI)	<i>p</i> value
Age	0.036	1.037	(1.023-1.050)	0.000***
gender male	-0.49	0.613	(0.084-4.450)	0.628
stage2	0.668	1.951	(1.117-3.405)	0.019*
stage3	1.374	3.95	(2.189-7.126)	0.000***
stage4	2.718	15.143	(7.074-32.417)	0.000***
CDH1	0.014	1.014	(0.913-1.127)	0.792
CDH2	0.101	1.106	(0.944-1.297)	0.213
CDH4	-0.066	0.936	(0.609-1.439)	0.764
CDH11	-0.025	0.976	(0.828-1.150)	0.769
CDH12	-0.291	0.747	(0.431-1.295)	0.299
CDH13	0.264	1.302	(1.053-1.611)	0.015*

The coefficient represents the regression coefficient. HR represents the hazard ratio, and 95% confidential interval are showed in (95% CI).

**Supplementary Table 1B. Univariate Cox regression analysis of CDH1/2/4/11/12/13 and age, gender, tumor stage with overall survival in molecular subtype-Luminal of breast cancer (BRCA) patients.**

Univariate	BRCA-luminal			
	Overall survival			
	Coefficient	HR	(95% CI)	<i>p</i> value
Age	0.039	1.039	(1.020-1.059)	0.000***
gender male	-15.811	0	(0.000-Inf)	0.995
stage2	0.559	1.749	(0.899-3.403)	0.1
stage3	1.106	3.021	(1.448-6.303)	0.003**
stage4	2.223	9.232	(3.471-24.552)	0.000***
CDH1	0.069	1.071	(0.917-1.252)	0.387
CDH2	0.159	1.172	(0.947-1.451)	0.144
CDH4	-0.197	0.821	(0.312-2.160)	0.69
CDH11	-0.032	0.969	(0.761-1.234)	0.798
CDH12	-0.419	0.658	(0.297-1.454)	0.3
CDH13	0.331	1.392	(0.973-1.992)	0.071

The coefficient represents the regression coefficient. HR represents the hazard ratio, and 95% confidential interval are showed in (95% CI).

**Supplementary Table 1C. Univariate Cox regression analysis of CDH1/2/4/11/12/13 and age, gender, tumor stage with overall survival in molecular subtype-HER2 of breast cancer (BRCA) patients.**

<b>BRCA-HER2</b>				
<b>Univariate</b>	<b>Overall survival</b>			
	<b>Coefficient</b>	<b>HR</b>	<b>(95% CI)</b>	<b>p value</b>
Age	0.086	1.09	(1.018-1.168)	0.014*
stage2	-1.178	0.308	(0.022-4.285)	0.381
stage3	0.474	1.606	(0.112-22.999)	0.727
stage4	3.033	20.763	(1.181-365.073)	0.038*
CDH1	-0.404	0.668	(0.429-1.040)	0.074
CDH2	0.459	1.583	(0.653-3.835)	0.309
CDH4	-29.735	0	(0-0.072)	0.032*
CDH11	0.4	1.492	(0.351-6.339)	0.587
CDH12	3.279	26.541	(1.308-538.706)	0.033*
CDH13	-0.442	0.643	(0.043-9.605)	0.749

The coefficient represents the regression coefficient. HR represents the hazard ratio, and 95% confidential interval are showed in (95% CI).

**Supplementary Table 1D. Univariate Cox regression analysis of CDH1/2/4/11/12/13 and age, gender, tumor stage with overall survival in molecular subtype-Basal of breast cancer (BRCA) patients.**

<b>BRCA-basal</b>				
<b>Univariate</b>	<b>Overall survival</b>			
	<b>Coefficient</b>	<b>HR</b>	<b>(95% CI)</b>	<b>p value</b>
Age	0.023	1.023	(0.986-1.063)	0.226
stage2	18.162	77244950	(2.8e+07-2.1e+08)	0.000***
stage3	19.179	2.13e+08	(7.5e+07-6.1e+08)	0.000***
stage4	22.124	4.06e+09	(3.7e+08-4.5e+10)	0.000***
CDH1	-0.048	0.953	(0.651-1.395)	0.805
CDH2	-0.26	0.771	(0.553-1.074)	0.124
CDH4	-0.089	0.915	(0.617-1.358)	0.659
CDH11	0.427	1.533	(1.064-2.209)	0.022*
CDH12	0.899	2.457	(1.224-4.935)	0.012*
CDH13	0.156	1.169	(0.684-2.000)	0.567

The coefficient represents the regression coefficient. HR represents the hazard ratio, and 95% confidential interval are showed in (95% CI).



**Supplementary Table 2. Pathway analysis of genes co-expressed cadherin 1 (CDH1) from the MetaCore database (with p-value < 0.05 set as the cutoff value) (Supplementary Table 2 and Figure 8).**

#	Maps	p-Value	Network objects from active data
1	Immune response_B cell antigen receptor (BCR) pathway	1.298E-16	STIM1, Calcineurin A (catalytic), GRB2, alpha-4/beta-1 integrin, ICAM1, c-Rel (NF-kB subunit), H-Ras, NF-kB p50/c-Rel, ERK1/2, EGR1, c-Raf-1, BCAP, Fibronectin, CD19, VAV-1, Rac1, IP3 receptor, BAD, Syk, Cyclin D2, Shc, PI3K reg class IA (p85), GSK3 beta, Rb protein, CD79A, CDK4, FKHR, MEK6(MAP2K6), VAV-2, MEK2(MAP2K2), GSK3 alpha/beta, Bcl-XL, MEK1/2, CDC42, WASP, Actin cytoskeletal, NF-kB, AKT(PKB), NF-kB p50/p65, PDK (PDPK1), TAK1(MAP3K7), NF-AT2(NFATC1), MEKK4(MAP3K4), MEK1(MAP2K1), VCAM1, RelA (p65 NF-kB subunit), LRRK1, B-Raf, NF-kB1 (p50), K-RAS, ETS1, Lyn, PIP5KIII, CIN85, CD79 complex, PP2A catalytic, PIP5KI, PKC-beta2, NFKBIA, PI3K cat class IA (p110-delta), CARD11, CDK6, HPK1(MAP4K1), PKC-beta, p70 S6 kinase1, Calmodulin, CalDAG-GEFIII, CKLFSF7, MEKK1(MAP3K1), ATF-2, MALT1, IKK-beta, PLC-gamma, CD79B, Bcl-10, Calcineurin B (regulatory), PLC-gamma 2, p38 MAPK, Elk-1
2	Oxidative stress_ROS-induced cellular signaling	6.173E-16	Casein kinase II, alpha chains, p38alpha (MAPK14), Tuberin, SREBP1 (nuclear), SCD, ERK1/2, EGR1, VEGF-A, PKA-reg (cAMP-dependent), TXNIP (VDUP1), p21, Bak, Cytochrome c, FASN, E2f1, Syk, Bax, GSK3 beta, FTH1, IRP2, GRP75, MDM2, IL-6, NF-kB, AKT(PKB), Catalase, NF-kB p50/p65, Cyclin B1, c-Src, TNF-alpha, NOTCH1 (NICD), Thioredoxin, Chk2, ACACA, RelA (p65 NF-kB subunit), KEAP1, IRP1, HIF1A, SRX1, AMPK alpha subunit, Pin1, NIK(MAP3K14), Isoform p66 Shc, Glutaredoxin 1, NFKBIA, HSPA1A, GSTP1, COX-2 (PTGS2), ELAVL1 (HuR), HSF1, PKC-beta, NOTCH3 (3ICD), PRKD1, p70 S6 kinase1, GPX1, PKC, LKB1, PTEN, MEKK1(MAP3K1), HES1, HSP27, IKK-beta, DLC1 (Dynein LC8a), c-Abl, Cyclin D1, JNK(MAPK8-10), HIF-prolyl hydroxylase, HDAC1, SAE2, SP1, p53, NRF2, ADAM17, p38 MAPK, APEX, PAI1, NALP3
3	Development_Negative regulation of WNT/Beta-catenin signaling in the cytoplasm	6.950E-16	Casein kinase I delta, NOTCH1 receptor, CXXC4, VHL, DP1, NKD1, PP1-cat, RIPK4, Presenilin 1, Alpha-1 catenin, Laforin, FAF1, Casein kinase I epsilon, Beta-catenin, CYLD, CXXC5, DAB2, Nucleoredoxin, Dsh, Casein kinase I alpha, Rac1, YAP1 (YAp65), G-protein alpha-13, WWP1, STK4, SIAH1, GSK3 alpha/beta, LATS2, G-protein beta/gamma, WDR26, Skp2/TrCP/FBXW, TAZ, Axin, RACK1, HECTD1, LRP5/LRP6, Prickle-1, c-Cbl, STK3, Tcf(Lef), E2F1, Amer1, PP2A catalytic, SENP2, RNF185, A20, Cull1/Rbx1 E3 ligase, YAP1/TAZ, CDK6, ELAVL1 (HuR), PEG3, WNT5A, Malin, PKC-alpha, Porf-2, WNT, Beclin 1, Cyclin D1, p53, NKD2, DACT3, Frizzled, DACT1
4	Immune response_IFN-alpha/beta signaling via PI3K and NF-kB pathways	1.750E-15	Tuberin, AKT1, Cyclin D3, ISG15, IRS-2, Tyk2, RPS6, DHFR, NMI, eIF4E, ERK1/2, c-Raf-1, CDC25A, IFN-alpha/beta receptor, p21, IFNAR1, PKC-epsilon, CDK1 (p34), I-kB, p70 S6 kinases, PI3K reg class IA (p85), GSK3 beta, NF-kB2 (p100), Rb protein, CDK4, EMSY, IFN-alpha, p19, ISG54, CAK complex, CREB1, p130, MEK1/2, RSAD2, b-Myb, NF-kB, AKT(PKB), PDK (PDPK1), p107, PU.1, pRB/E2F4, IFI17, PI3K cat class IA, RelA (p65 NF-kB subunit), NF-kB2 (p52), PKC-delta, TRAF2, p130/E2F4, E2F1, p107/E2F4, IFNAR2, eIF4B, p90RSK1, eIF4G1/3, NIK(MAP3K14), MNK1, CDK2, PCNA, 4E-BP1, GBP1, IFIT1, E2F4, PKC-alpha, Cyclin E, eIF4A, FOXO3A, IRF7, MNK2(GPRK7), Cyclin A
5	Immune response_IL-4-induced regulators of cell growth, survival, differentiation and metabolism	2.174E-14	ATP6V1B2, RARbeta, DHA2, MCM5, IL-4R type I, CCR2, PPAR-alpha, SOCS1, CDC25A, p21, Cytochrome c, STAT1, Loricrin, CPT-1A, Filaggrin, EGR2 (Krox20), Bax, CDK4, FKHR, SOCS3, Bcl-XL, ACADM, FasL(TNFSF6), Osteoprotegerin, AKT(PKB), PPAR-gamma, GATA-3, A-FABP, MMP-13, PLEKHF1, ANGPTL4, MCM4, IL-4R type II, Cyclin D, CYP2E1, IL4RA, Bcl-6, SK4/IK1, Cathepsin V, CDK2, CDK6, AP-1, Cyclin E, HSD3B1, FOXO3A, PERC, STAT5, Cyclin A, STAT6, LPL
6	Neurogenesis_NGF/TrkA MAPK-mediated signaling	1.343E-13	SPHK1, NEFL, TrkA, ERK5 (MAPK7), CDK5, GRB2, APS, Fra-1, H-Ras, ERK1/2, MEF2C, CrkL, EGR1, PP2A regulatory, SGK1, PKA-reg (cAMP-dependent), CRK, c-Raf-1, FRS2, DNAJA3 (TID1), p21, VGF, PKC-epsilon, Ephrin-A receptor 2, IP3 receptor, TY3H, Shc, MAPKAPK2, PLC-gamma 1, MEK6(MAP2K6), MAP2K5 (MEK5), KIDINS220, CREB1, MEK1/2, PLAUR (uPAR), M-Ras, RGS2, p107, Stromelysin-1, c-Src, KCTD11, GAB2, SHPS-1, MATK, RIN, B-Raf, NF-kB1 (p50), JunB, K-RAS, PKC-delta, PP2A catalytic, C3G, SH2B, p90Rsk, p130CAS, NGF, AP-1, Calmodulin, MAGI-2, PKC-lambda/iota, SHP-2, Cyclin D1, SORBS1, MMP-10, SP1, PVR, JMJD3, RIT, p38 MAPK, Elk-1, PKA-cat (cAMP-dependent), FosB
7	Development_Differentiation of white adipocytes	4.070E-13	p38alpha (MAPK14), SREBP1 (nuclear), GRB2, BMP4, H-Ras, ERK1/2, FOXC2, c-Raf-1, SMAD4, PRKAR1A, SREBP1 precursor, Shc, HIVEP2, Rb protein, Resistin, FTase-alpha, MEK2(MAP2K2), CREB1, MEK1/2, PPARGC1 (PGC1-alpha), INSIG1, p107, PPAR-gamma, TAK1(MAP3K7), MEK1(MAP2K1), A-FABP, CIDEC, p90RSK1, LIPS, RIP140, PSAT, Factor D, FTase, TAB1, Angiotensinogen, LXR-alpha, BMPR1A, SMAD1, Leptin, BMP2, LPL, Perilipin, C/EBPalpha, C/EBPdelta
8	Role of activation of WNT signaling in the progression of lung cancer	1.531E-12	DVL-3, RUNX3, WNT3A, FZD6, Oct-3/4, NKD1, SFRP2, Krm1, Lef-1, DVL-1, TCF7L2 (TCF4), DKK1, FZD8, Beta-catenin, Matrilysin (MMP-7), VEGF-A, p21, Dsh, Rac1, ING4, GSK3 beta, FZD2, Survivin, Axin2, EZH2, SKP2, FZD9, FZD7, DVL-2, Axin, CD147, RUVBL1, WNT4, ROR2, hASH1, WNT9A, Tcf(Lef), Porcn, WNT3, FZD3, ARD1, WNT1, SFRP4, WNT2B, WNT5A, LKB1, MEKK1(MAP3K1), WNT, WNT10B, LRP6, SUZ12, Cyclin D1, SFRP1, p38 MAPK, Frizzled, NOTCH3

9	Development_Negative regulation of WNT/Beta-catenin signaling in the nucleus	2.248E-12	ZNF703, Casein kinase I delta, AKT1, Calcineurin A (catalytic), RUNX3, Oct-3/4, VHL, Lef-1, PGAM5, Alpha-1 catenin, TCF7L2 (TCF4), 14-3-3, Jade-1, Casein kinase I epsilon, Beta-catenin, VEGF-A, BCL9/B9L, PC1-CTT, TLE, Dsh, Menin, GSK3 beta, Nephrocystin-4, HDAC2, HIC1, LATS2, RANBP3, CtBP, PJA2, HIC5, PPAR-gamma, Axin, TAK1(MAP3K7), SOX9, TCF7 (TCF1), KDM2, LRP5/LRP6, TRRAP, WWOX, NARF, c-Cbl, PKC-delta, Tcf(Lef), E2F1, SOX17, SENP2, Cul1/Rbx1 E3 ligase, NLK, RNF43, WNT5A, SOX2, WNT, FOXO3A, eNOS, CHIBBY, HDAC1, Plakoglobin, RUVBL2, CDX1, Frizzled, Histone H1, DACT1
10	Stellate cells activation and liver fibrosis	2.435E-12	COL1A1, GRO-2, Biglycan, TNF-R2, GRB2, ICAM1, WNT3A, CCL2, H-Ras, Beta-catenin, c-Raf-1, TRADD, SMAD4, PDGF-R-alpha, DAB2, Dsh, Smoothed, I-kB, Shc, PI3K reg class IA (p85), GSK3 beta, RIPK1, MEK2(MAP2K2), MMP-2, COL1A2, ERK2 (MAPK1), AKT(PKB), PDGF receptor, NF-kB p50/p65, TNF-R1, ERK1 (MAPK3), TNF-alpha, MEK1(MAP2K1), PI3K cat class IA, PTCH1, TRAF2, Tcf(Lef), TGF-beta receptor type II, IL1RAP, KLF6, NIK(MAP3K14), TIMP1, TRAF1, ACTA2, Cyclin D1, IRAK1/2, SMAD3, SPI, Elk-1, Frizzled, TLR2, PDGF-R-beta
11	Development_Positive regulation of WNT/Beta-catenin signaling in the cytoplasm	3.380E-12	Casein kinase II, alpha chains, Bcl-9, EGF, BIG1, GRB2, IRS-2, NKD1, UBE2B, PPI-cat, RIPK4, Alpha-1 catenin, 14-3-3, Beta-catenin, TGIF, SMAD4, Dsh, Rac1, YAP1 (YAp65), CDK1 (p34), PPP2R2A, SIAH1, USP25, GSK3 alpha/beta, ERK2 (MAPK1), AKT(PKB), Axin, GSKIP, HECTD1, ITGB1, LRP5/LRP6, SIAH2, Tcf(Lef), 14-3-3 zeta/delta, TGT, HSP105, PKA-reg type II (cAMP-dependent), PP2A catalytic, RNF220, COX-2 (PTGS2), Travid, BIG2, Miz-1, USP9X, WNT, USP7, Joubertin, PP2C alpha, JNK(MAPK8-10), SMAD3, NKD2, MITF, PKA-cat (cAMP-dependent), Frizzled, SET7, DACT1 p38alpha (MAPK14), Maspin, PLSCR3, Calcineurin A (catalytic), MPTP complex, Apaf-1, Cathepsin H, Granzyme B, ROCK1, ERK1/2, MUL1, RAD9A, PP2C, VDAC 2, Bik, Bak, Cytochrome c, Caspase-8, OPA1, Endonuclease G, NIP3, BAD, GZMH, Bax, SOD1, RASSF1, PINK1, PPI-cat alpha, AMBRA1, Mitofusin 1, Caspase-2, Bcl-XL, MTCH2, VDAC 1, MIDUO, Calpain 1(mu), Mcl-1, Cathepsin D, Granzyme K, Cathepsin L, IFI27, Aif, GC1QBP, PKC-delta, 14-3-3 zeta/delta, MAPI, Pin1, PP2A catalytic, PARL, Caspase-9, Metaxin 1, BMF, JSAP1, RAD9, CDK2, ATF-2, SLC25A3, TIMM8A, tBid, Beclin 1, HtrA2, Cyclin A, JNK(MAPK8-10), JNK2(MAPK9), Caveolin-1, DNMI1 (DRP1), Calcineurin B (regulatory), Smac/Diablo, p38 MAPK, Bid
12	Apoptosis and survival_Regulation of apoptosis by mitochondrial proteins	4.849E-12	IL-7 receptor, MHC class II, ICOS-L, IL-7, Tyk2, IFN-gamma, BATF, CXCR5, CD28, OX40(TNFRSF4), KLF2, SLAM, IFN-alpha/beta receptor, STAT1, TRIM, I-kB, PI3K reg class IA (p85), FKHR, IFN-alpha, RIPK1, CD4, CD84, IL-6, CTLA-4, Fyn, NF-kB, AKT(PKB), ICOS, IL-2, CD40L(TNFSF5), BAFF(TNFSF13B), CD80, Osteopontin, PI3K cat class IA, DDX6, PI3K reg class IA (p85-alpha), MCPIP, TRAF2, BAFF-R, IL4RA, NIK(MAP3K14), Bcl-6, A20, JAK3, CARD11, RC3H2, 4E-BP1, Hedls, c-Maf, p70 S6 kinase1, MALT1, IKK-beta, CXCL13, SAP, PD-1, Bcl-10, TLR7, CD40(TNFRSF5), IL-21 receptor, STAT6, CD86, BLIMP1 (PRDI-BF1)
13	T follicular helper cell dysfunction in SLE	4.885E-12	RECK, ERK5 (MAPK7), GRB2, CCL2, H-Ras, eIF4E, ERK1/2, MEF2C, EGR1, MSK1/2 (RPS6KA5/4), c-Raf-1, HDAC4, p21, Angiotensin II, p47-phox, Syk, Shc, p70 S6 kinases, FKHR, cPLA2, MEK6(MAP2K6), MAP2K5 (MEK5), MMP-2, CREB1, IL-6, MEK1/2, G-protein beta/gamma, PPARGC1 (PGC1-alpha), Fyn, AKT(PKB), Catalase, PDK (PDPK1), c-Src, PDGF-D, MEKK4(MAP3K4), Pyk2(FAK2), JAK2, Osteopontin, PI3K cat class IA, PI3K reg class IA (p85-alpha), PKC-delta, ETS1, EGFR, AGTR1, MNK1, PLD2, p90Rsk, CaMK II delta, COX-2 (PTGS2), ELAVL1 (HuR), 4E-BP1, p130CAS, Calmodulin, SOD3 (EC-SOD), MMP-14, G-protein alpha-q, Cyclin D1, ATOX1, SPI, ADAM17, p38 MAPK, Elk-1, PAI1, PKA-cat (cAMP-dependent), PDGF-R-beta, ATP7A
14	Signal transduction_Angiotensin II/ AGTR1 signaling via p38, ERK and PI3K	2.049E-11	FHL3, Casein kinase I delta, Sirtuin3, MCM5, RUNX3, VHL, FBXW7, SART1, KLF2, VCP, SKP1, UBXD7, Ubiquitin, ING4, GSK3 beta, MCM7, LAMP2, OS-9, EAF2, MDM2, HSP40, MCM2, HSP90, Calpain 1(mu), HSP70, SAT2, EGLN1, RACK1, DEC2, HSC70, PRDX2, CITED2, HIF1A, ARD1, PSMA7, Sirtuin2, HSP90 beta, Cul1/Rbx1 E3 ligase, AML1 (RUNX1), FHL1 (SLIM1), PTEN, Sirtuin7, SSAT, Elongin C, HIF-prolyl hydroxylase, PRDX4, CHIP, RUVBL2, p53, CITED4
15	Transcription_Negative regulation of HIF1A function	3.026E-11	

**Supplementary Table 3. Pathway analysis of genes co-expressed cadherin 2 (CDH2) from the MetaCore database (with p-value < 0.05 set as the cutoff value) (Supplementary Table 3 and Supplementary Figure 4).**

#	Maps	p-Value	Network objects from active data
1	Cell adhesion_ECM remodeling	2.504E-18	MMP-13, TIMP3, SERPINE2, MSN (moesin), MMP-1, IL-8, MMP-14, MMP-2, Versican, MMP-12, IGF-1 receptor, Matrilysin (MMP-7), PLAUR (uPAR), alpha-5/beta-1 integrin, Actin cytoskeletal, MMP-10, Collagen IV, TIMP2, Fibronectin, Nidogen, Stromelysin-1, LAMA4, MMP-9, PAI1, PLAU (UPA), Syndecan-2, Collagen I, Kallikrein 3 (PSA), Collagen III
2	Cytoskeleton remodeling_Regulation of actin cytoskeleton organization by the kinase effectors of Rho GTPases	2.188E-15	Talin, RhoA, WRCH-1, MRCKalpha, Rac1-related, Cdc42 subfamily, RhoJ, Vinculin, MSN (moesin), ERM proteins, F-Actin cytoskeleton, Spectrin, MRLC, ARPC1B, RhoA-related, Caldesmon, Actin cytoskeletal, Alpha-actinin, Filamin A, RhoC, LIMK1, RhoB, TC10, MyHC, LIMK, MLCK, MRCK
3	IL-1 beta- and Endothelin-1-induced fibroblast/ myofibroblast migration and extracellular matrix production in asthmatic airways	1.775E-12	COL1A1, COL4A1, EDNRB, TIMP3, MMP-1, ERK1/2, MMP-2, Versican, IL-1RI, COL1A2, CTGF, PDGF-R-alpha, Thrombospondin 1, Fibronectin, Stromelysin-1, PAI1, EDNRA, Collagen I, PDGF-R-beta, Collagen III
4	TGF-beta-induced fibroblast/ myofibroblast migration and extracellular matrix production in asthmatic airways	4.672E-12	COL1A1, Biglycan, TGF-beta 2, ITGB1, COL4A1, MMP-13, TIMP3, Tenascin-C, MMP-1, ERK1/2, MMP-2, COL1A2, COL5A1, Collagen IV, TIMP2, ITGA5, Fibronectin, Stromelysin-1, MMP-9, PAI1, Collagen I, MEK4(MAP2K4), Collagen III, Thrombospondin 2
5	Role of TGF-beta 1 in fibrosis development after myocardial infarction	6.420E-12	COL1A1, Biglycan, EDNRB, Tenascin-C, MMP-1, MMP-2, ACTA2, COL1A2, CTGF, Angiotensin II, TIMP2, Thrombospondin 1, Fibronectin, Prolyl endopeptidase, MMP-9, PAI1, EDNRA, Collagen I, Collagen III
6	Glucocorticoid-induced elevation of intraocular pressure as glaucoma risk factor	1.080E-11	RhoA, ITGB1, WNT5A, ROR2, COL4A1, MMP-1, Filamin B (TABP), Antileukoproteinase 1, SERPINA3 (ACT), WNT2, MMP-2, Actin cytoskeletal, Alpha-actinin, Filamin A, Srp40, Collagen IV, Thrombospondin 1, Fibronectin, Stromelysin-1, PKC-epsilon, alpha-V/beta-5 integrin, PAI1, LAMA1, MLCK
7	Transcription_HIF-1 targets	3.805E-10	G3P2, Tfr1, TGF-beta 2, Adipophilin, Carbonic anhydrase XII, Lysyl oxidase, ROR-alpha, Adrenomedullin, HIF1A, P4HA2, REDD1, MMP-2, Galectin-1, PLAUR (uPAR), P4HA1, 5'-NTD, GLUT3, ENO1, Angiopoietin 2, CTGF, Thrombospondin 1, MMP-9, PAI1, Carbonic anhydrase IX, Stanniocalcin 2, LRP1, PKM2, IBP3
8	Protein folding and maturation_Posttranslational processing of neuroendocrine peptides	2.237E-09	PAM, Trypsin, AVP-NPII, OT-NPI, GRP(1-27), AVP-Gly, GRP(18-27), GRP(1-27)Gly, AVP extracellular region, GRP precursor, OT, PCSK5, OT-Gly, GRP(1-17), Neurophysin-II, OT-Gly-Lys-Arg, NPI, ProGRP, AVP-Gly-Lys-Arg
9	Development_Positive regulation of WNT/Beta-catenin signaling at the receptor level	7.111E-09	Biglycan, RECK, ROR2, FZD2, WNT7B, LYPD6, Tenascin-C, Glypican-3, Tcf(Lef), SFRP2, WNT, ERK1/2, WLS, TMEM59, RAP-2A, Filamin A, MKK7 (MAP2K7), GPR124, Stromelysin-1, WNT5B, Frizzled
10	Cell adhesion_Tight junctions	1.170E-08	RhoA, Rich1, JAM3, Cingulin, Tubulin alpha, F-Actin, ARP3, INADL, MRLC, ACTR3, CGNL1, ZO-3, Actin cytoskeletal, PARD6, Claudin-1, Actin, Tubulin (in microtubules)
11	Beta-catenin-dependent transcription regulation in colorectal cancer	2.542E-08	MTS1 (S100A4), LAMC2, LAMC2 (80kDa), Calcyclin, Tenascin-C, IL-8, TCF7L2 (TCF4), Fascin, MMP-14, Lamin A/C, Beta-catenin, PLAUR (uPAR), LAMC2 (100kDa), Claudin-1, PLAU (UPA)

12	Cytoskeleton remodeling_Regulation of actin cytoskeleton nucleation and polymerization by Rho GTPases	2.568E-08	RhoA, RhoD, DRF, RhoF (Rif), Profilin, Rac1-related, Cdc42 subfamily, BAIAP2, FMNL3, FMNL2, F-Actin cytoskeleton, RhoA-related, Actin cytoskeletal, RhoC, RhoB, TC10, FNBP1
13	Cell adhesion_Integrin-mediated cell adhesion and migration	3.065E-08	Talin, RhoA, p130CAS, ITGB1, p190-RhoGEF, VCAM1, PKC, Vinculin, PINCH, Zyxin, F-Actin cytoskeleton, alpha-5/beta-1 integrin, Actin cytoskeletal, Alpha-parvin, Alpha-actinin, Collagen IV, Fibronectin, PARD6, Collagen I, Collagen III
14	Development_Negative regulation of WNT/Beta-catenin signaling in the cytoplasm	3.961E-08	WWP1, Prickle-1, WNT5A, STK4, SIAH1, PKC-alpha, Tcf(Lef), WNT, Amer1, beta-TrCP, Alpha-1 catenin, Beclin 1, NEDD4L, LATS2, Beta-catenin, Skp2/TrCP/FBXW, Nucleoredoxin, SENP2, NKD2, DACT3, Frizzled, DACT1, CDK6
15	FAK1 signaling in melanoma	4.004E-08	Talin, RhoA, p130CAS, ITGB1, ARCGAP22, PKC-alpha, ERK1/2, MMP-14, MMP-2, alpha-5/beta-1 integrin, Actin cytoskeletal, TIMP2, RhoC, ITGA5, Fibronectin, PLAU (UPA)

**Supplementary Table 4. Pathway analysis of genes co-expressed cadherin 4 (*CDH4*) from the MetaCore database (with p-value < 0.05 set as the cutoff value) (Supplementary Table 4 and Supplementary Figure 5).**

#	Maps	p-Value	Network objects from active data
1	Protein folding and maturation_POMC processing	2.428E-13	PAM, proACTH, POMC, N-POMC, beta-Endorphin extracellular region, gamma-LPH, ACTH 1-17, Joining peptide (JP), DA-alphaMSH, gamma-MSH, beta-LPH, gamma2-MSH, beta-MSH, N-POC, gamma3-MSH, ACTH, alpha-MSH, CLIP
2	Beta-catenin-dependent transcription regulation in colorectal cancer	1.638E-11	COX-2 (PTGS2), ID2, MTS1 (S100A4), LAMC2, LAMC2 (80kDa), Calcyclin, Tenascin-C, IL-8, CDX2, L1CAM, Fascin, MMP-14, PLAUR (uPAR), LAMC2 (100kDa), SOX9, PLAU (UPA), MDR1, YAP1 (YAp65)
3	Cell adhesion_ECM remodeling	2.422E-11	MMP-13, SERPINE2, Caveolin-2, MSN (moesin), MMP-1, IL-8, EGFR, MMP-14, MMP-2, MMP-12, HB-EGF, Matrilysin (MMP-7), PLAUR (uPAR), Actin cytoskeletal, Collagen IV, TIMP2, Kallikrein 1, Stromelysin-1, LAMA4, PLAU (UPA), Syndecan-2, Kallikrein 3 (PSA)
4	Transcription_HIF-1 targets	2.755E-08	ID2, Adipophilin, Lysyl oxidase, Transferrin, ROR-alpha, Endothelin-1, Adrenomedullin, HIF1A, P4HA2, LOXL4, MMP-2, Galectin-1, PLAUR (uPAR), 5'-NTD, GLUT3, ENO1, CTGF, p21, IBP1, MGF, HGF receptor (Met), PGK1, SDF-1, MDR1, IBP3
5	Development_Regulation of epithelial-to-mesenchymal transition (EMT)	2.916E-08	N-cadherin, Endothelin-1, E2A, WNT, TGF-beta receptor type II, SLUG, EGFR, SIP1 (ZFHX1B), MMP-2, PDGF-A, IL-1RI, Caldesmon, ACTA2, Tropomyosin-1, PDGF-R-alpha, TWIST1, HGF receptor (Met), Vimentin, Frizzled, TGF-beta receptor type I
6	Role of stellate cells in progression of pancreatic cancer	5.083E-08	RECK, MMP-13, CCL2, IL-8, TGF-beta receptor type II, EGFR, ERK1/2, MMP-2, PDGF-A, HB-EGF, IL-6, Galectin-1, ACTA2, CTGF, PDGF-R-alpha, PDGF receptor, OSF-2, Stromelysin-1, TGF-beta receptor type I
7	Development_YAP/TAZ-mediated co-regulation of transcription	8.820E-08	ID2, TEF-3, Endothelin-1, FKHR, SOD2, HIF1A, CDX2, SLUG, SIP1 (ZFHX1B), Cyr61, ID3, HBP17, TAZ, CTGF, TWIST1, SOX9, YAP1 (YAp65), CDK6
8	Role of Tissue factor-induced Thrombin signaling in cancerogenesis	2.122E-07	MLCP (cat), MMP-13, PKC-alpha, IL-8, EGFR, G-protein alpha-i family, MRLC, ERK1/2, MMP-2, Angiopoietin 1, Actin cytoskeletal, Coagulation factor X, ERK2 (MAPK1), G-protein alpha-q/11, Tissue factor, PLC-beta3, ERK1 (MAPK3), MLCK, IP3 receptor
9	Expression targets of Tissue factor signaling in cancer	1.791E-06	ITGB1, VEGF-C, GFPT2, IL-8, Cyr61, PLAUR (uPAR), Coagulation factor X, CTGF, Tissue factor, PLAU (UPA)
10	Role of TGF-beta 1 in fibrosis development after myocardial infarction	2.492E-06	TMSB4X, EDNRB, Endothelin-1, Tenascin-C, MMP-1, TGF-beta receptor type II, MMP-2, ACTA2, Ac-SDKP, CTGF, TIMP2, Thymosin beta-4, TGF-beta receptor type I
11	MAPK-mediated proliferation of normal and asthmatic smooth muscle cells	2.689E-06	Amphiregulin, EDNRB, PLC-beta, Endothelin-1, PKC-alpha, EGFR, G-protein alpha-i family, ERK1/2, PDGF-A, HB-EGF, PDGF-C, PDGF-R-alpha, PDGF receptor, p90Rsk, IP3 receptor, TGF-beta receptor type I
12	G protein-coupled receptors signaling in lung cancer	2.940E-06	PGE2R4, Amphiregulin, EDNRB, Endothelin-1, IL-8, EGFR, G-protein alpha-i family, NTSR1, ERK1/2, MMP-2, PGE2R1, HB-EGF, Galpha(i)-specific peptide GPCRs, TGF-alpha, Galanin, Galpha(q)-specific peptide GPCRs, G-protein alpha-q/11, HB-EGF(mature), SDF-1

13	Cell adhesion_Desmosomes	3.919E-06	Keratin 17, Desmocollin 3, Keratin 14, Keratin 5, Keratin 1, Plakophilin 1, Desmoglein 3, Vimentin, DSC2
14	Bone metastases in Prostate Cancer	4.695E-06	Endothelin-1, CCL2, WNT, G-protein alpha-i family, DKK1, PTHR1, PTHrP, SDF-1, Frizzled, IBP3, Kallikrein 3 (PSA)
15	Signal transduction_PDGF signaling via MAPK cascades	5.014E-06	COX-2 (PTGS2), SPHK1, MMP-13, ERK1/2, MMP-2, PDGF-A, PDGF-C, IL-6, EGR1, PDGF-R-alpha, ERK2 (MAPK1), p21, PDGF receptor, Tissue factor, Stromelysin-1, p90Rsk, Phox1 (PRRX1)

---

**Supplementary Table 5. Pathway analysis of genes co-expressed cadherin 7 (CDH7) from the MetaCore database (with p-value < 0.05 set as the cutoff value) (Supplementary Table 5 and Supplementary Figure 6).**

#	Maps	p-Value	Network objects from active data
1	Cell cycle_Chromosome condensation in prometaphase	2.632E-18	Condensin, TOP1, Cyclin B, Histone H3, CAP-G, CAP-G/G2, CAP-H/H2, CAP-C, Cyclin A, CNAP1, CAP-D2/D3, Aurora-B, TOP2, BRRN1, Aurora-A, CAP-E, CDK1 (p34)
2	Cell cycle_The metaphase checkpoint	2.852E-16	HZwint-1, ZW10, Survivin, Nek2A, CENP-A, CDC20, MAD2a, CENP-H, SPBC25, BUB3, Aurora-B, HEC, CENP-E, BUB1, Aurora-A, PLK1, CDCA1, CENP-F, Zwilch, AF15q14
3	Cell cycle_Role of APC in cell cycle regulation	2.885E-16	Cyclin B, ORC1L, CKS1, Nek2A, CDC20, MAD2a, BUB3, Tome-1, Cyclin A, Aurora-B, CDC25A, BUB1, Geminin, Emi1, Aurora-A, PLK1, Securin, CDK1 (p34), CDK2
4	DNA damage_ATM/ATR regulation of G2/M checkpoint: cytoplasmic signaling	9.173E-15	p38alpha (MAPK14), Chk2, Chk1, Brca1, Histone H3, CDC25C, UBE2C, PP1-cat, Nucleolysin TIAR, 14-3-3, B56G, JAB1, PP2A regulatory, Aurora-B, JNK2(MAPK9), CDC25A, Cyclin B1, Aurora-A, PLK1, p38 MAPK, DCK, CDK1 (p34)
5	Cell cycle_Spindle assembly and chromosome separation	1.398E-14	Tubulin alpha, Cyclin B, Separase, ZW10, Nek2A, CDC20, MAD2a, Importin (karyopherin)-alpha, KNSL1, Aurora-B, HEC, TPX2, CSE1L, Aurora-A, Securin, Ran, CDK1 (p34), Tubulin (in microtubules)
6	DNA damage_Intra S-phase checkpoint	2.323E-13	PCNA, Chk2, MCM3, Chk1, MCM7, Brca1, SMC3, CDC7, Histone H3, MCM5, FANCD2, DTL (hCdt2), MCM4, FANCI (KIAA1794), PP1-cat, MCM10, PP1-cat alpha, Histone H2AX, Cyclin A, CDC25A, MCM2, Claspin, p38 MAPK, CDK2, CDC45L
7	DNA damage_ATM/ATR regulation of G2/M checkpoint: nuclear signaling	1.213E-11	HSF1, Chk2, Chk1, Brca1, Wee1, Cyclin B, Cyclin B2, CDC25C, PALB2, MDM2, Histone H2AX, Cyclin A, RBBP8 (CtIP), Cyclin B1, Claspin, PLK1, CDK1 (p34), CDK2
8	Cell cycle_Role of Nek in cell cycle regulation	4.024E-11	Tubulin beta, Tubulin gamma, PI3K cat class IA, Tubulin alpha, Histone H3, Nek2A, MAD2a, HEC, Cyclin B1, TPX2, PDK (PDPK1), Aurora-A, Ran, CDK1 (p34), Tubulin (in microtubules)
9	Cell cycle_Start of DNA replication in early S phase	5.728E-10	MCM3, CDC7, ORC1L, MCM5, RPA3, DP1, MCM4, MCM10, ORC6L, MCM4/6/7 complex, MCM2, Geminin, CDK2, CDC45L
10	Abnormalities in cell cycle in SCLC	1.651E-09	PCNA, E2F2, Histone H3, CKS1, CDK4, BMI-1, MDM2, Cyclin A, Aurora-B, Cyclin B1, CDK1 (p34), Cyclin E2, CDK2
11	Ubiquinone metabolism	2.963E-09	NDUFA8, NDUFB3, NDUFS8, NDUFS3, DAP13, NDUFS5, NDUFAB1, NDUFB1, NDUFB5, NDUFC1, NDUFV3, NDUFA7, NDUFA9, NDUFS4, COQ3, NDUFB2, coenzyme Q2 homolog, prenyltransferase (yeast), NDUFA4, NDUFB6, NDUFB8
12	Cell cycle_Cell cycle (generic schema)	3.800E-09	Cyclin B, E2F2, CDC25C, CDK4, E2F5, DP1, Cyclin A, CDC25A, p107, CDK1 (p34), CDK2
13	ATP/ITP metabolism	4.216E-09	AK2, CSL4, POLR1A, RRP4, RRM2B, PPA5, RRM2, RRP46, ADSS, ACYP2, Ribonucleotide reductase, POLR2I, POLR2B, RRP40, POLR2G, RPA16, RPA39, POLR2D, POLR2J, Adenosine kinase, PM/SCL-75, HPRT, POLR3K, Small RR subunit, RRM1, 5'-NT1B
14	Cell cycle_Initiation of mitosis	4.695E-09	Wee1, Cyclin B2, Histone H3, CDC25C, FOXM1, Kinase MYT1, Lamin B, KNSL1, Cyclin B1, PLK1, CDK1 (p34), CDK7
15	Cell cycle_Sister chromatid cohesion	1.312E-08	PCNA, TOP1, SMC3, Cyclin B, RFC3, Separase, Histone H3, DERPC, DCC1, Securin, CDK1 (p34)

**Supplementary Table 6. Pathway analysis of genes co-expressed cadherin 11 (*CDH11*) from the MetaCore database (with p-value < 0.05 set as the cutoff value) (Supplementary Table 6 and Supplementary Figure 7).**

#	Maps	p-Value	Network objects from active data
1	Cell adhesion_ECM remodeling	2.784E-19	MMP-13, TIMP3, SERPINE2, Caveolin-2, PLAT (TPA), MSN (moesin), MMP-1, IL-8, IGF-2, MMP-14, MMP-2, Versican, MMP-12, Matrilysin (MMP-7), PLAUR (uPAR), alpha-5/beta-1 integrin, MMP-10, TIMP2, IGF-1, Fibronectin, Kallikrein 1, Nidogen, Stromelysin-1, LAMA4, PAI1, PLAU (UPA), Syndecan-2, Collagen I, Kallikrein 3 (PSA), Collagen III
2	IL-1 beta- and Endothelin-1-induced fibroblast/ myofibroblast migration and extracellular matrix production in asthmatic airways	2.862E-18	COL1A1, IL-1 beta, AP-1, EDNRB, TIMP3, Decorin, CCL2, MMP-1, HAS2, c-Jun, MMP-2, Versican, IL-1RI, c-Jun/c-Fos, COL1A2, CTGF, PDGF-R-alpha, Thrombospondin 1, Fibronectin, Stromelysin-1, PAI1, EDNRA, Collagen I, PDGF-R-beta, Collagen III
3	Development_Regulation of epithelial-to-mesenchymal transition (EMT)	6.645E-18	IL-1 beta, HEY1, VE-cadherin, N-cadherin, TGF-beta 2, TGF-beta 3, WNT, TGF-beta receptor type II, SLUG, ZO-1, Lef-1, c-Jun, Sno-N, SIP1 (ZFHX1B), MMP-2, IL-1RI, Caldesmon, ACTA2, Tropomyosin-1, PDGF-R-alpha, TWIST1, Fibronectin, Vimentin, TCF8, Claudin-1, PAI1, PDGF-D, Frizzled, EDNRA, FGFR1, PDGF-R-beta
4	Role of TGF-beta 1 in fibrosis development after myocardial infarction	4.860E-14	COL1A1, Biglycan, TMSB4X, EDNRB, Tenascin-C, MMP-1, SMAD7, TGF-beta receptor type II, MMP-2, ACTA2, Ac-SDKP, COL1A2, CTGF, TIMP2, Thymosin beta-4, Thrombospondin 1, Fibronectin, PAI1, EDNRA, Collagen I, Collagen III
5	TGF-beta-induced fibroblast/ myofibroblast migration and extracellular matrix production in asthmatic airways	8.853E-14	COL1A1, Biglycan, TGF-beta 2, ITGB1, AP-1, MMP-13, TIMP3, Decorin, TGF-beta 3, Tenascin-C, MMP-1, HAS2, TGF-beta receptor type II, c-Jun, MMP-2, c-Jun/c-Fos, COL1A2, COL5A1, TIMP2, ITGA5, Fibronectin, Stromelysin-1, PAI1, Collagen I, Collagen III, Thrombospondin 2
6	Development_TGF-beta-dependent induction of EMT via SMADs	1.227E-12	ID2, HEY1, N-cadherin, TGF-beta 2, TGF-beta 3, ETS1, TGF-beta receptor type II, SLUG, Lef-1, SIP1 (ZFHX1B), MMP-2, TGF-beta, TWIST1, Fibronectin, Vimentin, TCF8, Claudin-1, PAI1, ILK
7	Role of adhesion of SCLC cells in tumor progression	1.634E-11	RhoA, N-cadherin, ITGB1, VCAM1, alpha-4/beta-1 integrin, Tenascin-C, alpha-V/beta-1 integrin, MMP-14, MMP-2, CDC42, alpha-5/beta-1 integrin, PTHrP, CD9, Caveolin-1, Fibronectin, Stromelysin-1, SDF-1, CXCR4
8	TGF-beta 1-mediated induction of EMT in normal and asthmatic airway epithelium	2.237E-11	COL1A1, IL-1 beta, N-cadherin, AP-1, Tenascin-C, SMAD7, ETS1, TGF-beta receptor type II, SLUG, ZO-1, c-Jun, MMP-2, ACTA2, c-Jun/c-Fos, CTGF, TWIST1, DAB2, Fibronectin, Vimentin, PAI1
9	Development_Role of proteases in hematopoietic stem cell mobilization	2.666E-11	Cathepsin G, VCAM1, alpha-4/beta-1 integrin, MMP-14, MMP-2, alpha-5/beta-1 integrin, DPP4, MGF, Fibronectin, c-Kit, Cathepsin K, SDF-1, CXCR4
10	Role of stellate cells in progression of pancreatic cancer	5.084E-11	COL1A1, RECK, MMP-13, c-Fos, CCL2, IL-8, TGF-beta receptor type II, c-Jun, MMP-2, Galectin-1, ID1, ACTA2, alpha-5/beta-1 integrin, COL1A2, CTGF, PDGF-R-alpha, PDGF receptor, OSF-2, Fibronectin, Stromelysin-1, Collagen I, PDGF-R-beta, Collagen III
11	Signal transduction_WNT/Beta-catenin signaling in tissue homeostasis	7.895E-11	Cyclin D2, FGF18, Cyclin A2, FKHR, BACE1, Tcf(Lef), IL-8, WNT, SLUG, Lef-1, Pitx2, TCF7L2 (TCF4), Connexin 43, MMP-2, Versican, Beta-catenin, KLF4, PAI1, Frizzled



12	TGF-beta signaling via SMADs in breast cancer	9.851E-11	TGF-beta 2, MMP-13, MTS1 (S100A4), RUNX2, NOX4, JunB, TGF-beta 3, IL-8, ETS1, TGF-beta receptor type II, SLUG, Fascin, MMP-14, ITGB5, PTHrP, CTGF, TWIST1, FOXQ1 (HFH1), PAI1, GLI-2
13	Glucocorticoid-induced elevation of intraocular pressure as glaucoma risk factor	1.112E-10	RhoA, ITGB1, ROCK, WNT5A, ROR2, GCR Beta, GCR, PLAT (TPA), MMP-1, Elastin, Filamin B (TABP), WNT2, MMP-2, CDC42, GCR Alpha, Thrombospondin 1, Fibronectin, Stromelysin-1, alpha-V/beta-5 integrin, PAI1, LAMA1, MLCK, FGFR1
14	Production and activation of TGF-beta in airway smooth muscle cells	1.946E-10	RhoA, TGF-beta 2, ROCK, AP-1, c-Fos, TGF-beta 3, TGF-beta receptor type II, PAR2, G-protein alpha-i family, c-Jun, EGR1, c-Jun/c-Fos, TGF-beta, Beta-tryptase 2, Tryptase, PAI1, PLAU (UPA)
15	Development_TGF-beta-dependent induction of EMT via RhoA, PI3K and ILK	5.404E-10	RhoA, TGF-beta 2, TGF-beta 3, PINCH, TGF-beta receptor type II, SLUG, ZO-1, Lef-1, ROCK1, Beta-catenin, Caldesmon, ACTA2, Tropomyosin-1, HIC5, Fibronectin, Vimentin, Claudin-1, Actin, ILK

**Supplementary Table 7. Pathway analysis of genes co-expressed cadherin 12 (*CDH12*) from the MetaCore database (with p-value < 0.05 set as the cutoff value) (Supplementary Table 7).**

#	Maps	p-Value	Network objects from active data
1	Cytoskeleton remodeling_Regulation of actin cytoskeleton organization by the kinase effectors of Rho GTPases	1.414E-09	RhoA, WRCH-1, DMPK, PAK, Rac1-related, Cdc42 subfamily, RhoJ, ERM proteins, Spectrin, MRLC, SLC9A1, RhoA-related, Alpha adducin, RhoC, RhoB, TC10, MyHC, MRCK
2	Development_Negative regulation of WNT/Beta-catenin signaling in the cytoplasm	5.128E-07	ELAVL1 (HuR), KLHL12, WWP1, STK4, Porf-2, WNT, beta-TrCP, Itch, Alpha-1 catenin, NEDD4L, GSK3 alpha/beta, Skp2/TrCP/FBXW, TAZ, Cyclin D1, CXXC5, RNF185, Axin, YAP1/TAZ
3	LRRK2 in neurons in Parkinson's disease	1.038E-06	GSK3 beta, AP-2 alpha subunits, Beta-adaptin 2, PKC-zeta, MARKK, Tau (MAPT), RAB-5B, AP2A2, CHIP, PKA-cat (cAMP-dependent), VIL2 (ezrin)
4	Development_Positive regulation of WNT/Beta-catenin signaling in the cytoplasm	3.932E-06	PPP2R2A, TBL1X, Bcl-9, Trabid, USP25, WNT, USP7, Alpha-1 catenin, Joubertin, FAK1, GSK3 alpha/beta, IGF-1 receptor, SMAD3, Makorin-1, Axin, PKA-cat (cAMP-dependent)
5	Cytoskeleton remodeling_Regulation of actin cytoskeleton nucleation and polymerization by Rho GTPases	6.154E-06	RhoA, RhoD, RhoF (Rif), CYFIP2, Rac1-related, Cdc42 subfamily, BAIAP2, RhoA-related, RhoC, RhoB, TC10, FNBP1
6	Development_Positive regulation of STK3/4 (Hippo) pathway and negative regulation of YAP/TAZ function	7.507E-06	RhoA, STK4, AMPK beta subunit, Adenylate cyclase, beta-TrCP, CCDC85C, Itch, Alpha-1 catenin, EBP50, Skp2/TrCP/FBXW, TAZ, MARKK, Axin, PKA-cat (cAMP-dependent), Alpha-catenin
7	Development_Negative regulation of WNT/Beta-catenin signaling in the nucleus	7.966E-06	NF-AT5, TBL1X, GSK3 beta, Oct-3/4, WNT, Alpha-1 catenin, Jade-1, P15RS, CHIBBY, BCL9/B9L, GLI-3R, PC1-CTT, CHD8, TLE, HIC5, Axin, Histone H1
8	PI3K signaling in gastric cancer	1.560E-05	ELAVL1 (HuR), PI3K reg class IA (p85), GSK3 beta, PI3K reg class IA, PTEN, HSP27, FAK1, ErbB3, Cyclin D1, PRNP, G-protein alpha-q/11, MDR1
9	Signal transduction_mTORC2 downstream signaling	2.056E-05	RhoA, Tuberin, GSK3 beta, SREBP1 (nuclear), PKC, STK4, NEDD4L, GSK3 alpha/beta, PKC-zeta, IGF-1 receptor, Cyclin D1, Adenylate cyclase type IX, PKA-cat (cAMP-dependent), PREX1
10	Signal transduction_Cyclic AMP signaling	3.383E-05	PKC, cAMP-GEFI, PHK alpha, PHK gamma, GSK3 alpha/beta, Adenylate cyclase type VI, PKC-zeta, CREB1, Adenylate cyclase type IX, PKA-cat (cAMP-dependent)
11	Regulation of lipid metabolism_Regulation of lipid metabolism via LXR, NF-Y and SREBP	3.383E-05	SREBP1 precursor, Importin (karyopherin)-beta, ACLY, SREBP1 (nuclear), AMPK beta subunit, RARalpha, RXRA, CREB1, SPI, SREBP1 (Golgi membrane)
12	Signal transduction_IGF-1 receptor signaling pathway	7.566E-05	Androgen receptor, PI3K reg class IA (p85), GSK3 beta, SREBP1 (nuclear), Bcl-2, Cyclin D, FAK1, PKC-zeta, IGF-1 receptor, MNK2(GPRK7), MKK7 (MAP2K7), ACSA
13	WNT signaling in gastric cancer	1.292E-04	GSK3 beta, CD44, WNT, beta-TrCP, WNT3, Skp2/TrCP/FBXW, Cyclin D1, Axin, FBXW11
14	DNA damage_ATM/ATR regulation of G1/S checkpoint	1.306E-04	ELAVL1 (HuR), Chk2, SMG1, FBXW7, PP2A structural, beta-TrCP, PP2A regulatory, Cyclin D1, PER3, FBXW11
15	Main pathways of Schwann cells transformation in neurofibromatosis type 1	1.344E-04	Tuberin, PI3K reg class IA (p85), Amphiregulin, GSK3 beta, ErbB2, PTEN, Bcl-2, FAK1, ErbB3, Neurofibromin, IGF-1 receptor, BRD4, Cyclin D1, ErbB4

**Supplementary Table 8. Pathway analysis of genes co-expressed cadherin 13 (*CDH13*) from the MetaCore database (with p-value < 0.05 set as the cutoff value) (Supplementary Table 8 and Supplementary Figure 8).**

#	Maps	p-Value	Network objects from active data
1	Development_Regulation of epithelial-to-mesenchymal transition (EMT)	3.068E-16	IL-1 beta, HEY1, VE-cadherin, N-cadherin, TGF-beta 2, WNT, TGF-beta receptor type II, SLUG, ZO-1, SIP1 (ZFHX1B), MMP-2, PDGF-A, Caldesmon, ACTA2, Tropomyosin-1, PDGF-R-alpha, TWIST1, Fibronectin, Jagged1, Vimentin, TCF8, DLL4, Claudin-1, PAI1, PDGF-D, Frizzled, EDNRA, FGFR1, PDGF-R-beta
2	Role of stellate cells in progression of pancreatic cancer	3.846E-16	COL1A1, MEK1(MAP2K1), NGF, RECK, MMP-13, c-Fos, IL-8, TGF-beta receptor type II, alpha-V/beta-3 integrin, MEK2(MAP2K2), MMP-2, PDGF-A, HB-EGF, Galectin-1, ID1, ACTA2, alpha-5/beta-1 integrin, SOS, COL1A2, CTGF, PDGF-R-alpha, PDGF receptor, OSF-2, Fibronectin, NFKBIA, Collagen I, PDGF-R-beta, Collagen III
3	Cell adhesion_ECM remodeling	2.966E-15	MMP-13, TIMP3, SERPINE2, Caveolin-2, PLAT (TPA), IL-8, MMP-2, Versican, MMP-12, HB-EGF, PLAUR (uPAR), alpha-5/beta-1 integrin, Actin cytoskeletal, MMP-10, Collagen IV, TIMP2, Fibronectin, Kallikrein 1, Nidogen, LAMA4, PAI1, PLAU (UPA), Syndecan-2, Collagen I, Kallikrein 3 (PSA), Collagen III
4	IL-1 beta- and Endothelin-1-induced fibroblast/ myofibroblast migration and extracellular matrix production in asthmatic airways	9.808E-14	COL1A1, IL-1 beta, AP-1, COL4A1, EDNRB, TIMP3, Decorin, HAS2, MMP-2, Versican, COL1A2, NF-kB, CTGF, PDGF-R-alpha, Thrombospondin 1, Fibronectin, PAI1, EDNRA, Collagen I, PDGF-R-beta, Collagen III
5	TGF-beta-induced fibroblast/ myofibroblast migration and extracellular matrix production in asthmatic airways	2.572E-11	COL1A1, Biglycan, TGF-beta 2, ITGB1, AP-1, COL4A1, MMP-13, TIMP3, Decorin, Tenascin-C, HAS2, TGF-beta receptor type II, MMP-2, COL1A2, COL5A1, Collagen IV, TIMP2, ITGA5, Fibronectin, PAI1, Collagen I, Collagen III, Thrombospondin 2
6	Role of TGF-beta 1 in fibrosis development after myocardial infarction	5.509E-11	COL1A1, Biglycan, EDNRB, Tenascin-C, TGF-beta receptor type II, MMP-2, AGTR1, ACTA2, COL1A2, CTGF, Angiotensin II, TIMP2, Thrombospondin 1, Fibronectin, PAI1, EDNRA, Collagen I, Collagen III
7	MAPK-mediated proliferation of normal and asthmatic smooth muscle cells	3.070E-10	LPAR2, Rb protein, EDNRB, c-Fos, PLAT (TPA), G-protein alpha-I family, MKP-1, PDGF-A, HB-EGF, PDGF-C, MEK1/2, G-protein beta/gamma, SOS, PDGF-R-alpha, PDGF receptor, Elk-1, PAI1, p90Rsk, EDNRA, FGFR1, PDGF-R-beta
8	Stimulation of TGF-beta signaling in lung cancer	7.310E-10	IL-1 beta, N-cadherin, TGF-beta 2, I-kB, ITGB1, Vinculin, TGF-beta receptor type II, SLUG, MMP-2, ACTA2, EGR1, VEGF-A, TGF-beta, Tropomyosin-1, MMP-28, Fibronectin, Vimentin, PAI1, Tropomyosin-2
9	Cell adhesion_PLAU signaling	1.144E-09	STAT3, MEK1(MAP2K1), LAMC2, NF-kB2 (p52), alpha-V/beta-1 integrin, alpha-V/beta-3 integrin, G-protein alpha-I family, F-Actin cytoskeleton, MRLC, PLAUR (uPAR), alpha-5/beta-1 integrin, VEGFR-2, SOS, NF-kB, Caveolin-1, MYLK1, sUPAR, alpha-V/beta-5 integrin, PLAU (UPA), MLCK, STAT1, PDGF-R-beta
10	Glucocorticoid-induced elevation of intraocular pressure as glaucoma risk factor	2.691E-09	ITGB1, WNT5A, COL4A1, GCR Beta, GCR, PLAT (TPA), ITGB3, alpha-V/beta-3 integrin, WNT2, MMP-2, Actin cytoskeletal, GCR Alpha, LAMB3, Collagen IV, Thrombospondin 1, Fibronectin, alpha-V/beta-5 integrin, PAI1, LAMA1, MLCK, FGFR1
11	Stromal-epithelial interaction in Prostate Cancer	3.849E-09	Keratin 17, TGF-beta 2, Tenascin-C, TGF-beta receptor type II, MMP-2, Versican, PDGF-A, ACTA2, PDGF-R-alpha, HIC5, TIMP2, Fibronectin, Vimentin, PDGF-D, FGFR1, Collagen I, PDGF-R-beta

12	Development_TGF-beta-dependent induction of EMT via MAPK	3.859E-09	MEK1(MAP2K1), TGF-beta 2, ITGB1, MLK3(MAP3K11), AP-1, c-Fos, NOX4, ITGB3, alpha-V/beta-1 integrin, TGF-beta receptor type II, MEK2(MAP2K2), MMP-2, TGF-beta, SOS, Fibronectin, Vimentin, Claudin-1, PAI1
13	TGF-beta 1-mediated induction of EMT in normal and asthmatic airway epithelium	8.956E-09	COL1A1, IL-1 beta, N-cadherin, AP-1, Tenascin-C, ITGB3, TGF-beta receptor type II, SLUG, ZO-1, MMP-2, ACTA2, CTGF, TWIST1, Fibronectin, Jagged1, Vimentin, PAI1
14	Development_TGF-beta-dependent induction of EMT via SMADs	1.255E-08	HEY1, N-cadherin, TGF-beta 2, TGF-beta receptor type II, SLUG, SIP1 (ZFHX1B), MMP-2, TGF-beta, TWIST1, Fibronectin, Jagged1, Vimentin, TCF8, Claudin-1, PAI1
15	Signal transduction_Angiotensin II/AGTR1 signaling via Notch, Beta-catenin and NF-kB pathways	2.318E-08	COL1A1, HEY1, I-kB, PRKD1, NF-kB2 (p100), NF-kB2 (p52), IL-8, Connexin 43, MMP-2, AGTR1, Axin2, Beta-catenin, ACTA2, HEY2, Angiotensinogen, VEGF-A, NF-kB, CTGF, NIK(MAP3K14), Angiotensin II, Fibronectin, YAP1 (Yap65)

---

**Supplementary Table 9. Pathway analysis of genes co-expressed cadherin 15 (*CDH15*) from the MetaCore database (with p-value < 0.05 set as the cutoff value) (Supplementary Table 9 and Supplementary Figure 9).**

#	Maps	p-Value	Network objects from active data
1	Transcription_HIF-1 targets	6.658E-17	PDK1, NIX, P4HA2, PFKL, REDD1, SLC9A1, VEGF-A, Cyclin G2, 5'-NTD, GLUT3, ENO1, p21, MSH6, Carbonic anhydrase IX, PGK1, Stanniocalcin 2, NIP3, MDR1, AK3, IBP3, ID2, Adipophilin, LOXL4, MMP-2, PLAUR (uPAR), WT1, Alpha-1B adrenergic receptor, DEC1 (Stra13), ALDOC, c-Myc, Epo, SDF-1, CXCR4, LRP1, PKM2, G3P2, ARNT, Heme oxygenase 1, TGF-beta 2, Ceruloplasmin, Lysyl oxidase, ROR-alpha, Adrenomedullin, CITED2, HIF1A, HXK1, HIF-1, GPI, P4HA1, FGF2, Angiopoietin 2, IBP1, MGF, Thrombospondin 1, TfR1, GLUT1, Carbonic anhydrase XII, Transferrin, SOX2, CX3CR1, TGM2, Galectin-1, NOXA, CTGF, MCT4, LDHA, ABCG2, p53, HGF receptor (Met), Leptin, MMP-9, PAII
2	Oxidative stress_ROS-induced cellular signaling	7.281E-17	Casein kinase II, alpha chains, Tuberin, SREBP1 (nuclear), SCD, ERK1/2, EGR1, VEGF-A, PKA-reg (cAMP-dependent), TXNIP (VDUP1), IKK (cat), p21, Bak, Cytochrome c, FASN, E2I, Carbonic anhydrase IX, Syk, IL-1 beta, Bax, GSK3 beta, FTL, IKK-alpha, FTH1, IRP2, GRP75, MDM2, IL-6, GADD45 alpha, NF-kB, AKT(PKB), Catalase, Cyclin B1, c-Src, PUMA, NOTCH1 (NICD), Thioredoxin, Heme oxygenase 1, PLK3 (CNK), Chk2, Adrenomedullin, HIF1A, IL-8, SRX1, AMPK alpha subunit, Pin1, NIK(MAP3K14), Glutaredoxin 1, p300, NFKBIA, HSPA1A, GSTP1, TR1, ELAVL1 (HuR), HSF1, PKC-beta, PRKD1, Sirtuin1, GPX1, PKC, LKB1, PTEN, MEKK1(MAP3K1), HES1, IKK-beta, DLC1 (Dynein LC8a), NOXA, Cyclin D1, HIF-prolyl hydroxylase, HDAC1, SAE2, SP1, p53, NRF2, ADAM17, p38 MAPK, APEX, PAII, mTOR, NALP3
3	Development_Negative regulation of WNT/Beta-catenin signaling in the cytoplasm	6.919E-14	Casein kinase I delta, NOTCH1 receptor, CXXC4, NKD1, PP1-cat, RIPK4, APC protein, Alpha-1 catenin, Casein kinase I epsilon, Beta-catenin, CYLD, CXXC5, Nucleoredoxin, Dsh, Casein kinase I alpha, WWP1, STK4, SIAH1, Itch, GSK3 alpha/beta, Ankyrin-G, G-protein beta/gamma, WDR26, Skp2/TrCP/FBXW, TAZ, Axin, KCTD1, RACK1, KLHL12, E-cadherin, HECTD1, Prickle-1, HIPK2, STK3, Tcf(Lef), HUWE1, Amer1, beta-TrCP, PP2A catalytic, PR72, SENP2, A20, Cull1/Rbx1 E3 ligase, YAP1/TAZ, MAP1LC3A, CDK6, ELAVL1 (HuR), PEG3, WNT5A, PKC-alpha, Porf-2, WNT, Beclin 1, NEDD4L, Cyclin D1, p53, NKD2, DACT3, Frizzled, Siah1/SIP/Ebi E3 ligase, DACT1
4	Neurophysiological process_Dynein-dynactin motor complex in axonal transport in neurons	8.348E-13	Nude, ERK1/2, DCTN1(p150Glued), Importin (karyopherin)-alpha, HDAC6, APP, DYNC111, Vimentin, Ubiquitin, Hap-1, TMEM108, Centractins, DYNLL, ORP1, Dynein 1, cytoplasmic, heavy chain, Tctex-1, Alpha-centractin, MAPRE3(EB3), DYNLT, HAP40, PRNP, AKT(PKB), Snapin, PAFAH alpha (LIS1), MAPRPE1(EB1), DYI2, Tubulin (in microtubules), Importin (karyopherin)-beta, Dynein 1, cytoplasmic, light chains, TrkC, Sortilin, BPGK1, TrkB, JSAP1, NGF, RILP (Rab interacting lysosomal protein), Kinesin heavy chain, Bassoon, Kinesin light chain, Carboxypeptidase H, Dynein 1, cytoplasmic, intermediate chains, BDNF, NUDEL, SPTBN2
5	G protein-coupled receptors signaling in lung cancer	1.444E-12	SSTR2, c-Fos, CD44, ERK1/2, PGE2R1, HB-EGF, VEGF-A, PKA-reg (cAMP-dependent), BDKRB2, Galanin, G-protein alpha-q/11, CCL5, I-kB, GRP-R, CaMK II, Amphiregulin, CNR1, IKK-alpha, GALR2, NTSR1, MMP-2, Bcl-XL, G-protein beta/gamma, Galpha(i)-specific peptide GPCRs, VIP, TGF-alpha, Galpha(i)-specific cannabis GPCR, AKT(PKB), PDK (PDPK1), c-Src, SDF-1, CXCR4, RhoA, Pyk2(FAK2), PGE2R4, G-protein alpha-12 family, IL-8, G-protein alpha-12, EGFR, G-protein alpha-i family, Galpha(q)-specific peptide GPCRs, PGE2R3, HB-EGF(mature), SSTR3, STAT3, EDNRB, Calmodulin, GRP(1-27), NT, VIP receptor 1, Cyclin D1, VIP receptor 2, SSTR5, ADAM17, PKA-cat (cAMP-dependent), EDNRA
6	Transcription_Negative regulation of HIF1A function	2.066E-12	FHL3, p14ARF, Casein kinase I delta, Sirtuin3, MCM5, RUNX3, COMMD1 (MURR1), FBXW7, SART1, KLF2, VCP, Sirtuin6, SKP1, UBXD7, Ubiquitin, ING4, GSK3 beta, EGLN2, MCM7, Elongin B, LAMP2, EAF2, MDM2, MCM2, HSP90, Calpain 1(mu), HSP70, SAT2, EGLN1, RACK1, PLK3 (CNK), HSC70, PRDX2, CITED2, HIF1A, MTG16 (CBFA2T3), ARD1, PSMA7, Sirtuin2, HSP90 beta, Cull1/Rbx1 E3 ligase, AML1 (RUNX1), Sirtuin1, HIF3A, PTEN, SSAT, Elongin C, HIF-prolyl hydroxylase, PRDX4, CHIP, p53, CITED4
7	Chemotaxis_Lysophosphatidic acid signaling via GPCRs	4.803E-12	LPAR3, c-Fos, H-Ras, LARG, ROCK1, ERK1/2, PRK1, HB-EGF, Beta-catenin, EGR1, HDAC7, G-protein alpha-q/11, p21, PKC-epsilon, TRIP6, IP3 receptor, LPAR2, PI3K reg class IA (p85), Bax, GSK3 beta, PLC-beta, FKHR, PLEKHG2, DIA1, HAS2, Caspase-3, Cyr61, CREB1, Bcl-XL, MEK1/2, G-protein beta/gamma, CDC42, Actin cytoskeletal, N-CoR, TAZ, MSK1, AKT(PKB), PDK (PDPK1), c-Src, RhoA, Tiam1, E-cadherin, cPKC (conventional), G-protein alpha-12 family, PLC-eta 1, PKC-delta, Tcf(Lef), IL-8, EGFR, G-protein alpha-i family, F-Actin cytoskeleton, MKL2, mTORC1, Caspase-9, LIMK, PLD2, CD36, G-protein gamma 12, MEK4(MAP2K4), 4E-BP1, p130CAS, ROCK, PRKD1, PAK, PDZ-RhoGEF, PKC, Vinculin, ATF-2, PLC-delta 1, Bcl-2, FasR(CD95), SIVA1, Rho GTPase, MKL1, CTGF, p53, PLC-beta3, ADAM17, p38 MAPK, Elk-1, mTOR, PREX1

8	Development_Positive regulation of WNT/Beta-catenin signaling in the cytoplasm	7.694E-12	Casein kinase II, alpha chains, TBL1X, Bcl-9, BIG1, IRS-2, NKD1, IRS-1, UBE2B, PP1-cat, RIPK4, APC protein, Alpha-1 catenin, 14-3-3, Beta-catenin, TGIF, SMAD4, Makorin-1, Dsh, USP47, ZBED3, CDK1 (p34), PPP2R2A, SIAH1, USP25, PR130, Insulin receptor, GSK3 alpha/beta, IGF-1 receptor, ERK2 (MAPK1), AKT(PKB), Axin, HECTD1, ITGB1, SIAH2, HIPK2, Tcf(Lef), 14-3-3 zeta/delta, TGT, HSP105, PKA-reg type II (cAMP-dependent), PP2A catalytic, Trabd, BIG2, USP9X, WNT, Jouberin, PP2C alpha, SMAD3, Parathyroid hormone, NKD2, MITF, PKA-cat (cAMP-dependent), Frizzled, SET7, DACT1  IP10, ISG15, TCF7L2 (TCF4), RIG-G, ERK1/2, GCH1, Beta-catenin, Matrilysin (MMP-7), PRMT1, ZNF145, SMAD4, PIAS1, Apo-2L(TNFSF10), p21, IFNAR1, VAV-1, STAT1, PL scramblase 1, ULK1, IKK-epsilon, Ubiquitin, TAP1 (PSF1), MAPKAPK2, PKC-theta, IFN-alpha, ISG54, Axin2, p130, MSK1, RSAD2, AKT(PKB), p27KIP1, FZD7, HIP-2, Lck, CD45, PKR, PKC-delta, MEK3(MAP2K3), IRF9, MEK4(MAP2K4), Ku80, MEKK1(MAP3K1), SP5, Filamin B (TABP), FOXO3A, FasR(CD95), IRF7, Cyclin D1, HDAC1, SMAD3, p38 MAPK, mTOR
9	Immune response_IFN-alpha/beta signaling via MAPKs	1.507E-11	CLEC12A, Fc epsilon RI gamma, MSR1, Endoplasmic, gp91-phox, FCGR3A, Rac2, CLEC4C, VCP, TAP, Rab-3C, VAV-1, p47-phox, Syk, Rab-6, IP-30, Adipophilin, HYOU1, IRAP, MyD88, C1q, cPLA2, Calreticulin, MHC class I, HSP60, TLR9, HSP90, Syntaxin 4, HSP70, Rab8B, LRP1, EHD1, Cathepsin L, Dectin-1, Rab-4A, SEC61 complex, FCGRT, LLIR, Cytochrome b-558, CLEC9A, HSP105, Rab-32, Fc gamma RII alpha, Rab-35, RanBPM, Rab-33A, Cathepsin B, HSPA1A, SEC22B, Fc gamma RI, DAP12, CD74, Rab-11A, CD8, UFO, Rab-10, OLR1, IKK-beta, TLR7, CD40(TNFRSF5), RAB-5B, TRIF (TICAM1), CHIP, SNAP-23, Rab-34, TLR2  GAB1, CD44, ERK1/2, Beta-catenin, EGR1, Fibronectin, PI3K reg class IA (p85), GSK3 beta, N-Ras, Bcl-XL, TWIST1, AKT(PKB), alpha-MSH, MC1R, HGF, MEK1(MAP2K1), N-cadherin, E-cadherin, PI3K cat class IA, Desmoglein 1, HIF1A, C/EBPbeta, RXRA, PKC-beta2, PKC-alpha, ATF-2, SLUG, Cyclin D1, Plakoglobin, HGF receptor (Met), p38 MAPK, Elk-1, MITF
10	Immune response_Antigen presentation by MHC class I: cross-presentation	2.580E-11	MHC class II, IL-1 alpha, Calcineurin A (catalytic), ICAM1, CD44, CD28, MSK1/2 (RPS6KA5/4), HDAC7, IP3 receptor, I-kB, PI3K reg class IA (p85), PKC-theta, MyD88, IKK-alpha, PLC-gamma 1, NR2, ITK, Caspase-3, IL-1RI, CREB1, G-protein beta/gamma, CD83, NF-kB, AKT(PKB), HSP70, SDF-1, CXCR4, RhoA, Pyk2(FAK2), CD80, PI3K cat class IA, Lck, CD45, Slp76, HIP1, MEK3(MAP2K3), PSMC2, MEF2, NIK(MAP3K14), LAT, NR2A, RhoGDI alpha, MEK4(MAP2K4), ROCK, Calmodulin, PKC-alpha, CD3, IKK-beta, IP3R1, PSD-95, IRAK1/2, CD40(TNFRSF5), Calcineurin B (regulatory), p38 MAPK, TLR2  SPHK1, NEFL, c-Fos, Fra-1, H-Ras, ERK1/2, MEF2C, HB-EGF, EGR1, PP2A regulatory, SGK1, PKA-reg (cAMP-dependent), FRS2, p21, VGF, PKC-epsilon, Ephrin-A receptor 2, IP3 receptor, TY3H, MAPKAPK2, PLC-gamma 1, Ca/DAG-GEFII, N-Ras, SNX26 (TCGAP), MAP2K5 (MEK5), KIDINS220, CREB1, MEK1/2, PLAUR (uPAR), Flotillin-1, M-Ras, MSK1, RGS2, p107, Stromelysin-1, c-Src, GAB2, Sequestosome 1(p62), SHPS-1, MATK, Efs/Sin, RIN, NF-kB1 (p50), K-RAS, PKC-delta, MEK3(MAP2K3), SOS, PP2A catalytic, C3G, SH2B, p90Rsk, p130CAS, NGF, Calmodulin, MAGI-2, SHP-2, SUR-8, Cyclin D1, SORBS1, SP1, PVR, JMJD3, SHB, RIT, p38 MAPK, Elk-1, PKA-cat (cAMP-dependent), FosB
11	HGF signaling in melanoma	8.917E-11	MIG, IL-18R1, MHC class II, IP10, CTAG2, DHFR, Granzyme B, IFN-gamma, MAGE-1 antigen, Apo-2L(TNFSF10), CD19, Dsk2 (ubiquilin-2), Perforin, STAT1, MAGE-3, IFN-alpha, ACAT2, CD4, CD27(TNFRSF7), MHC class I, MAGE-4 antigen, G-protein beta/gamma, NXF2, Kappa chain (Ig light chain), MAGEB2, FasL(TNFSF6), NF-kB, CT47A, SDF-1, CXCR4, IL-2, CD40L(TNFSF5), G3P2, Syndecan-1, MAGEC1, GAS11, CD38, I-TAC, T-bet, G-protein alpha-i family, AID, IL4RA, Bcl-6, IRF4, RGS1, Btk, CXCR3, STAT3, CD8, CXorf61, SOX2, ATF-2, FasR(CD95), CXCL13, KTN1, CD40(TNFRSF5), STAT6, MAGEC2, p53, IL-21, BLIMP1 (PRDI-BF1)  gp130, IP10, c-Fos, GAB1, ESR1 (nuclear), H-Ras, ERK1/2, HSD17B1, Vimentin, Carbonic anhydrase IX, MDR1, STAT1, MUC1, Survivin, PI3K reg class IA, CYP19, IL-6, Bcl-XL, MEK1/2, TWIST1, AKT(PKB), c-Myc, N-cadherin, E-cadherin, PI3K cat class IA, NF-kB1 (p50), C/EBPbeta, JAB1, SOS, IL6RA, STAT3, SHP-2, Bcl-2, Fascin, S100A7, AKT2, Cyclin D1, SNAIL1, Jagged1, IL-6 receptor, C/EBPdelta
12	CHDI_Correlations from Replication data_Causal network (positive correlations)	9.062E-11	
13	Neurogenesis_NGF/ TrkA MAPK-mediated signaling	9.356E-11	
14	Role of tumor-infiltrating B cells in anti-tumor immunity	1.033E-10	
15	IL-6 signaling in breast cancer cells	1.105E-10	